Supporting Information

Probing and Engineering Key Residues for Bis-*C*-glycosylation and Promiscuity of a *C*-Glycosyltransferase

Dawei Chen,[†] Shuai Fan,[‡] Ridao Chen,[†] Kebo Xie,[†] Sen Yin,[†] Lili Sun,[§] Jimei Liu,[†] Lin Yang,[§] Jianqiang Kong,[†] Zhaoyong Yang,[‡] and Jungui Dai[*,†]

[†] State Key Laboratory of Bioactive Substance and Function of Natural Medicines, Institute of Materia Medica, Chinese Academy of Medical Sciences and Peking Union Medical College, 1 Xian Nong Tan Street, Beijing 100050, China.

[‡] Institute of Medicinal Biotechnology, Chinese Academy of Medical Sciences and Peking Union Medical College, 1 Tian Tan Xi Li, Beijing 100050, China.

[§]College of Life and Environmental Sciences, Minzu University of China, 27 Zhong Guan Cun Southern Street, Beijing 100081, China

*Correspondence: jgdai@imm.ac.cn

Table of Contents

1. MS, ^{1}H and ^{13}C NMR data of *C*-glycosylated products

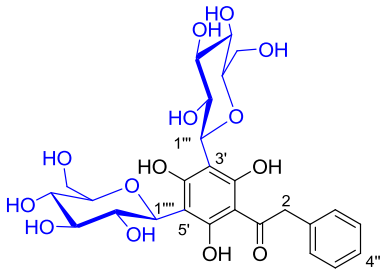

1a

2-Phenyl-3',5'-(bis-*C*-β-D-glucosyl)-2',4',6'-trihydroxyacetophenone (1a) (2.2 mg): ESI-MS *m/z* 567.13 $[M-H]^-$; HRMS (ESI^+) calcd. for $C_{26}H_{33}O_{14}$ $[M+H]^+$: 569.1865; found: 569.1816. ^{1}H NMR (400 M, CD_3OD-d_4): Aglycon: δ = 7.24-7.19 (5H, m, H-2"-6"). Glycosyl: δ = 4.94 (2H, d, J = 9.7 Hz, H-1''', 1''''), 3.89-3.42 (12H, m, Glc); ^{13}C NMR (150 M, CD_3OD-d_4): Aglycon: δ = 205.5 (C=O), 163.4 (C-4'), 162.9 (C-2', 6'), 137.2 (C-1"), 131.0 (C-2", 6"), 129.3 (C-3", 5"), 127.6 (C-4"), 106.2 (C-1'), 104.6 (C-3', 5'), Glycosyl: δ = 82.9 (C-5''', 5''''), 79.3 (C-3''', 3''''), 76.9 (C-1''', 1''''), 74.3 (C-2''', 2''''), 71.2 (C-4''', 4''''), 62.0 (C-6''', 6'''').[1,2]

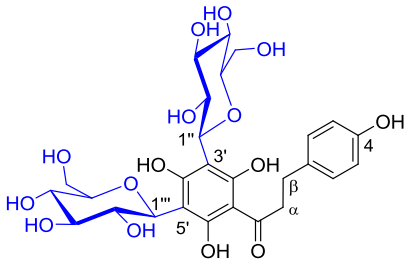

2a

Phloretin 3',5'-bis-*C*-β-D-glucoside (2a) (2.9 mg): ESI-MS *m/z* 597.11 $[M-H]^-$. ^{1}H NMR (400 M, CD_3OD-d_4): Aglycon: δ = 7.04 (2H, d, J = 7.3 Hz, H-2, 6), 6.68 (2H, d, J = 7.3 Hz, H-3, 5), 3.34 (2H, t, J = 7.4 Hz, H-β), 2.87 (2H, t, J = 7.4 Hz, H-α). Glycosyl: δ =4.94 (2H, d, J = 9.7 Hz, H-1", 1'''), 3.87-3.42 (12H, m, Glc); ^{13}C NMR (150 M, CD_3OD-d_4): Aglycon: δ = 207.3 (C=O), 163.3 (C-4'), 162.4 (C-2', 6'), 156.6 (C-4), 134.0 (C-1), 130.5 (C-2, 6), 116.2 (C-3, 5), 106.3 (C-1'), 104.5 (C-3', 5'), 48.0 (C-α), 31.2 (C-β). Glycosyl: δ = 82.9 (C-5", 5'''), 79.3 (C-3", 3'''), 76.9 (C-1", 1'''), 74.3 (C-2", 2'''), 71.2 (C-4", 4'''), 62.0 (C-6", 6''').[1]

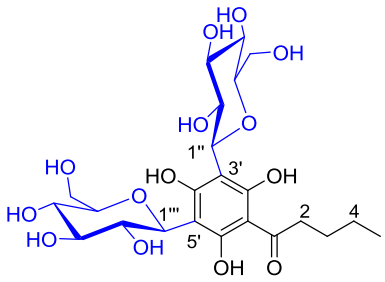

3a

1-(3',5'-Bis-*C*-β-D-glucosyl-2',4',6'-trihydroxyphenyl) pentan-1-one (3a) (8.1 mg): ESI-MS *m/z* 533.14 $[M-H]^-$; HRMS (ESI^+) calcd. for $C_{23}H_{35}O_{14}$ $[M+H]^+$: 535.2021; found: 535.1979. ^1H NMR (400 MHz, CD_3OD-d_4): Aglycon: δ = 3.13 (2H, m, H-2), 1.66 (2H, m, H-3), 1.41 (2H, m, H-4), 0.97 (3H, t, *J* = 7.0, H-5). Glycosyl: δ = 4.96 (2H, d, *J* = 9.7, H-1", 1'''), 3.90-3.46 (12H, m, Glc); ^{13}C NMR (150 MHz, CD_3OD-d_4) Aglycon: δ = 208.4 (C=O), 163.3 (C-4'), 162.3 (C-2', 6'), 106.4 (C-1'), 104.5 (C-3', 5'), 45.3 (C-2), 28.2 (C-3), 23.8 (C-4), 14.5 (C-5). Glycosyl: δ = 82.9 (C-5", 5'''), 79.3 (C-3", 3'''), 76.9 (C-1", 1'''), 74.3 (C-2", 2'''), 71.2 (C-4", 4'''), 62.0 (C-6", 6''').[1,3]

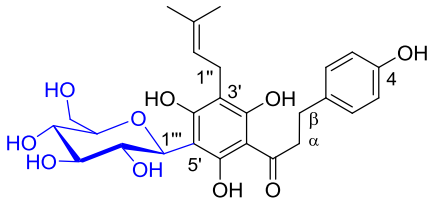

15a

3'-Dimethylallyphloretin 5'-*C*-β-D-glucoside (15a) (12.6 mg): ESI-MS *m/z* 503.26 $[M-H]^-$; HRMS (ESI^+) calcd. for $C_{26}H_{33}O_{10}$ $[M+H]^+$: 505.2068; found: 505.2025. ^1H NMR (400 M, CD_3OD-d_4): Aglycon: δ = 7.01 (2H, d, *J* = 8.4 Hz, H-2, 6), 6.65 (2H, d, *J* = 8.4 Hz, H-3, 5), 5.12 (1H, t, *J* = 7.0 Hz, H-2"), 3.30 (2H, t, *J* = 7.8 Hz, H-β), 3.23 (2H, d, *J* = 7.0 Hz, H-1"), 2.83 (2H, d, *J* = 7.8 Hz, H-α), 1.72 (3H, s, H-4"), 1.62 (3H, s, H-5"). Glycosyl: δ = 4.89 (overlap, H-1'''), 3.82 (1H, dd, *J* = 9.2, 3.2 Hz, H-2'''), 3.50 (1H, d, *J* = 9.5 Hz, H-6'''a), 3.43 (1H, d, *J* = 9.5 Hz, H-6'''b), 3.29-3.27 (3H, m, H-3'''-5'''); ^{13}C NMR (150 M, CD_3OD-d_4): Aglycon: δ = 207.2 (C=O), 163.2 (C-4'), 161.5 (C-4), 159.6 (C-2'), 159.4 (C-6'), 134.0 (C-3"), 131.8 (C-1), 130.3 (C-2, 6), 124.1 (C-2"), 116.1 (C-3, 5), 109.8 (C-3'), 106.8 (C-5'), 104.5 (C-1'), 47.8 (C-α), 31.4 (C-β), 25.9 (C-1"), 22.3 (C-4"), 17.9 (C-5"). Glycosyl: δ = 82.7 (C-5'''), 79.3 (C-3'''), 77.8 (C-1'''), 75.3 (C-2'''), 70.6 (C-4'''), 61.6 (C-6''').[4]

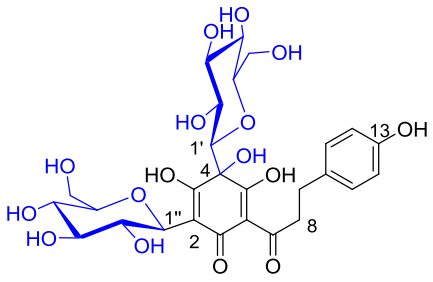

2c

2,4-Bis-*C*-β-D-glucopyranosyl-3,4,5-trihydroxy-6-[3-(4-hydroxyphenyl)-propanoyl]-2,5-cyclohexadien-1-one (2c) (8.1 mg): ESI-MS *m/z* 613.53 $[M-H]^-$; HRMS (ESI^+) calcd. for $C_{27}H_{34}O_{16}Na$ $[M+Na]^+$: 637.1739; found: 637.1697. ^1H NMR (600 M, CD_3OD-d_4): Aglycon: δ = 7.10 (2H, d, J = 7.6 Hz, H-11, 15), 6.69 (2H, d, J = 7.6 Hz, H-12, 14), 2.86 (2H, m, H-9), 2.75 (2H, m, H-8). Glycosyl: δ = 4.60 (1H, d, J = 9.8 Hz, H-1"), 4.51 (1H, d, J = 9.8 Hz, H-1'), 3.82-3.13 (12H, m, Glc); ^{13}C NMR (150 M, CD_3OD-d_4): Aglycon: δ = 197.8 (C-7), 196.6 (C-1), 191.8 (C-3), 185.9 (C-5), 156.5 (C-13), 134.4 (C-10), 130.6 (C-11, 15), 116.2 (C-12, 14), 105.2 (C-2), 100.9 (C-6), 86.0 (C-4), 42.4 (C-8), 32.7 (C-9). Glycosyl: δ = 87.6 (C-1'), 82.1 (C-5'), 81.5 (C-5"), 80.8 (C-3'), 79.9(C-3"), 75.2 (C-1"), 71.6 (C-2"), 70.6 (C-2'), 72.1 (C-4"), 71.5 (C-4'), 62.8 (C-6'), 62.5 (C-6").[1,5]

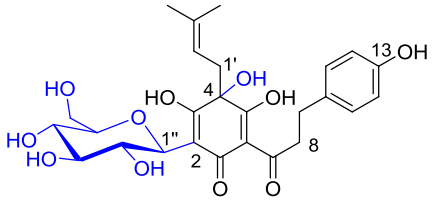

15b

2-*C*-β-D-Glucopyranosyl-4-dimethylally-3,4,5-trihydroxy-6-[3-(4-hydroxyphenyl)-propanoyl]-2,5-cyclohexadien-1-one (15b) (3.1 mg): ESI-MS *m/z* 519.37 $[M-H]^-$; HRMS (ESI^+) calcd. for $C_{26}H_{33}O_{11}$ $[M+H]^+$: 521.2017; found: 521.1976. ^1H NMR (500 M, CD_3OD-d_4): Aglycon: δ = 7.04 (2H, d, J = 8.4 Hz, H-11, 15), 6.65 (2H, d, J = 8.4 Hz, H-12, 14), 5.15 (1H, t, J = 6.8 Hz, H-2'), 2.97 (2H, t, J = 7.8 Hz, H-9), 2.74 (2H, m, H-8), 2.50 (2H, m, H-1'), 1.60 (3H, s, H-4'), 1.49 (3H, s, H-5'). Glycosyl: δ = 4.52 (1H, d, J = 9.9 Hz, H-1"), 3.81-3.18 (6H, m, Glc); ^{13}C NMR (150 M, CD_3OD-d_4): Aglycon: δ = 199.5 (C-7), 194.6 (C-1), 184.7 (C-3), 170.2 (C-5), 156.4 (C-13), 135.7 (C-3'), 134.2 (C-10), 130.4 (C-11, 15), 119.4 (C-2'), 116.0 (C-12, 14), 103.8 (C-6), 100.0 (C-2), 84.7 (C-4), 47.3 (C-8), 32.6 (C-9), 26.1 (C-1'), 21.6 (C-4'), 18.1 (C-5'). Glycosyl: δ = 82.1 (C-5"), 80.9 (C-3"), 75.5 (C-1"), 71.4 (C-2"), 71.3 (C-4"), 62.5 (C-6").[4,5]

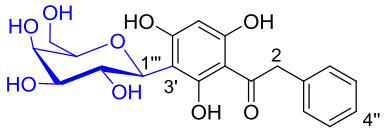

1c

2-Phenyl-3'-(*C*-β-D-galactosyl)-2',4',6'-trihydroxyacetophenone (1c) (2.0 mg): ESI-MS *m/z* 404.98 $[M-H]^-$; HRMS (ESI^+) calcd. for $C_{20}H_{23}O_9$ $[M+H]^+$: 407.1337; found: 407.1320. ^1H NMR (500 M, CD_3OD-d_4): Aglycon: δ= 7.36-7.14 (5H, m, H-2''-6''), 5.85 (1H, s, H-5'), 4.36 (2H, m, H-2). Glycosyl: δ = 4.79 (1H, d, J = 9.8 Hz, H-1'''), 4.02 (1H, t, J = 9.5 Hz, H-2'''), 3.92 (1H, d, J = 3.0 Hz, H-4'''), 3.72 (1H, dd, J = 11.5, 6.9 Hz, H-6'''a), 3.66 (1H, dd, J = 11.5, 5.0 Hz, H-6'''b), 3.59 (1H, dd, J = 6.9, 5.0 Hz, H-5'''), 3.52 (1H, dd, J = 9.5, 3.0 Hz, H-3'''); ^{13}C NMR (125 M, CD_3OD-d_4): Aglycon: δ = 204.7 (C=O), 164.9 (C-4'), 164.9 (C-2'), 164.4 (C-6'), 137.3 (C-1''), 130.8 (C-2'', 6''), 129.2 (C-3'', 5''), 127.4 (C-4''), 105.4 (C-3'), 105.0 (C-1'), 96.5 (C-5'), 50.7 (C-2). Glycosyl: δ = 80.8 (C-5'''), 76.3 (C-3'''), 76.3 (C-1'''), 71.5 (C-2'''), 70.6 (C-4'''), 62.9 (C-6''').[2,6]

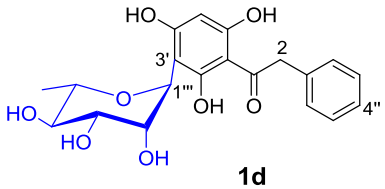

1d

2-Phenyl-3'-(*C*-α-L-rhamnosyl)-2',4',6'-trihydroxyacetophenone (1d) (1.4 mg): ESI-MS *m/z* 389.29 $[M-H]^-$; HRMS (ESI^+) calcd. for $C_{20}H_{23}O_8$ $[M+H]^+$: 391.1387; found: 391.1351. ^1H NMR (500 M, CD_3OD-d_4): Aglycon: δ = 7.24-7.16 (5H, m, H-2''-6''), 5.79 (1H, s, H-5'), 4.39 (1H, d, J = 15.5 Hz, H-2a), 4.31 (1H, d, J = 15.5 Hz, H-2b). Glycosyl: δ = 5.00 (1H, d, J = 0.9 Hz, H-1'''), 3.93 (1H, d, J = 3.2 Hz, H-2'''), 3.52 (1H, dd, J = 9.3, 3.2 Hz, H-3'''), 3.43 (1H, t, J = 9.3 Hz, H-4'''), 3.35 (1H, m, H-5'''), 1.33 (3H, d, J = 6.0 Hz, H-6'''); ^{13}C NMR (125 M, CD_3OD-d_4): Aglycon: δ = 204.7 (C=O), 164.1 (C-4'), 164.0 (C-2'), 162.5 (C-6'), 137.4 (C-1''), 130.8 (C-2'', 6''), 129.2 (C-3'', 5''), 127.4 (C-4''), 105.3 (C-3'), 103.4 (C-1'), 96.1 (C-5'), 50.6 (C-2). Glycosyl: δ = 78.7 (C-5'''), 77.8 (C-3'''), 75.7 (C-1'''), 73.8 (C-2'''), 73.5 (C-4'''), 18.4 (C-6''').[2,7]

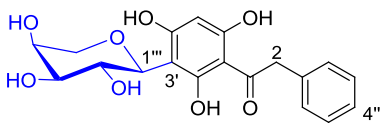

1e

2-Phenyl-3'-(*C*-α-L-arabinosyl)-2',4',6'-trihydroxyacetophenone (1e) (1.1 mg): ESI-MS *m/z* 375.06 $[M-H]^-$; HRMS (ESI^+) calcd. for $C_{19}H_{21}O_8$ $[M+H]^+$: 377.1231; found: 377.1193. ^1H NMR (500 M, CD_3OD-d_4): Aglycon: δ = 7.30-7.20 (5H, m, H-2''-6''), 5.91 (1H, s, H-5'), 4.40 (2H, m,

H-2). Glycosyl: δ = 4.75 (1H, d, *J* = 9.8 Hz, H-1'''), 4.10 (1H, t, *J* = 9.6 Hz, H-2'''), 4.00 (1H, d, *J* = 12.3 Hz, H-5'''a), 3.96 (1H, m, H-4'''), 3.69 (1H, d, *J* = 12.3 Hz, H-5'''b), 3.59 (1H, dd, *J* = 9.3, 2.9 Hz, H-3'''); ^{13}C NMR (150 M, CD_3OD-d_4): Aglycon: δ = 204.7 (C=O), 170.2 (C-4'), 165.2 (C-2'), 164.4 (C-6'), 137.4 (C-1''), 130.7 (C-2'', 6''), 129.2 (C-3'', 5''), 127.4 (C-4''), 105.4 (C-3'), 104.7 (C-1'), 95.7 (C-5'). Glycosyl: δ = 76.9 (C-3'''), 75.8 (C-1'''), 71.8 (C-5'''), 71.3 (C-2'''), 70.6 (C-4''').[8]

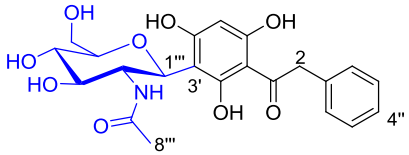

1f

2-Phenyl-3'-(*C*-β-D-*N*-acetylglucosaminyl)-2',4',6'-trihydroxyacetophenone (1f) (1.5 mg): ESI-MS *m/z* 446.17 $[M-H]^-$; HRMS (ESI^+) calcd. for $C_{22}H_{26}NO_9$ $[M+H]^+$: 448.1602; found: 448.1561. ^{1}H NMR (600 M, CD_3OD-d_4): Aglycon: δ = 7.30-7.18 (5H, m, H-2''-6''), 4.35 (2H, m, H-2). Glycosyl: δ = 4.92 (1H, d, *J* = 10.3 Hz, H-1'''), 3.86 (1H, d, *J* = 11.7 Hz, H-2'''), 3.78 (1H, dd, *J* = 12.1, 4.8 Hz, H-6'''a), 3.53-3.42 (3H, m, H-3'''-5'''), 3.39 (1H, m, H-6'''b), 1.68 (3H, s, H-8'''); ^{13}C NMR (150 M, CD_3OD-d_4): Aglycon: δ = 204.8 (C=O), 167.1 (C-4'), 165.3 (C-2'), 163.2 (C-6'), 137.4 (C-1''), 130.7 (C-2'', 6''), 129.2 (C-3'', 5''), 127.4 (C-4''), 103.8 (C-3'), 102.2 (C-1'), 49.6 (C-2). Glycosyl: δ = 173.2 (C-7'''), 82.7 (C-5'''), 77.3 (C-3'''), 75.1 (C-1'''), 71.8 (C-4'''), 62.4 (C-6'''), 55.7 (C-2'''), 22.6 (C-8''').[2,9]

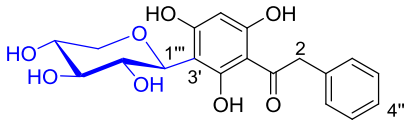

1g

2-Phenyl-3'-(*C*-β-D-xylosyl)-2',4',6'-trihydroxyacetophenone (1g) (3.2 mg): ESI-MS *m/z* 375.08 $[M-H]^-$; HRMS (ESI^+) calcd. for $C_{19}H_{21}O_8$ $[M+H]^+$: 377.1231; found: 377.1195. ^{1}H NMR (500 M, CD_3OD-d_4): Aglycon: δ = 7.29-7.19 (5H, m, H-2''-6''), 5.94 (1H, s, H-5'), 4.41 (2H, m, H-2). Glycosyl: δ = 4.74 (1H, d, *J* = 9.9 Hz, H-1'''), 4.09 (1H, t, *J* = 9.2 Hz, H-2'''), 3.97 (1H, t, *J* = 5.5 Hz, H-5'''a), 3.63 (1H, m, H-4'''), 3.38 (1H, m, H-3'''), 3.28 (1H, m, H-5'''b); ^{13}C NMR (150 M, CD_3OD-d_4): Aglycon: δ = 204.8 (C=O), 166.5 (C-4'), 165.4 (C-2'), 163.8 (C-6'), 137.4 (C-1''), 130.7 (C-2'', 6''), 129.2 (C-3'', 5''), 127.4 (C-4''), 105.3 (C-3'), 104.2 (C-1'), 95.7 (C-5'). Glycosyl: δ = 80.3 (C-3'''), 76.7 (C-1'''), 72.7 (C-2'''), 71.5 (C-5'''), 71.5 (C-4''').[2,8]

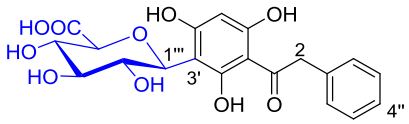

1h

2-Phenyl-3'-(*C*-β-D-glucuronyl)-2',4',6'-trihydroxyacetophenone (1h) (0.5 mg): ESI-MS *m/z* 419.21 $[M-H]^-$; HRMS (ESI^+) calcd. for $C_{20}H_{21}O_{10}$ $[M+H]^+$: 421.1186; found: 421.1150. ^1H NMR (600 M, CD_3OD-d_4): Aglycon: δ = 7.27-7.18 (5H, m, H-2"-6"), 5.92 (1H, s, H-5'), 4.38 (2H, m, H-2). Glycosyl: δ = 4.84 (1H, d, J = 10.1 Hz, H-1'''), 4.16 (1H, t, J = 9.4 Hz, H-2'''), 3.90 (1H, d, J = 9.8 Hz, H-5'''), 3.64 (1H, t, J = 9.4 Hz, H-3'''), 3.43 (1H, m, H-4'''); ^{13}C NMR (150 M, CD_3OD-d_4): Aglycon: δ = 204.7 (C=O), 166.7 (C-4'), 165.5 (C-2'), 163.9 (C-6'), 137.4 (C-1"), 130.7 (C-2", 6"), 129.2 (C-3", 5"), 127.4 (C-4"), 105.3 (C-3'), 103.7 (C-1'), 95.7 (C-5'), 52.7 (C-2). Glycosyl: δ = 171.4 (COO), 81.0 (C-5'''), 79.4 (C-3'''), 76.3 (C-1'''), 73.4 (C-2'''), 72.3 (C-4''').[2,10]

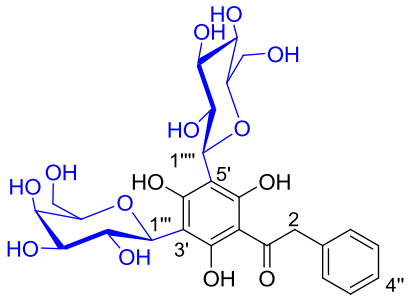

1ca

2-Phenyl-3'-(*C*-β-D-galactosyl)-5'-(*C*-β-D-glucosyl)-2',4',6'-trihydroxyacetophenone (1ca) (6.6 mg): ESI-MS *m/z* 567.42 $[M-H]^-$; HRMS (ESI^+) calcd. for $C_{26}H_{33}O_{14}$ $[M+H]^+$: 569.1865; found: 569.1836. ^1H NMR (400 M, CD_3OD-d_4): Aglycon: δ= 7.28-7.17 (5H, m, H-2"-6"), 4.43 (2H, m, H-2). Glycosyl: δ = 4.94 (1H, d, J = 9.8 Hz, H-1''''), 4.88 (1H, d, J = 9.9 Hz, H-1'''), 4.00-3.42 (12H, m, Glc, Gal); ^{13}C NMR (150 M, CD_3OD-d_4): Aglycon: δ = 205.3 (C=O), 163.3 (C-4'), 163.1 (C-2'), 162.6 (C-6'), 137.1 (C-1"), 130.8 (C-2", 6"), 129.2 (C-3", 5"), 127.5 (C-4"), 105.9 (C-5'), 105.1 (C-3'), 104.3 (C-1'), 51.0 (C-2). Glycosyl: δ = 82.7-61.9 (12C, C-1'''-6''', 1''''-6'''').[2,6]

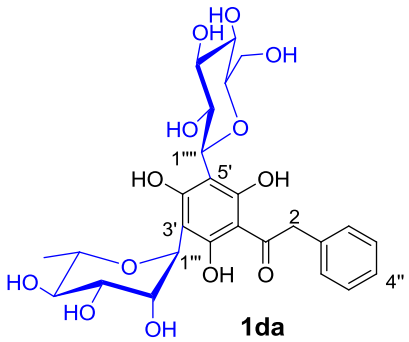

1da

2-Phenyl-3'-(*C*-α-L-rhamnosyl)-5'-(*C*-β-D-glucosyl)-2',4',6'-trihydroxyacetophenone (1da) (1.7 mg): ESI-MS *m/z* 551.31 $[M-H]^-$; HRMS (ESI^+) calcd. for $C_{26}H_{33}O_{13}$ $[M+H]^+$: 553.1876; found: 553.1851. ^1H NMR (400 M, CD_3OD-d_4): Aglycon: δ = 7.29-7.18 (5H, m, H-2"-6"), 4.41 (2H, m, H-2). Glycosyl: δ = 5.09 (1H, d, J = 0.8 Hz, H-1'''), 4.94 (1H, d, J = 9.8 Hz, H-1''''), 3.99-3.37 (10H, m, Glc, Rha), 1.37 (3H, d, J = 6.0 Hz, H-6'''); ^{13}C NMR (150 M, CD_3OD-d_4): Aglycon: δ = 205.3 (C=O), 168.8 (C-4'), 163.2 (C-2'), 162.8 (C-6'), 137.2 (C-1"), 130.9 (C-2", 6"), 129.2 (C-3", 5"), 127.4 (C-4"), 105.7 (C-5'), 104.1 (C-3'), 103.8 (C-1'), 50.9 (C-2). Glycosyl: δ = 82.6-61.8 (11C, C-1'''-5''', 1''''-6''''), 18.4 (C-6''').[2,7]

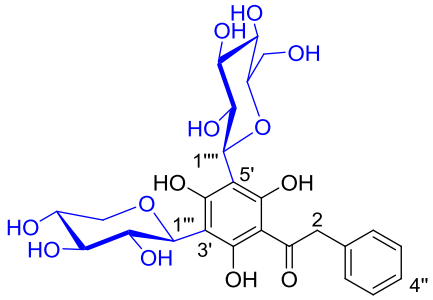

1ga

2-Phenyl-3'-(*C*-β-D-xylosyl)-5'-(*C*-β-D-glucosyl)-2',4',6'-trihydroxyacetophenone (1ga) (2.7 mg): ESI-MS *m/z* 537.15 $[M-H]^-$; HRMS (ESI^+) calcd. for $C_{25}H_{31}O_{13}$ $[M+H]^+$: 539.1759; found: 539.1717. ^1H NMR (400 M, CD_3OD-d_4): Aglycon: δ = 7.26-7.21 (5H, m, H-2"-6"), 4.40 (1H, m, H-2). Glycosyl: δ = 4.95 (1H, d, J = 9.7 Hz, H-1''''), 4.74 (1H, d, J = 11.7 Hz, H-1'''), 4.11-3.37 (13H, m, Glc, Xyl); ^{13}C NMR (150 M, CD_3OD-d_4): Aglycon: δ = 205.4 (C=O), 163.8 (C-4'), 163.2 (C-2'), 162.7 (C-6'), 137.0 (C-1"), 130.8 (C-2", 6"), 129.2 (C-3", 5"), 127.5 (C-4"), 106.1 (C-5'), 104.4 (C-3'), 104.4 (C-1'), 49.6 (C-2). Glycosyl: δ = 82.7-61.8 (11C, C-1'''-5''', 1''''-6'''').[2,8]

2. Supporting Tables

Table S1. Oligo-nucleotide primers used in the construction of chimeras library. The nucleotides in bold were the corresponding mutant sites. Chimeric genes were amplified by PCR using pET28a-MiCGTb or MiCGT as templates.

Mutants	Mutations	Primers (5′→3′)
MiCGTb-A	S60L, F62L, A64D	F: CTCT**CTT**CTC**CTC**TCT**GAT**TTTCCTCAGATCAC
		R: AATCAGAGAGGAGAAGAGAGATTGCTCGAGACTCGG
MiCGTb-B	V100A, T104N	F: CGCCGTTCA**GCT**CACCTTCTT**AAT**CCTCTCCTCTCT
		R: GATTAAGAAGGTGAGCTGAACGGCGAATAGCTTCCC
MiCGTb-C	I117L, T119I,	F: GCT**CTT**GTC**ATT**GAT**TCT**AGTTTG**GTT**TCCTCTGTTGTTCC
	T121S, I124V	R: CCAAACTAGAATCAATGACAAGAGCAGAGAGAGAAGGAGA
MiCGTb-D	I152E, A154T	F: TCTC**GAG**GAG**ACT**TTCCCAGCTTTTGTTGCATC
		R: GGGAAAGTCTCCTCGAGAGAACACATTCTG
MiCGTb-E	A225G, D226G,	F: AA**GGCGGC**ATC**CTTCCC**GGGATTAATGACAAAAG
	P228L, L229P	R: CCCGGGAAGGATGCCGCCTTCTAGTGCTTCAAATG
MiCGT-A	L60S, L62F, D64A	F: CT**AGT**CTC**TTC**TCT**GCT**TTTCCTCAGATCAC
		R: AAGCAGAGAAGAGACTAGAGATTGCTCGAGAC
MiCGT-B	A100V, N104T	F: CA**GTT**CACCTTCTC**ACT**CCTCTCCTCTCTTCC
		R: GGAGTGAGAAGGTGAACTGAACGGCGAATAGC
MiCGT-C	L117I, I119T,	F: GCT**ATT**GTC**ACA**GAT**ACT**AGTTTG**ATT**TCCTCTTTTGTTCC
	S121T, V124I	R: AAATCAAACTAGTATCTGTGACAATAGCAGAGAGAGGAGG
MiCGT-D	E152I, T154A	F: TCTC**ATC**GAG**GCT**TTCCCAGCTTTTGTTGC
		R: GAAAGCCTCGATGAGAGAACACATTCTGGT
MiCGT-E	G225A, G226D,	F: A**GCCGAC**ATC**CCGCTT**GGGATTAATGACAAAAGAG
	L228P, P229L	R: CCAAGCGGGATGTCGGCTTCTAGTGCTTCAAATGT
MiCGTb-S60L	S60L	AGTCTCGAGCAATCTCT**CTT**CTCTTCTCTG
		AAGAGAGATTGCTCGAGACTCGGCAACCGAAAC
MiCGTb-F62L	F62L	AGCAATCTCTAGTCTC**CTC**TCTGCTTTTCC
		AGAGGAGACTAGAGATTGCTCGAGACTCGG
MiCGTb-A64D	A64D	CTCTAGTCTCTTCTCT**GAT**TTTCCTCAGATCAC
		AATCAGAGAAGAGACTAGAGATTGCTCGAGACT
MiCGTb-V100A	V100A	F: GCTATTCGCCGTTCA**GCT**CACCTTCTCACT
		R: AGCTGAACGGCGAATAGCTTCCCACCGGAG
MiCGTb-T104N	T104N	F: TTCAGTTCACCTTCTC**AAT**CCTCTCCTCTC
		R: GATTGAGAAGGTGAACTGAACGGCGAATAG
MiCGTb-I152E	I152E	F: CAGAATGTGTTCTCTC**GAG**GAGGCTTTCCC
		R: TCCTCGAGAGAACACATTCTGGTTGATGAT
MiCGTb-A154T	A154T	F: TGTGTTCTCTCATCGAG**ACT**TTCCCAGCTT
		R: GTCTCGATGAGAGAACACATTCTGGTTGAT
MiCGT-E152I	E152I	F: CAGAATGTGTTCTCTC**ATC**GAGACTTTCCCAGC
		R: CGATGAGAGAACACATTCTGGTTGATGATGTGA
MiCGT-T154A	T154A	F: TGTGTTCTCTCGAGGAG**GCT**TTCCCAGCTT
		R: GCCTCCTCGAGAGAACACATTCTGGTTGAT
MiCGTb-S60	Site-saturation	CGAGTCTCGAGCAATCTCT**NNK**CTCTTCTCTGCTT
	mutagenesis	GMNNAGAGATTGCTCGAGACTCGGCAACCGAAACA
MiCGTb-V100	Site-saturation	GAAGCTATTCGCCGTTCA**NNK**CACCTTCTCACTCC
	mutagenesis	GGTGMNNTGAACGGCGAATAGCTTCCCACCGGAGG
MiCGTb-T104	Site-saturation	GTTCAGTTCACCTTCTC**NNK**CCTCTCCTCTCTTCC
	mutagenesis	GMNNGAGAAGGTGAACTGAACGGCGAATAGCTTCC
MiCGT-E152	Site-saturation	CAGAATGTGTTCTCTC**NNK**GAGACTTTCCC
	mutagenesis	CMNNGAGAGAACACATTCTGGTTGATGATG

Table S2. Seven MiCGT mutants at position 152 with high bis-*C*-glycosylation activity. The reactions were assayed with **1** as an acceptor and UDP-α-D-glucose (UDP-Glc) as a donor at 30 ℃ and pH 9.0.

Mutants	**Relative activity (%)**
MiCGTb	100
MiCGT-E152I	276.1±2.9
MiCGT-E152M	280.5±5.9
MiCGT-E152V	195.7±5.9
MiCGT-E152N	201.3±2.9
MiCGT-E152T	98.0±5.9
MiCGT-E152A	105.1±5.9
MiCGT-E152L	193.4±5.9

Table S3. Quadruple mutants of MiCGTb at position 60/100/104/152.

Mutants	Mutations
MiCGTb-GANM	S60G/V100A/T104N/I152M
MiCGTb-GAGM	S60G/V100A/T104G/I152M
MiCGTb-GSNM	S60G/V100S/T104N/I152M
MiCGTb-GSGM	S60G/V100S/T104G/I152M
MiCGTb-KANM	S60K/V100A/T104N/I152M
MiCGTb-KAGM	S60K/V100A/T104G/I152M
MiCGTb-KSNM	S60K/V100S/T104N/I152M
MiCGTb-KSGM	S60K/V100S/T104G/I152M

Table S4. Determination of kinetic parameters of MiCGTb and MiCGT variants for *C*-glycosylation. The kinetic parameters of the first *C*-glycosylation were assayed with **1** as an acceptor and UDP-Glc as a donor at 30 ℃ and pH 9.0. The kinetic parameters of the second *C*-glycosylation were assayed with mono-*C*-glucosides (**1b**) as acceptors and UDP-Glc as a donor at 30 ℃ and pH 9.0.

	2-Phenyl-2',4',6'-trihydroxyacetophenone (1)			**2-Phenyl-3'-(C-β-D-glucosyl)-2',4',6'-trihydroxyacetophenone (1b)**		
Mutants	K_m **(μM)**	k_{cat} **(min^{-1})**	k_{cat}/K_m **(M^{-1}min^{-1})**	K_m **(μM)**	k_{cat} **(min^{-1})**	k_{cat}/K_m **(M^{-1}min^{-1})**
MiCGTb	101±2.3	55.8±3.2	5.5×10^{5}	211.7±0.6	$(3.8\pm0.5)\times10^{-2}$	1.8×10^{2}
MiCGTb-GANM	83.2±2.3	32.8±1.7	3.9×10^{5}	219.7±1.5	$(4.6\pm0.9)\times10^{-2}$	2.1×10^{2}
MiCGTb-GAGM	78.1±1.9	34.9±2.1	4.5×10^{5}	354.7±5.2	0.13±0.1	3.6×10^{2}
MiCGTb-GSNM	36.6±2.1	19.2±2.3	5.3×10^{5}	213.8±2.4	$(5.8\pm0.3)\times10^{-2}$	2.7×10^{2}
MiCGTb-GSGM	189.5±3.4	50.7±1.5	2.7×10^{5}	227.6±1.8	$(9.5\pm1.1)\times10^{-2}$	4.2×10^{2}
MiCGTb-KANM	163.0±3.2	50.7±1.7	3.1×10^{5}	231.6±4.1	$(9.5\pm0.7)\times10^{-2}$	4.1×10^{2}
MiCGTb-KAGM	175.0±7.1	55.8±1.3	3.2×10^{5}	217.3±1.5	$(9.7\pm1.1)\times10^{-2}$	4.5×10^{2}
MiCGTb-KSNM	147.6±2.9	50.7±1.6	3.4×10^{5}	219.2±3.9	$(8.0\pm0.7)\times10^{-2}$	3.7×10^{2}
MiCGTb-KSGM	40.8±1.6	24.3±2.1	5.9×10^{5}	214.7±3.2	0.12±0.1	5.7×10^{2}
MiCGT-E152I	301.0±6.8	139.3±2.1	4.6×10^{5}	101.4±2.4	$(4.2\pm0.3)\times10^{-2}$	4.1×10^{2}
MiCGT-E152M	239.8±3.4	111.4±2.3	4.6×10^{5}	173.6±5.4	0.18±0.1	1.0×10^{3}
MiCGT-E152V	73.3±1.3	37.1±1.2	5.1×10^{5}	143.5±3.7	$(4.9\pm0.4)\times10^{-2}$	3.4×10^{2}
MiCGT-E152N	44.4±1.3	46.4±2.1	1.0×10^{6}	74.0±2.5	$(2.7\pm0.3)\times10^{-2}$	3.7×10^{2}
MiCGT-E152T	147.4±6.4	61.9±1.5	4.2×10^{5}	61.8±1.3	$(1.2\pm0.1)\times10^{-2}$	1.9×10^{2}
MiCGT-E152A	20.7±1.2	13.9±0.3	6.7×10^{5}	36.8±2.4	$(1.8\pm0.2)\times10^{-2}$	4.8×10^{2}
MiCGT-E152L	360.5±7.8	278.5±3.7	7.7×10^{5}	176.8±4.5	$(4.9\pm0.3)\times10^{-2}$	2.8×10^{2}

Table S5. Determination of kinetic parameters of MiCGTb-GAGM towards different sugar donors. The kinetic parameters of sugar donors were assayed with **1** as an acceptor at 30 ℃ and pH 9.0.

Sugar donors	K_m **(μM)**	k_{cat} **(min^{-1})**	k_{cat}/K_m **(M^{-1}min^{-1})**
UDP-α-D-glucose (**16**)	42.4 ±1.3	2.8 ±0.4	6.6×10^{4}
UDP-α-D-galactose (**18**)	236.8 ±12.7	$(9.2\pm1.2)\times10^{-2}$	388.9
UDP-β-L-rhamnose (**19**)	304.6 ±11.8	$(1.1\pm0.05)\times10^{-2}$	35.5
UDP-α-D-*N*-acetyl-glucosamine (**21**)	116.6 ±7.9	$(1.4\pm0.03)\times10^{-2}$	117.8
UDP-α-D-glucuronic acid (**23**)	76.5 ±2.7	$(5.4\pm0.9)\times10^{-3}$	70.5

3. Supporting Figures

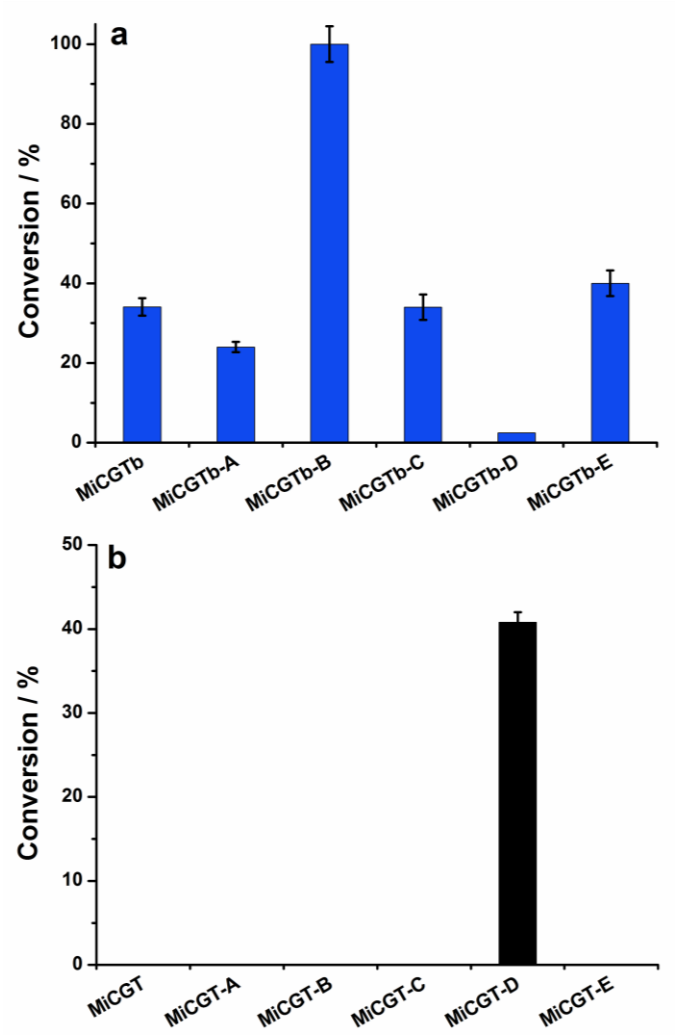

Figure S1. Percent conversion of **1a** by the MiCGTb–MiCGT chimeras through region swapping. (**a**) MiCGTb mutants; (**b**) MiCGT mutants. The above reactions were tested with **1** as an acceptor and UDP-Glc as a sugar donor at 30 ℃ and pH 9.0 for 12 h.

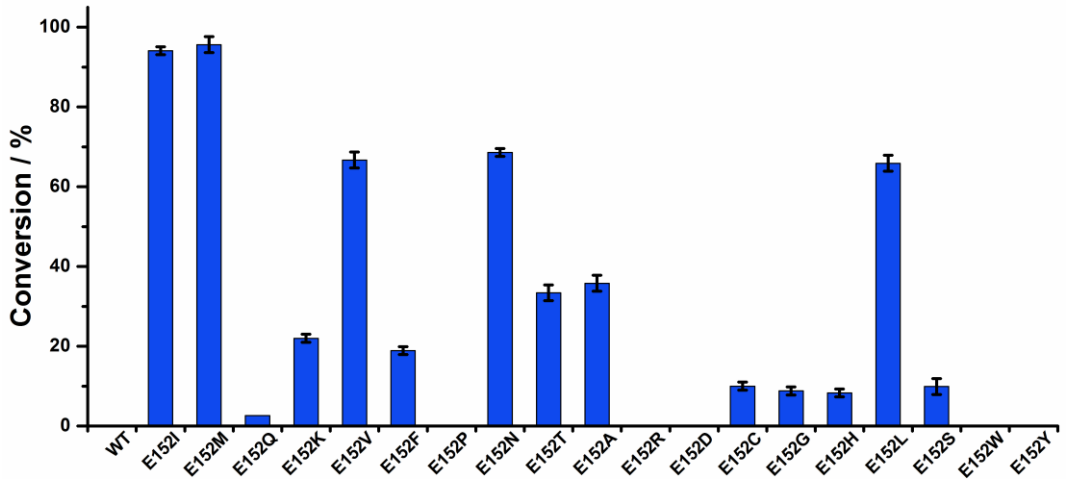

Figure S2. Percent conversion of **1a** by the site-saturation mutants of MiCGT at site 152. The residue 152 of MiCGT was substituted by other 19 amino acids by PCR using pET28a-MiCGT as templates. The above reactions were tested with **1** as an acceptor and UDP-Glc as a sugar donor at 30 ℃ and pH 9.0 for 12 h. WT: wild type.

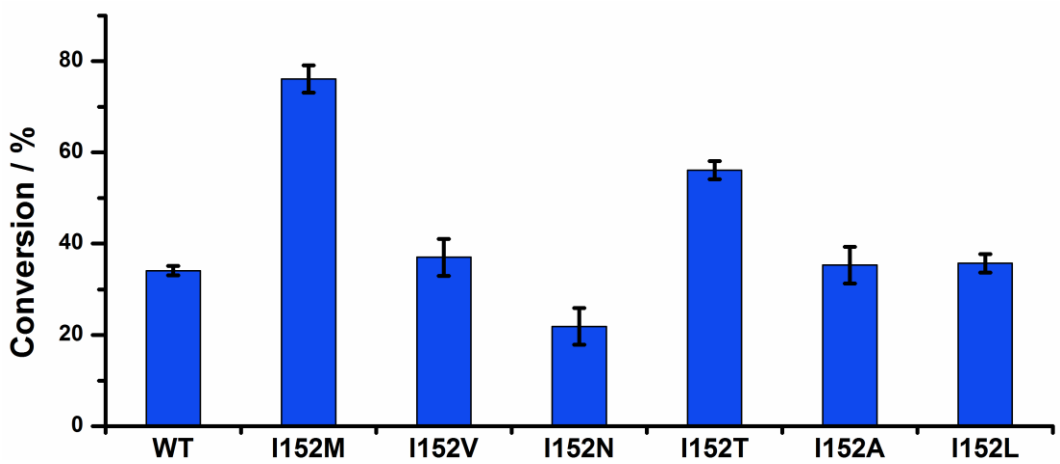

Figure S3. Percent conversion of **1a** by the MiCGTb mutants at site 152. The residue 152 of MiCGTb was substituted by methionine, valine, asparagine, threonine, alanine and leucine by PCR using pET28a-MiCGTb as templates. The above reactions were tested with **1** as an acceptor and UDP-Glc as a sugar donor at 30 ℃ and pH 9.0 for 12 h. WT: wild type.

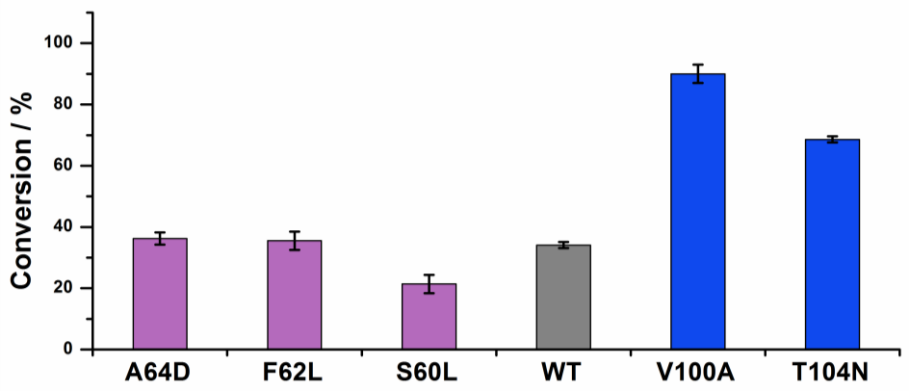

Figure S4. Percent conversion of **1a** by the MiCGTb mutants with single amino acid exchanges in A and B region of MiCGT. The above reactions were tested with **1** as an acceptor and UDP-Glc as a sugar donor at 30 ℃ and pH 9.0 for 12 h. WT: wild type.

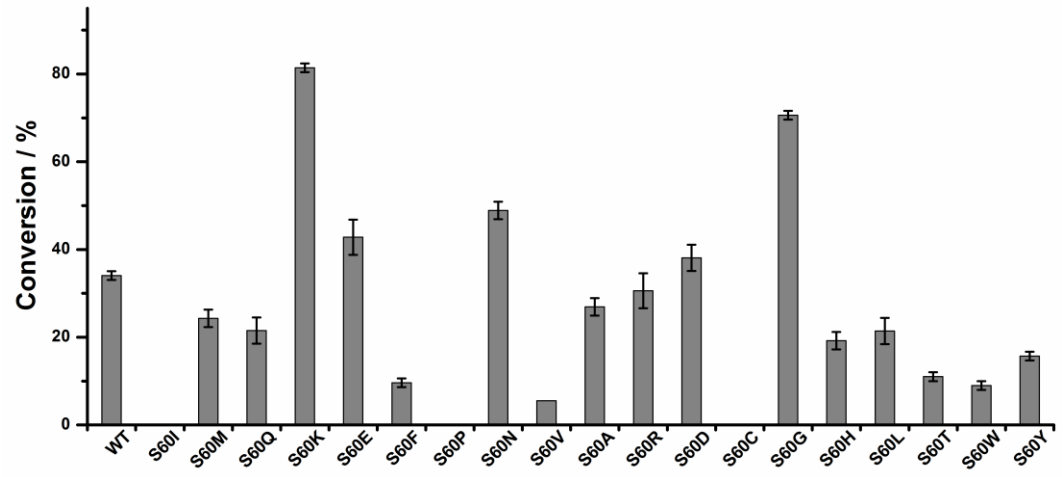

Figure S5. Percent conversion of **1a** by the site-saturation mutants of MiCGTb at site 60. The residue 60 of MiCGTb was substituted by other 19 amino acid by PCR using pET28a-MiCGTb as templates. The above reactions were tested with **1** as an acceptor and UDP-Glc as a sugar donor at 30 ℃ and pH 9.0 for 8 h. WT: wild type.

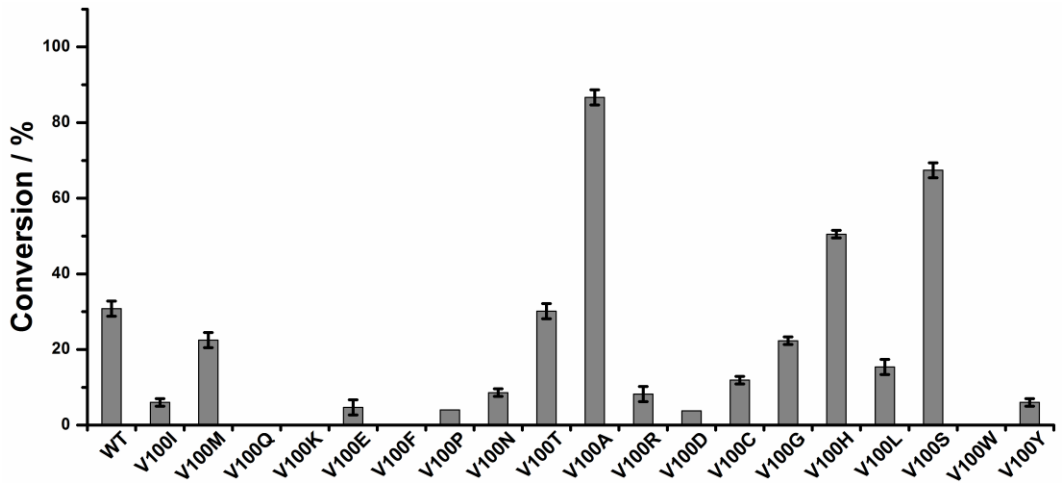

Figure S6. Percent conversion of **1a** by the site-saturation mutants of MiCGTb at site 100. The site 100 of MiCGTb was substituted by other 19 amino acid by PCR using pET28a-MiCGTb as templates. The above reactions were tested with **1** as an acceptor and UDP-Glc as a sugar donor at 30 ℃ and pH 9.0 for 8 h. WT: wild type.

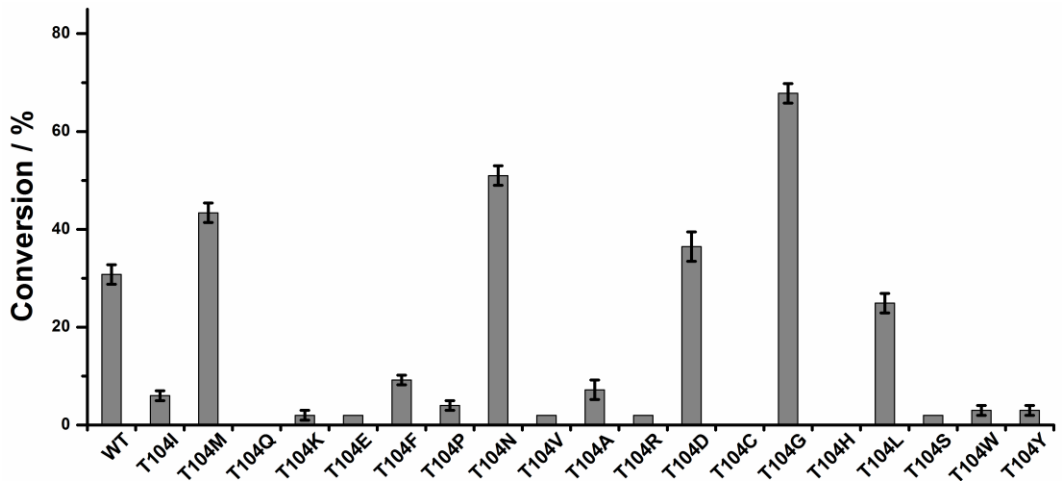

Figure S7. Percent conversion of **1a** by the site-saturation mutants of MiCGTb at site 104. The site 104 of MiCGTb was substituted by other 19 amino acid by PCR using pET28a-MiCGTb as templates. The above reactions were tested with **1** as an acceptor and UDP-Glc as a sugar donor at 30 ℃ and pH 9.0 for 8 h. WT: wild type.

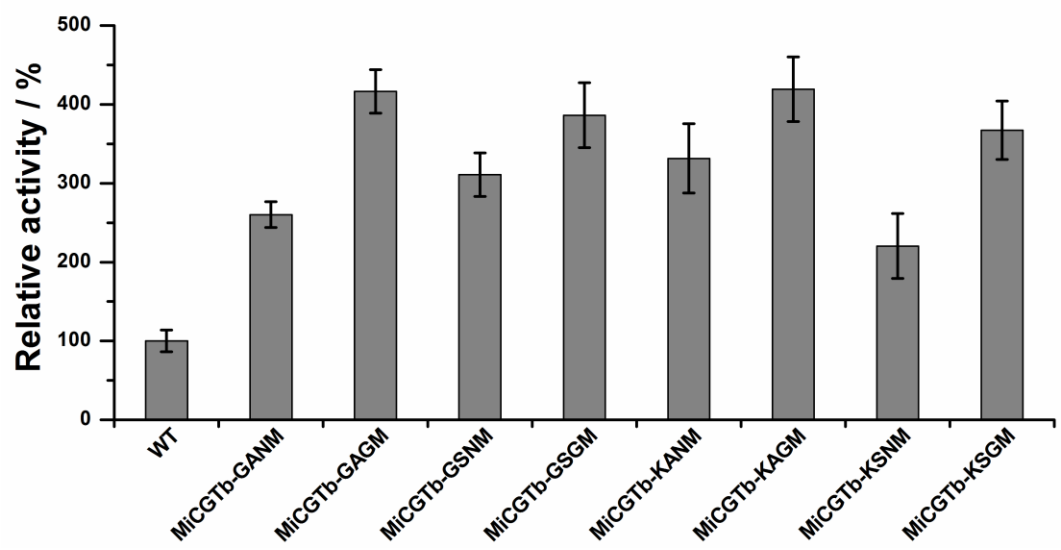

Figure S8. Relative activity of the quadruple-mutants of MiCGTb for bis-*C*-glycosylation. The above reactions were tested with **1** as an acceptor and UDP-Glc as a sugar donor at 30 ℃ and pH 9.0 for 60 min. WT: wild type.

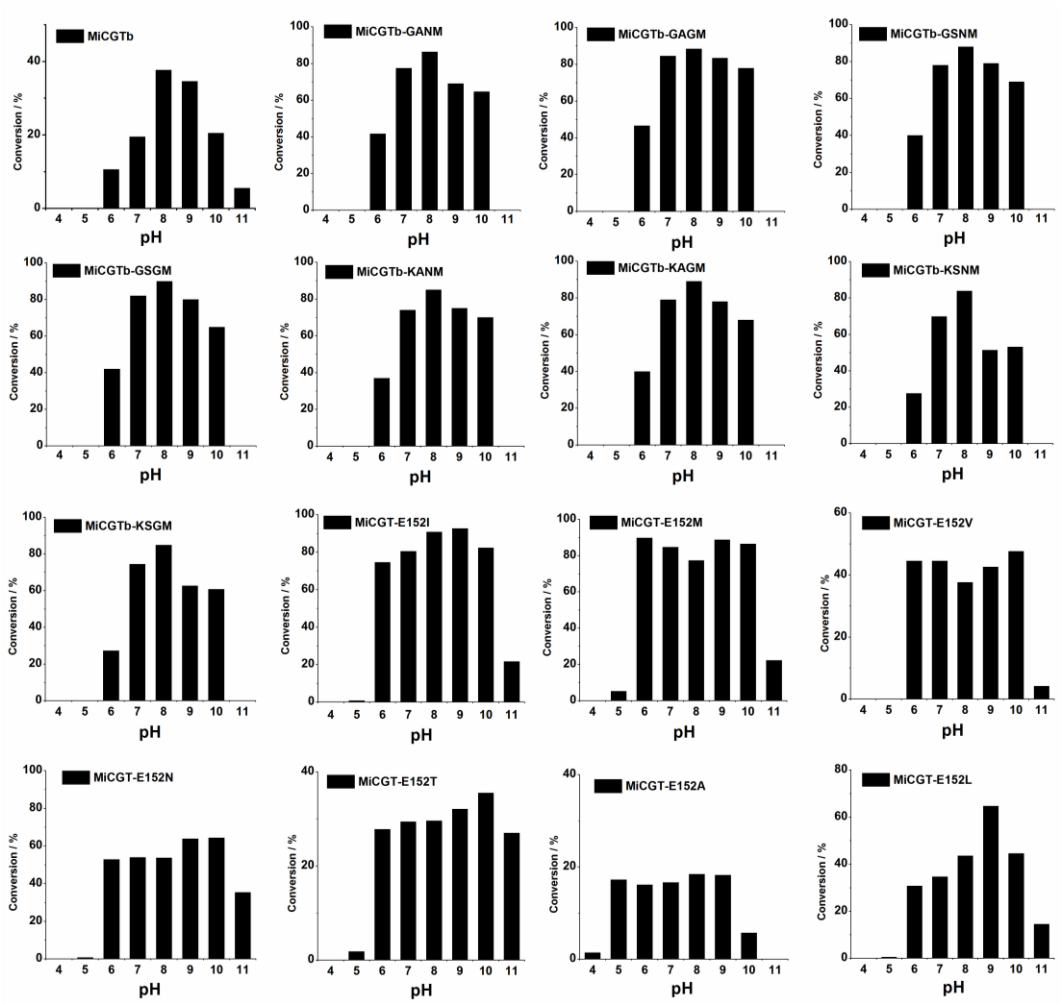

Figure S9. Effects of pH values on the conversion of **1a** by CGT mutants. The above reactions were conducted by using UDP-Glc as a sugar donor and **1** as an acceptor at 30 ℃ for 12 h.

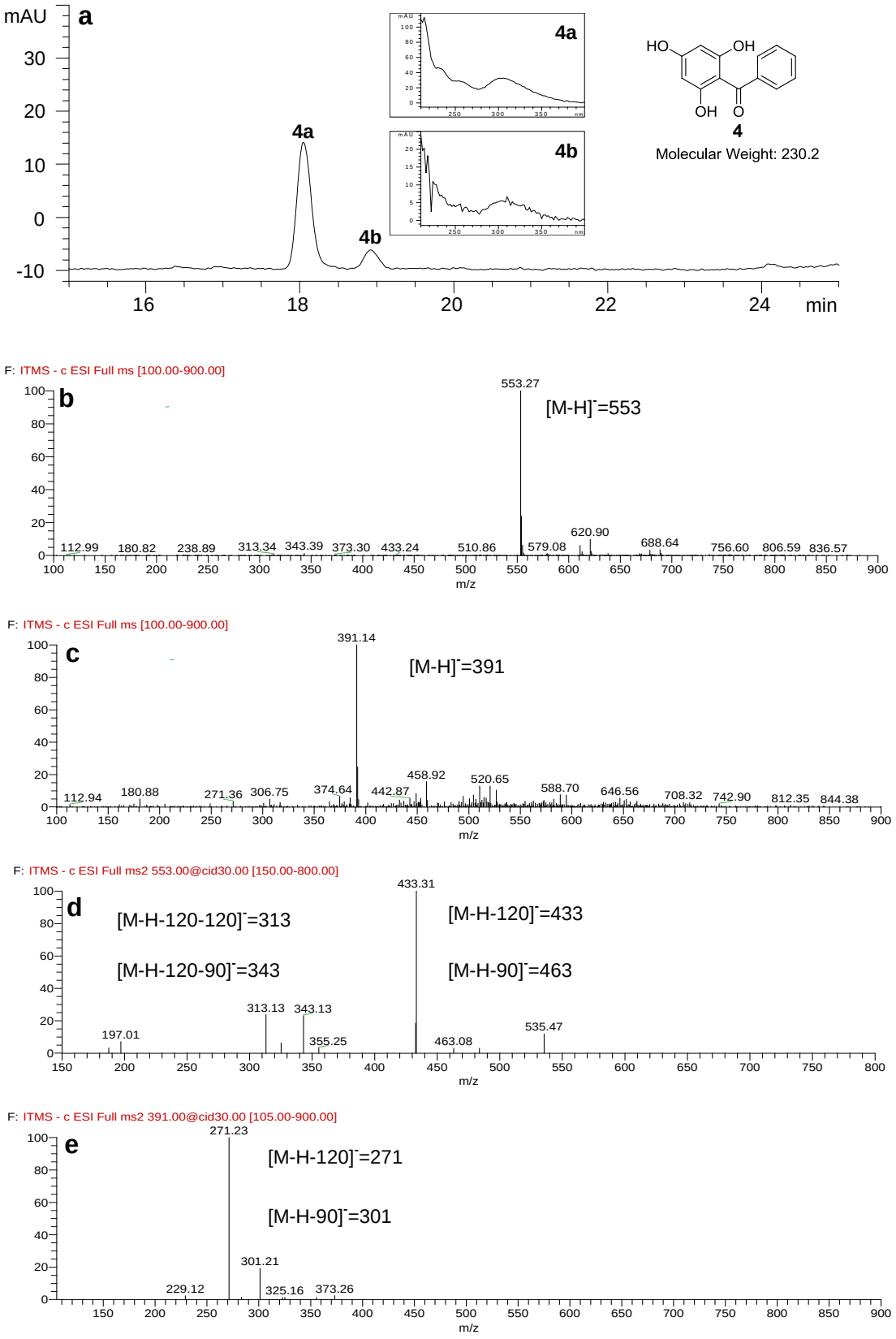

Figure S10. HPLC-DAD/ESI-MS analyses of *C*-glucosylated products by using **4** as an acceptor. (**a**) HPLC chromatogram and UV spectra of **4** and enzymatic products **4a** and **4b**; (**b**) and (**c**) Typical negative ion MS spectra for **4a** and **4b**; (**d**) and (**e**) Typical negative ion MS^2 spectra for **4a** and **4b**.

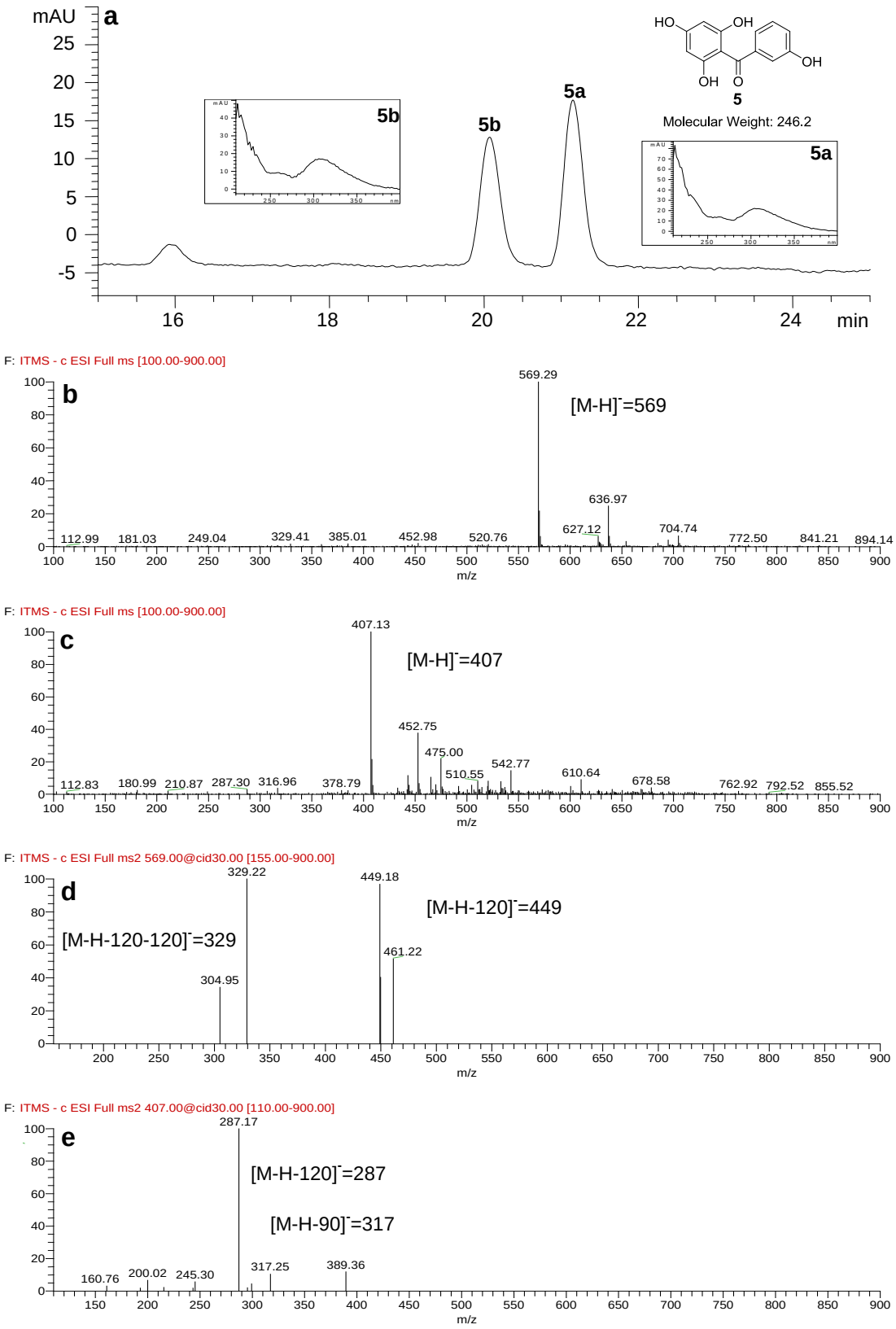

Figure S11. HPLC-DAD/ESI-MS analyses of *C*-glucosylated products by using **5** as an acceptor. (**a**) HPLC chromatogram and UV spectra of **5** and enzymatic products **5a** and **5b**; (**b**) and (**c**) Typical negative ion MS spectra for **5a** and **5b**; (**d**) and (**e**) Typical negative ion MS^2 spectra for **5a** and **5b**.

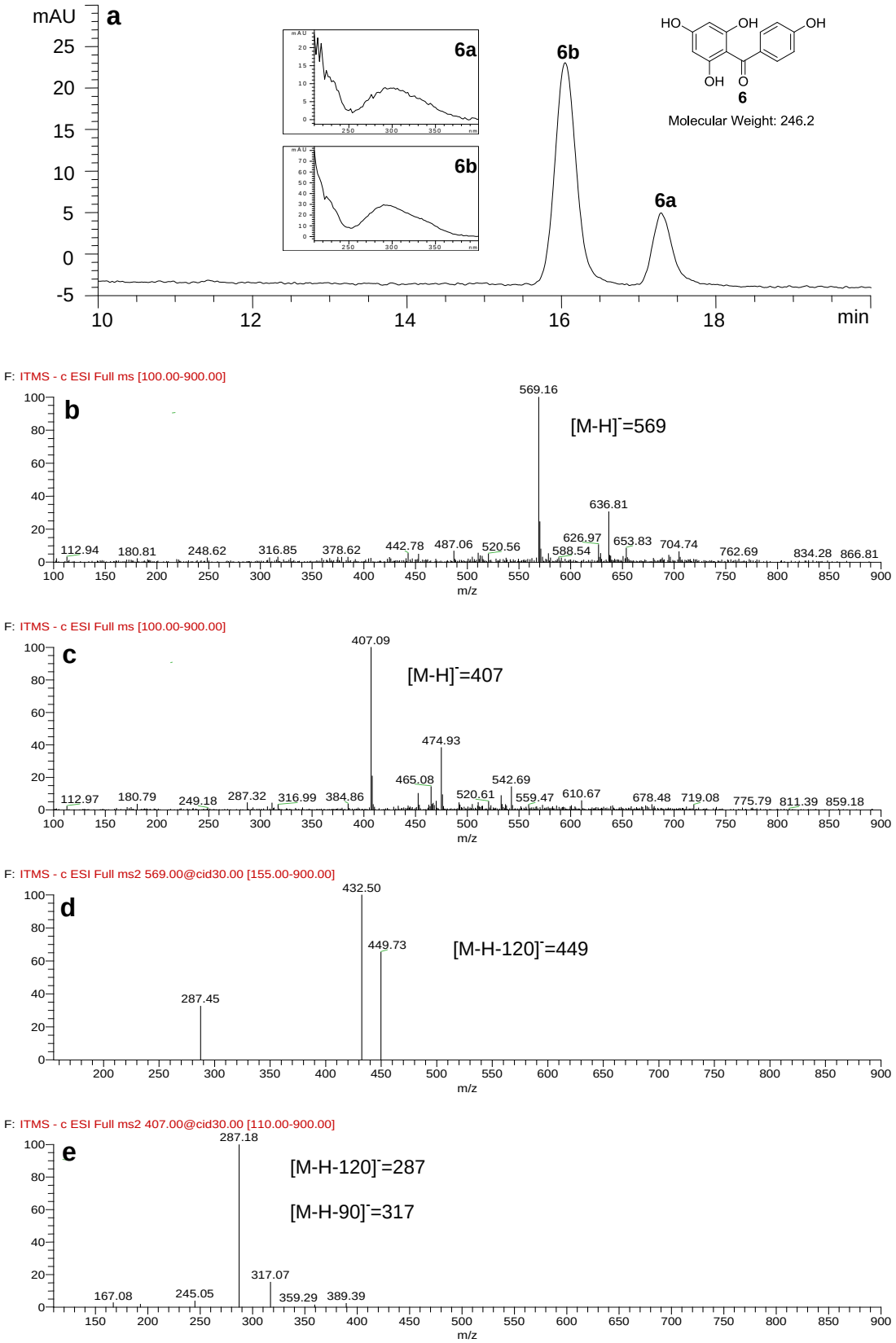

Figure S12. HPLC-DAD/ESI-MS analyses of *C*-glucosylated products by using **6** as an acceptor. (**a**) HPLC chromatogram and UV spectra of **6** and enzymatic products **6a** and **6b**; (**b**) and (**c**) Typical negative ion MS spectra for **6a** and **6b**; (**d**) and (**e**) Typical negative ion MS^2 spectra for **6a** and **6b**.

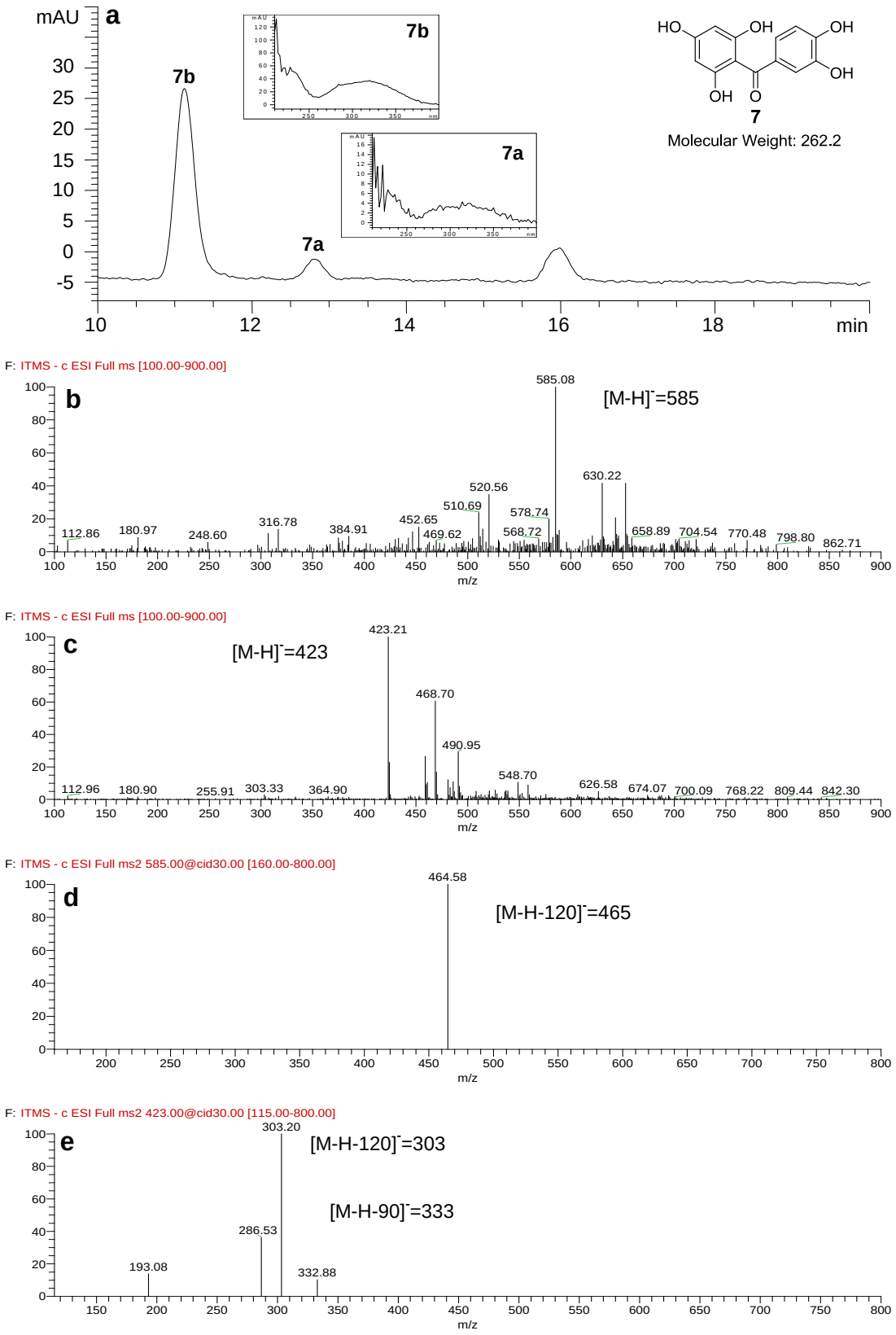

Figure S13. HPLC-DAD/ESI-MS analyses of *C*-glucosylated products by using **7** as an acceptor. (**a**) HPLC chromatogram and UV spectra of **7** and enzymatic products **7a** and **7b**; (**b**) and (**c**) Typical negative ion MS spectra for **7a** and **7b**; (**d**) and (**e**) Typical negative ion MS^2 spectra for **7a** and **7b**.

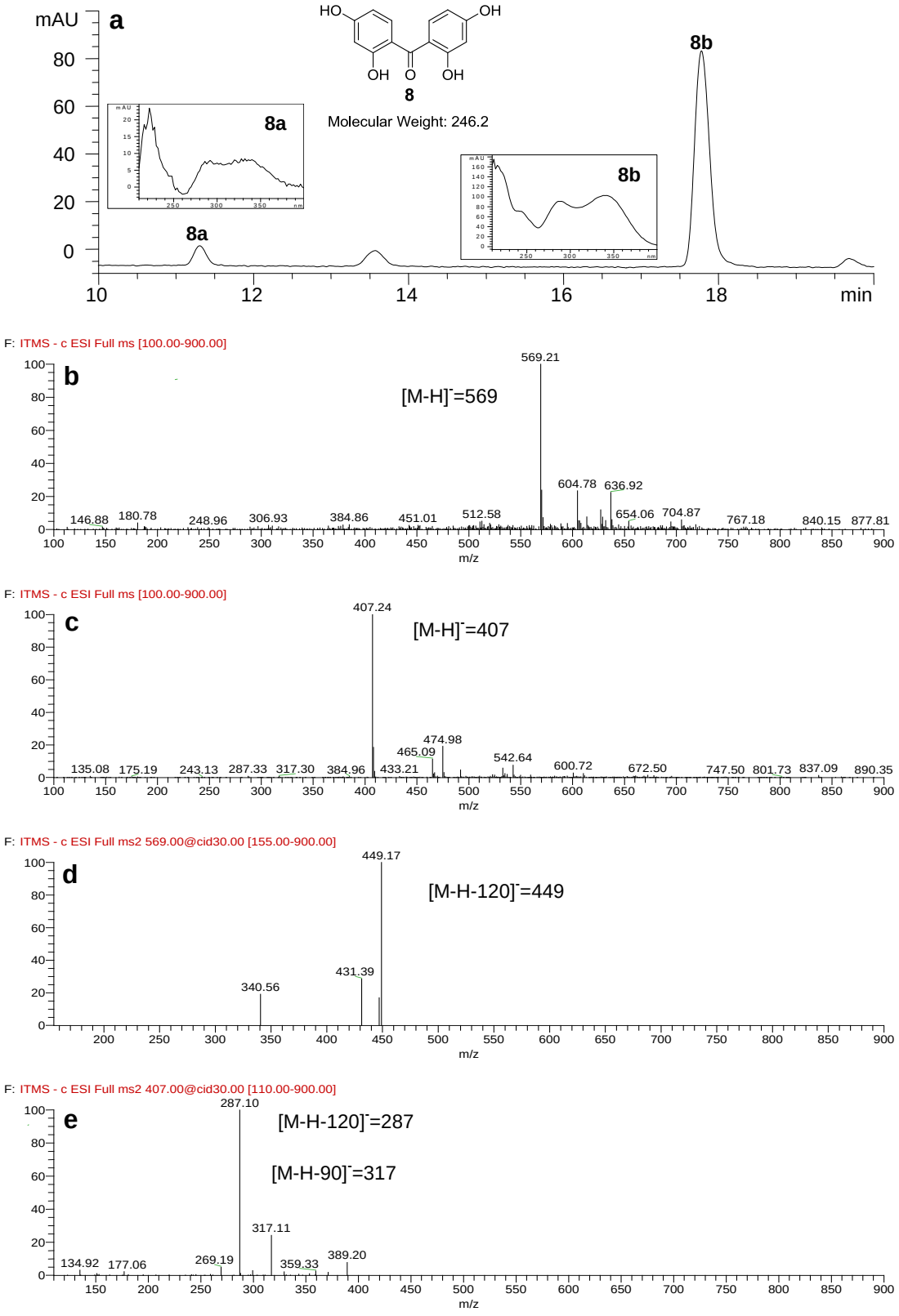

Figure S14. HPLC-DAD/ESI-MS analyses of *C*-glucosylated products by using **8** as an acceptor. (**a**) HPLC chromatogram and UV spectra of **8** and enzymatic products **8a** and **8b**; (**b**) and (**c**) Typical negative ion MS spectra for **8a** and **8b**; (**d**) and (**e**) Typical negative ion MS^2 spectra for **8a** and **8b**.

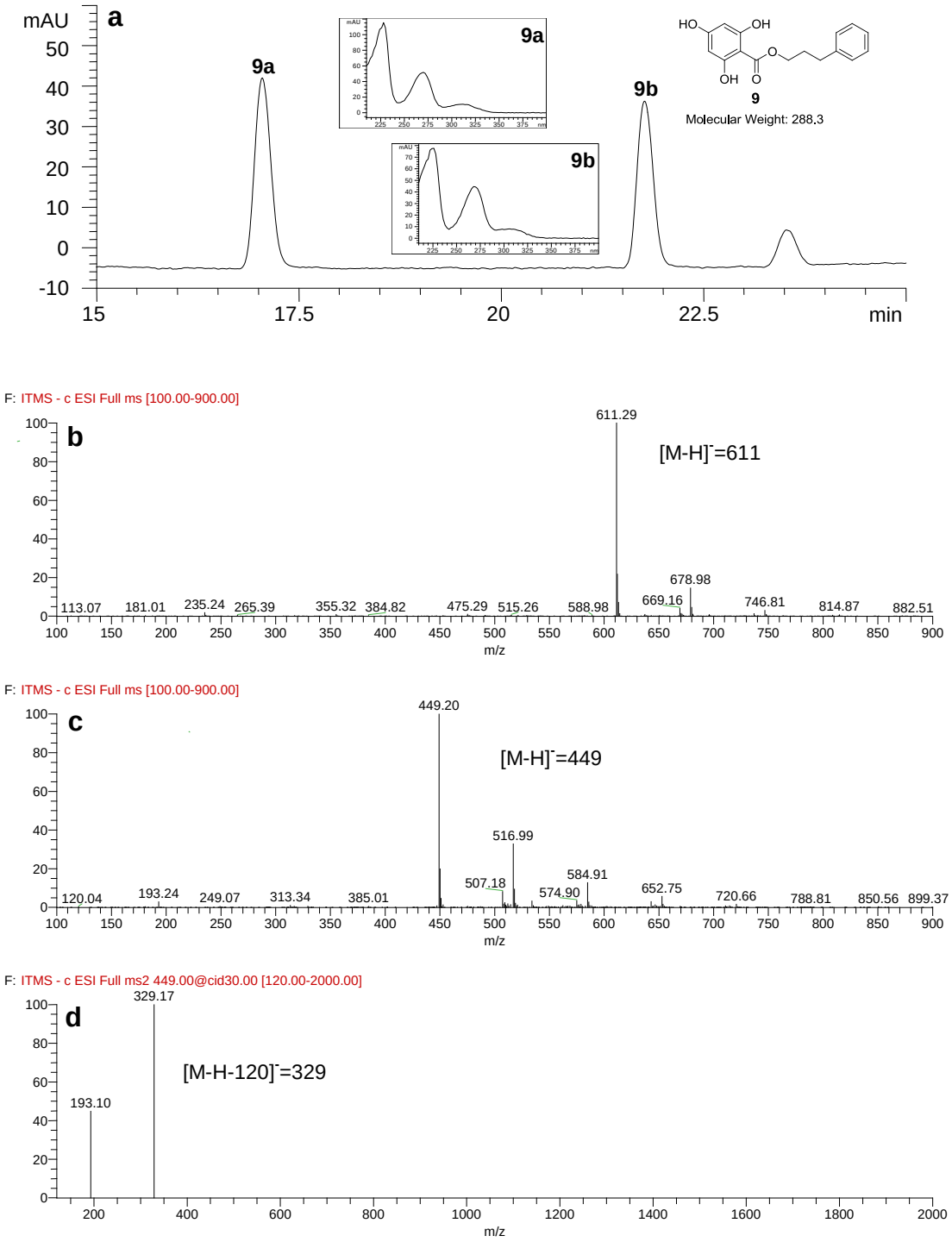

Figure S15. HPLC-DAD/ESI-MS analyses of *C*-glucosylated products using **9** as an acceptor. (**a**) HPLC chromatogram and UV spectra of **9** and enzymatic products **9a** and **9b**; (**b**) and (**c**) Typical negative ion MS spectra for **9a** and **9b**; (**d**) Typical negative ion MS^2 spectrum for **9b**.

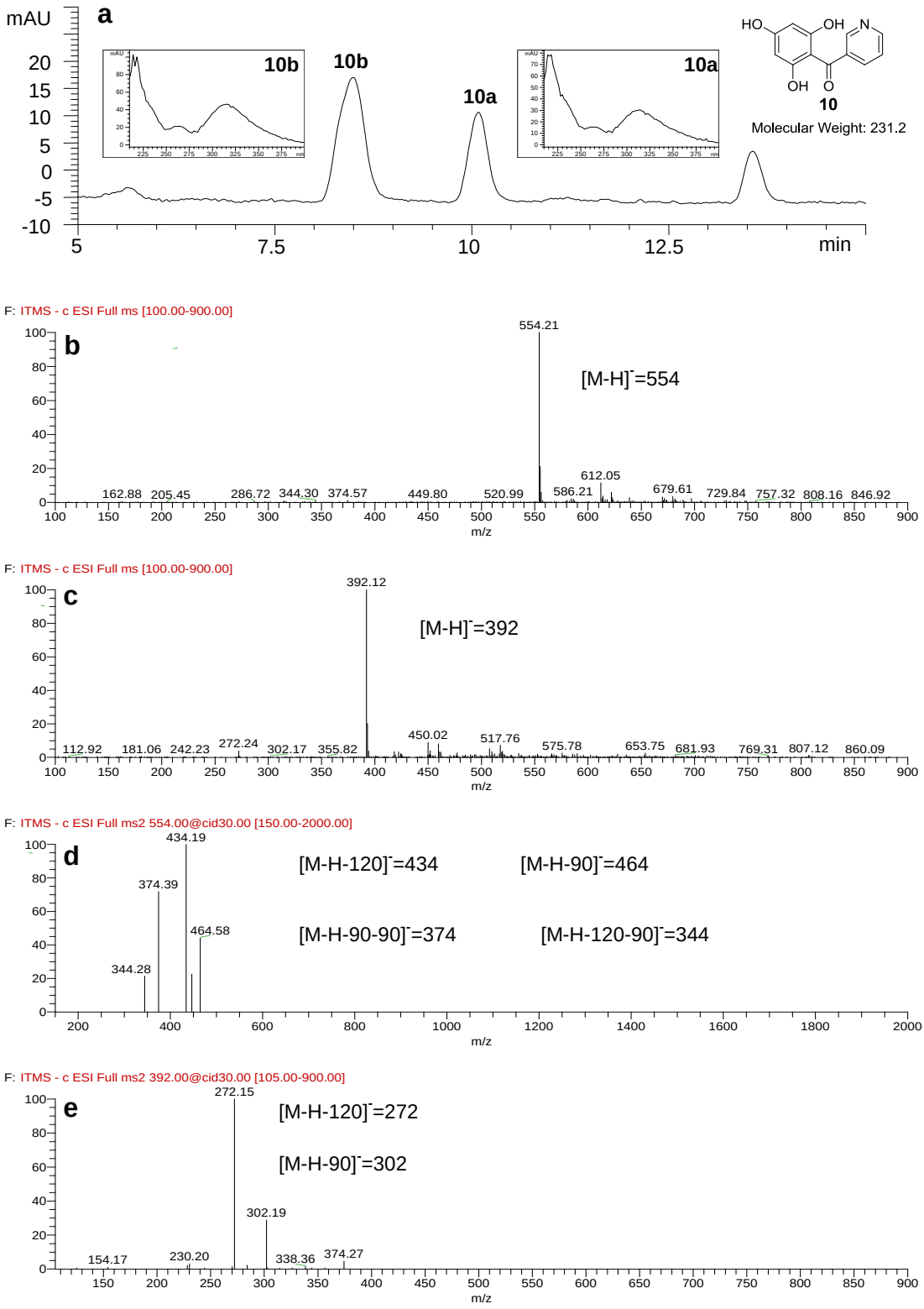

Figure S16. HPLC-DAD/ESI-MS analyses of *C*-glucosylated products using **10** as an acceptor. (**a**) HPLC chromatogram and UV spectra of **10** and enzymatic products **10a** and **10b**; (**b**) and (**c**) Typical negative ion MS spectra for **10a** and **10b**; (**d**) and (**e**) Typical negative ion MS^2 spectra for **10a** and **10b**.

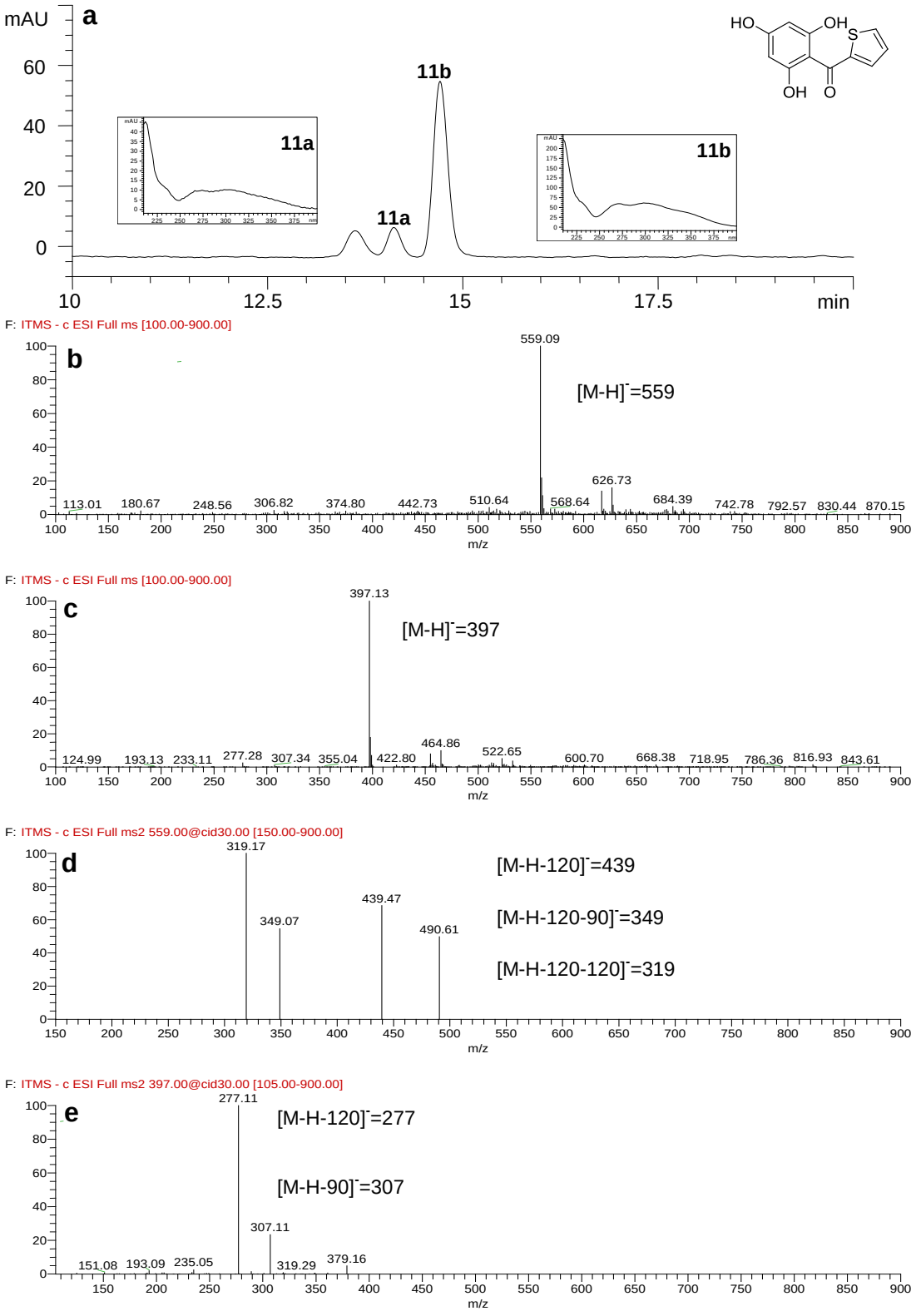

Figure S17. HPLC-DAD/ESI-MS analyses of *C*-glucosylated products using **11** as an acceptor. (**a**) HPLC chromatogram and UV spectra of **11** and enzymatic products **11a** and **11b**; (**b**) and (**c**) Typical negative ion MS spectra for **11a** and **11b**; (**d**) and (**e**) Typical negative ion MS^2 spectra for **11a** and **11b**.

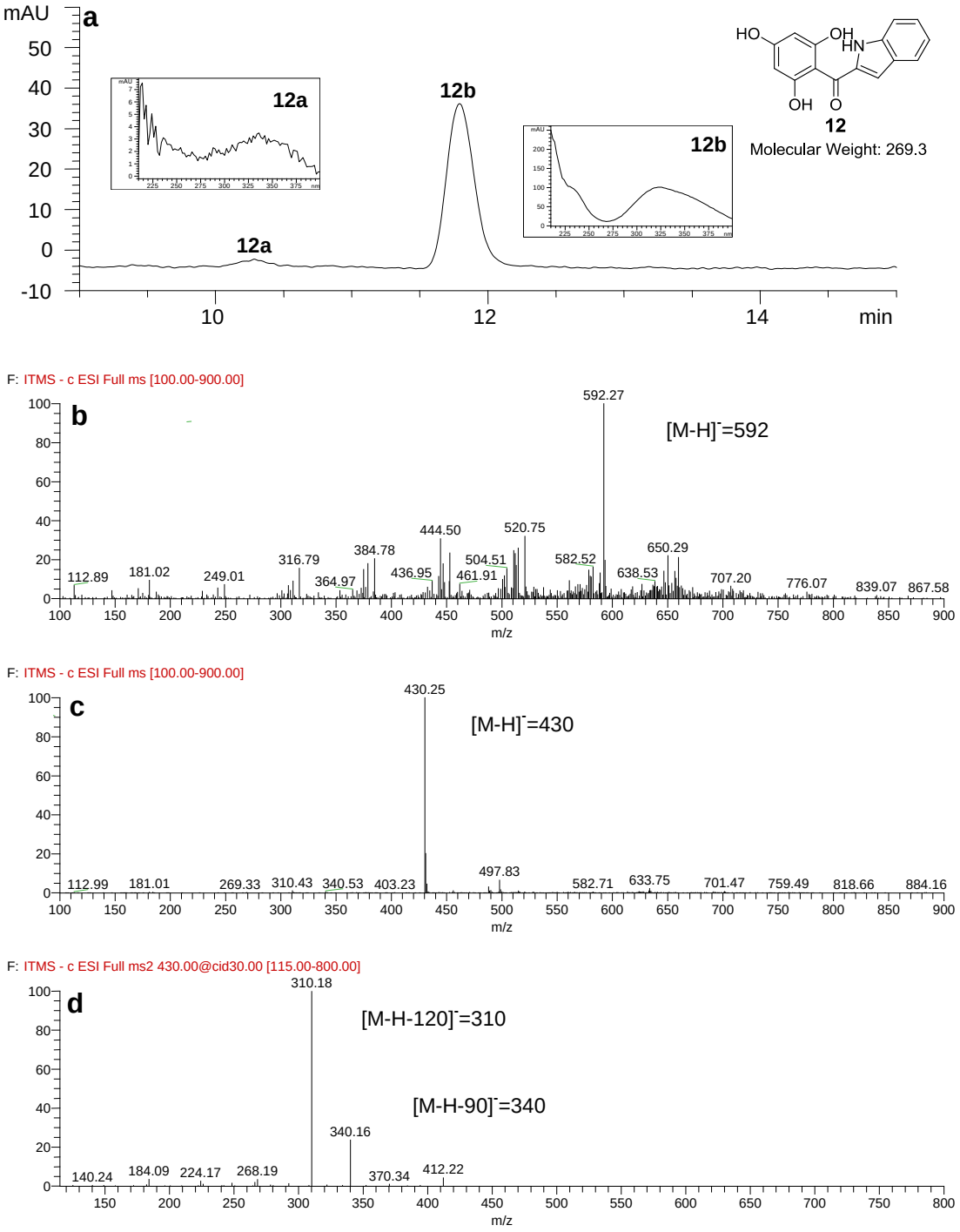

Figure S18. HPLC-DAD/ESI-MS analyses of *C*-glucosylated products using **12** as an acceptor. (**a**) HPLC chromatogram and UV spectra of **12** and enzymatic products **12a** and **12b**; (**b**) and (**c**) Typical negative ion MS spectra for **12a** and **12b**; (**d**) Typical negative ion MS^2 spectrum for **12b**.

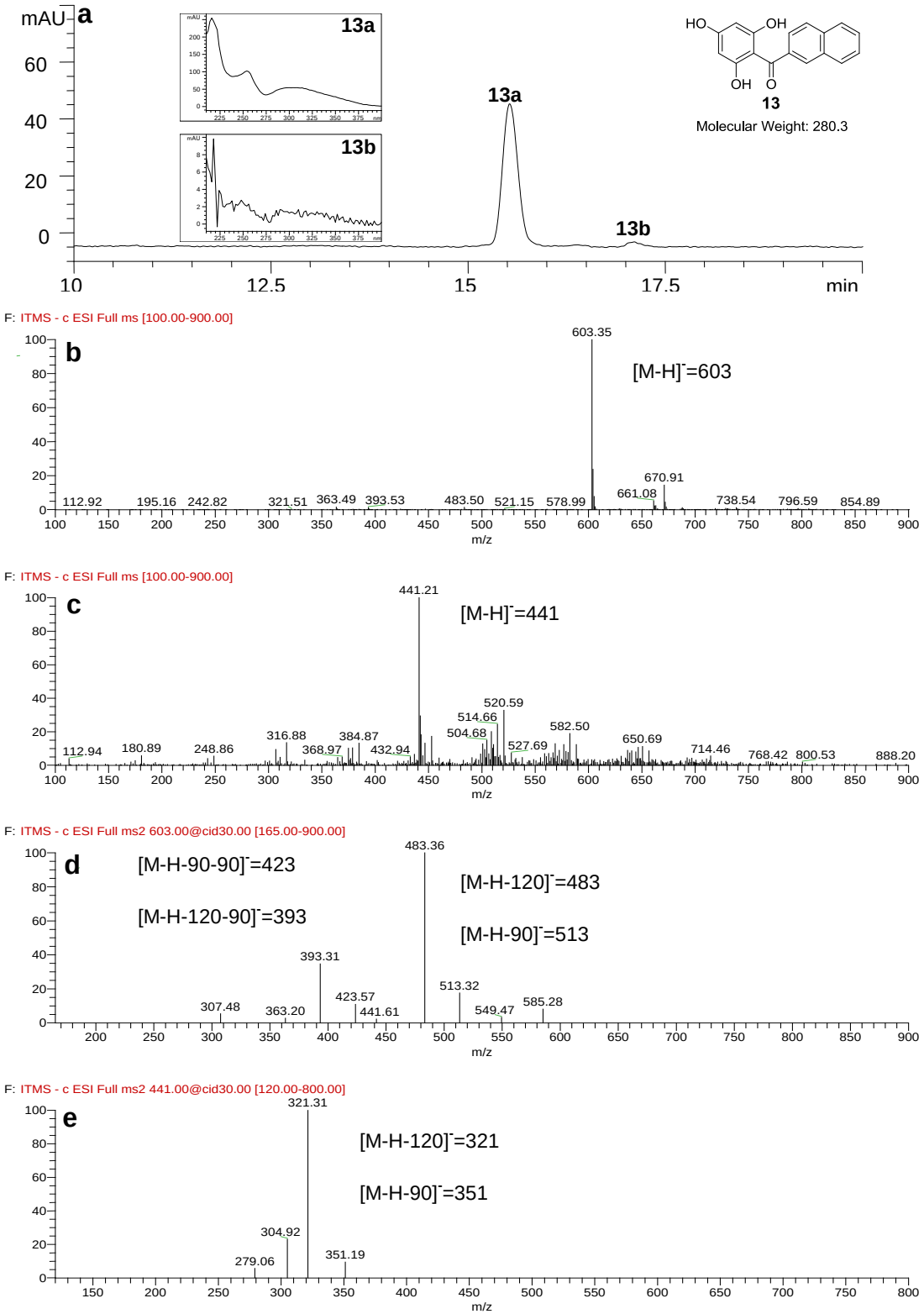

Figure S19. HPLC-DAD/ESI-MS analyses of *C*-glucosylated products using **13** as an acceptor. (**a**) HPLC chromatogram and UV spectra of **13** and enzymatic products **13a** and **13b**; (**b**) and (**c**) Typical negative ion MS spectra for **13a** and **13b**; (**d**) and (**e**) Typical negative ion MS^2 spectra for **13a** and **13b**.

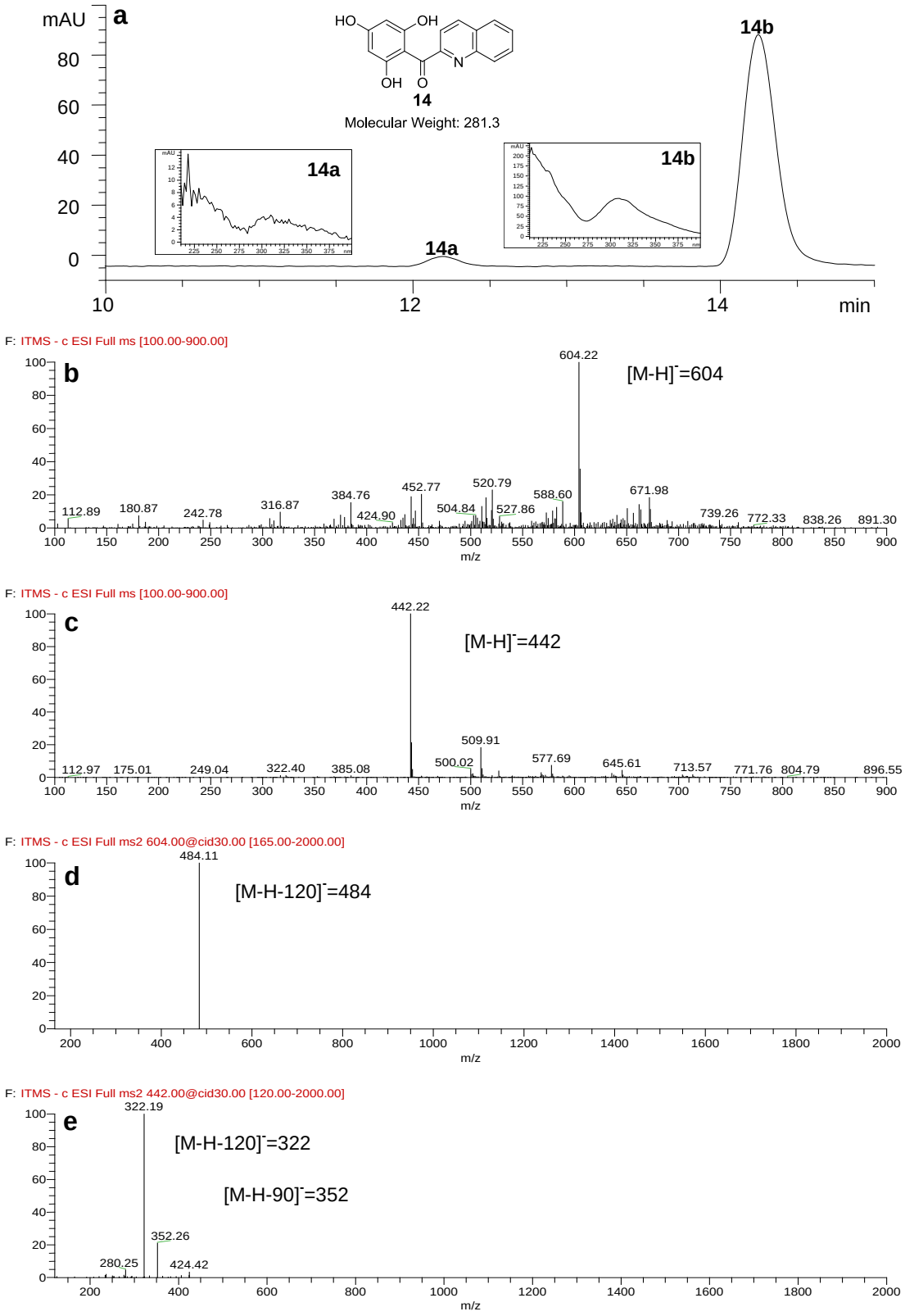

Figure S20. HPLC-DAD/ESI-MS analyses of *C*-glucosylated products using **14** as an acceptor. (**a**) HPLC chromatogram and UV spectra of **14** and enzymatic products **14a** and **14b**; (**b**) and (**c**) Typical negative ion MS spectra for **14a** and **14b**; (**d**) and (**e**) Typical negative ion MS^2 spectra for **14a** and **14b**.

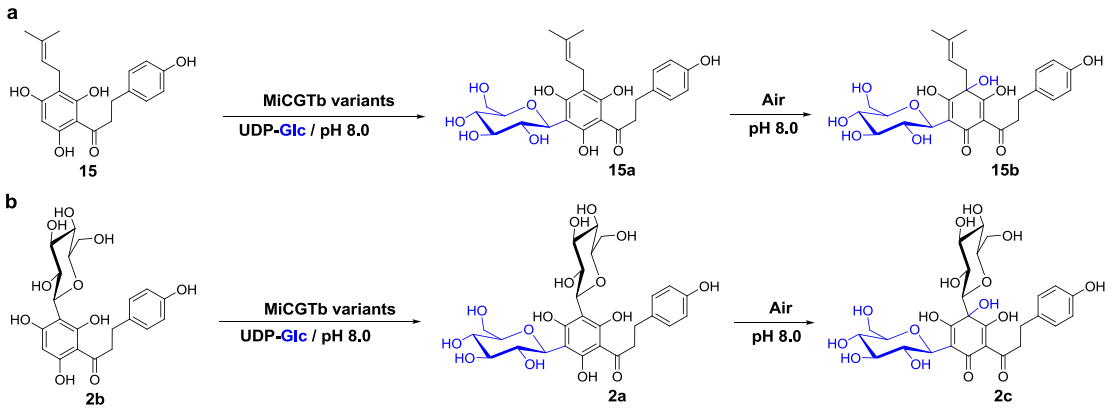

Figure S21. Phloretin derivatives with C-3' dimethylallyl or glycosyl substitution were catalyzed by MiCGTb variants to generate structurally diverse *C*-glucosides. (**a**) 3'-dimethylallyphloretin (**15**) was used as an acceptor and the *C*-glucosylated product spontaneously underwent oxidation to afford quinol *C*-glucoside **15b** at 30 ℃ and pH 8.0 (Na_2HPO_4-NaH_2PO_4 buffer) for 12 h; (**b**) 3'-glucosylphloretin (**2b**) was used as an acceptor and the *C*-glucosylated product spontaneously underwent oxidation to afford quinol *C*-glucoside **2c** at 30 ℃ and pH 8.0 (Na_2HPO_4-NaH_2PO_4 buffer) for 12 h.

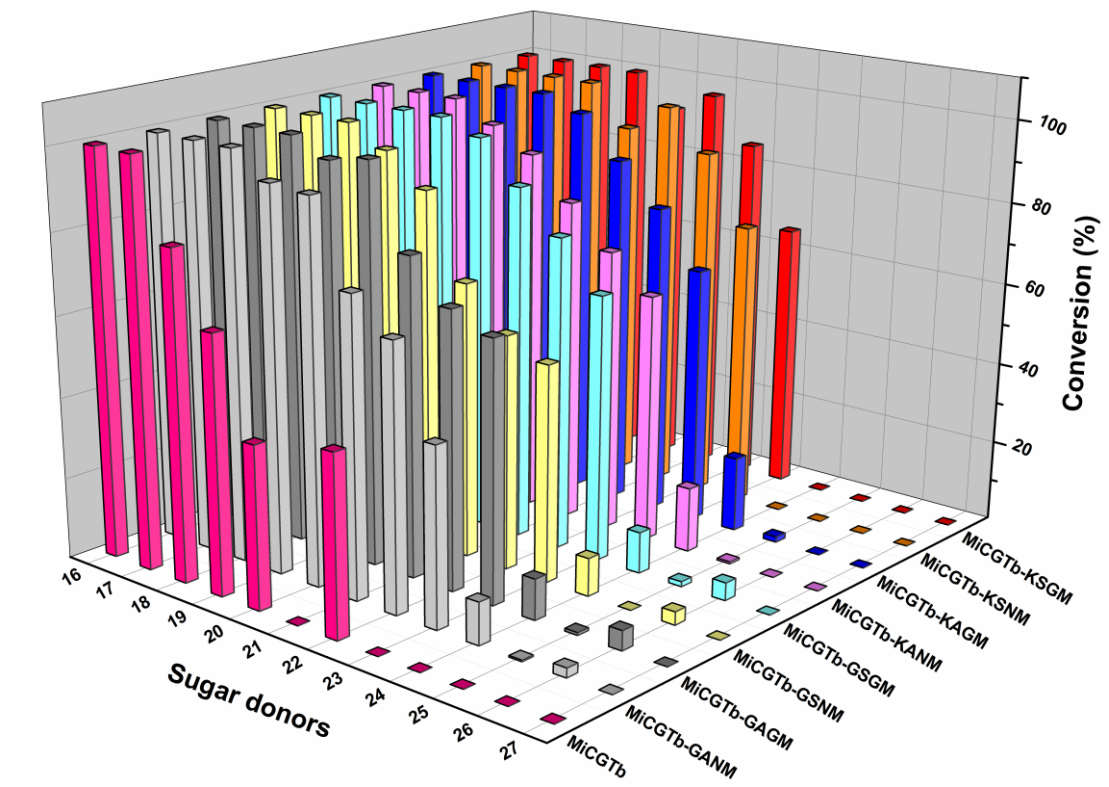

Figure S22. Sugar donor promiscuity of MiCGTb mutants using **1** as the sugar acceptor. The above reactions were conducted at 30 ℃ and pH 9.0 for 12 h. Mutants GANM, GAGM and GSGM exhibited *C*-glycosylation activity toward sugar donors **16**–**26**. Mutant GSNM has *C*-glycosylation capacity toward sugar donors **16**–**24** and **26**. Mutants KANM and KAGM have *C*-glycosylation capacity toward sugar donor **16**–**25**. Mutants KSNM and KSGM have *C*-glycosylation capacity toward sugar donor **16**–**23**.

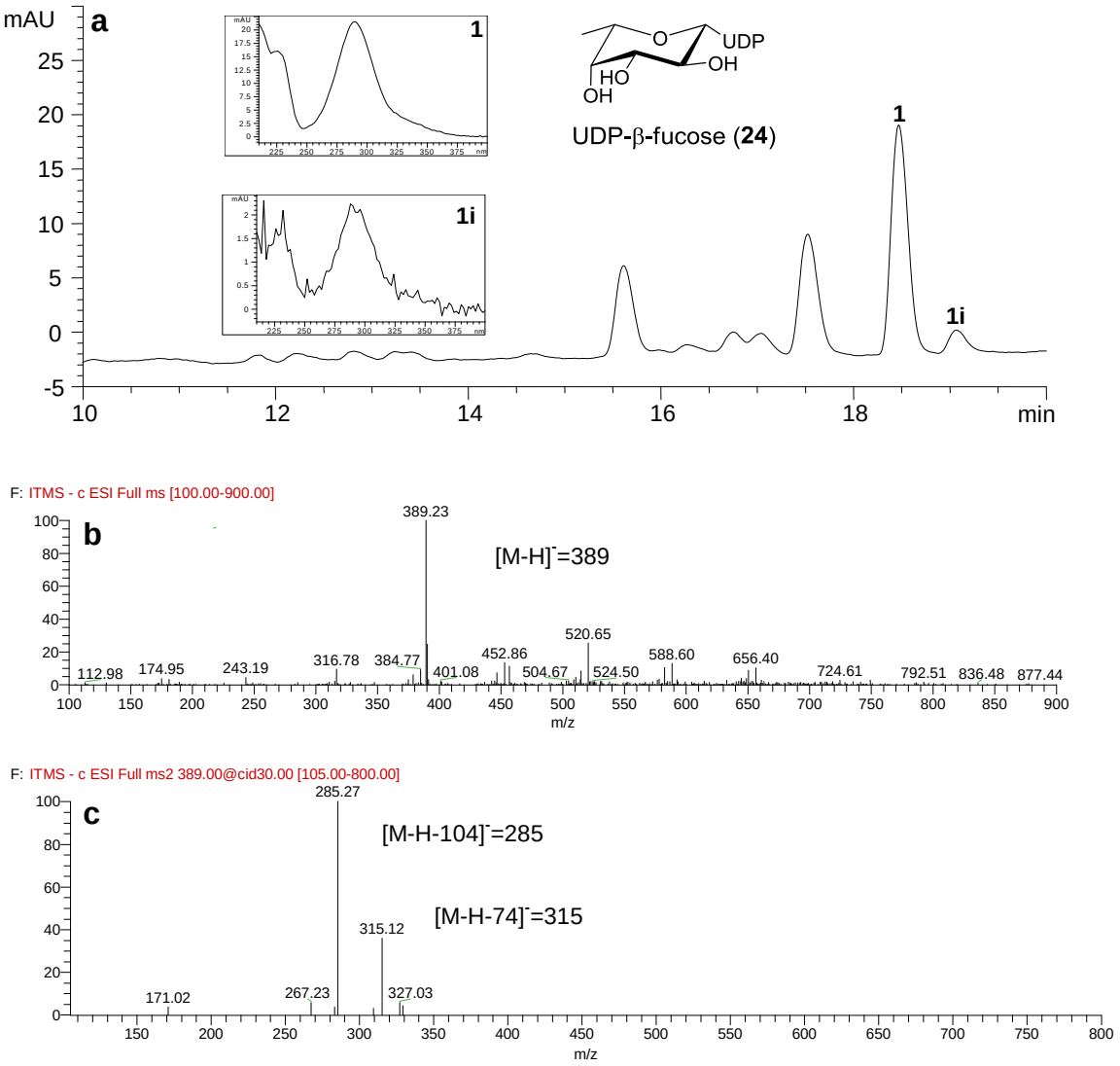

Figure S23. HPLC-DAD/ESI-MS analyses of enzymatic product using **24** as a sugar donor and **1** as an acceptor. (**a**) HPLC chromatogram and UV spectra of enzymatic product **1i**; (**b**) and (**c**) Typical negative ion MS and MS^2 spectra for **1i**.

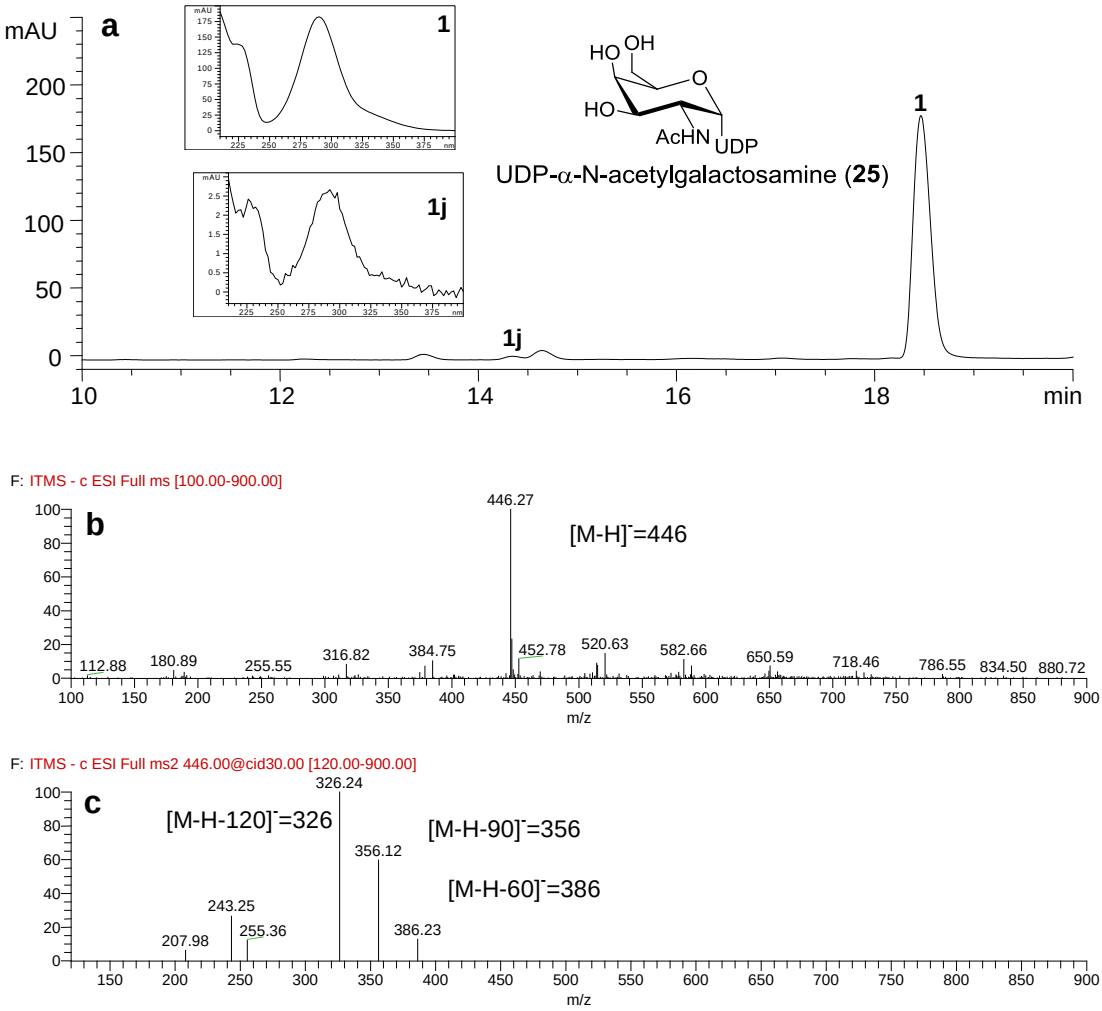

Figure S24. HPLC-DAD/ESI-MS analyses of enzymatic product using **25** as a sugar donor and **1** as an acceptor. (**a**) HPLC chromatogram and UV spectra of enzymatic product **1j**; (**b**) and (**c**) Typical negative ion MS and MS^2 spectra for **1j**.

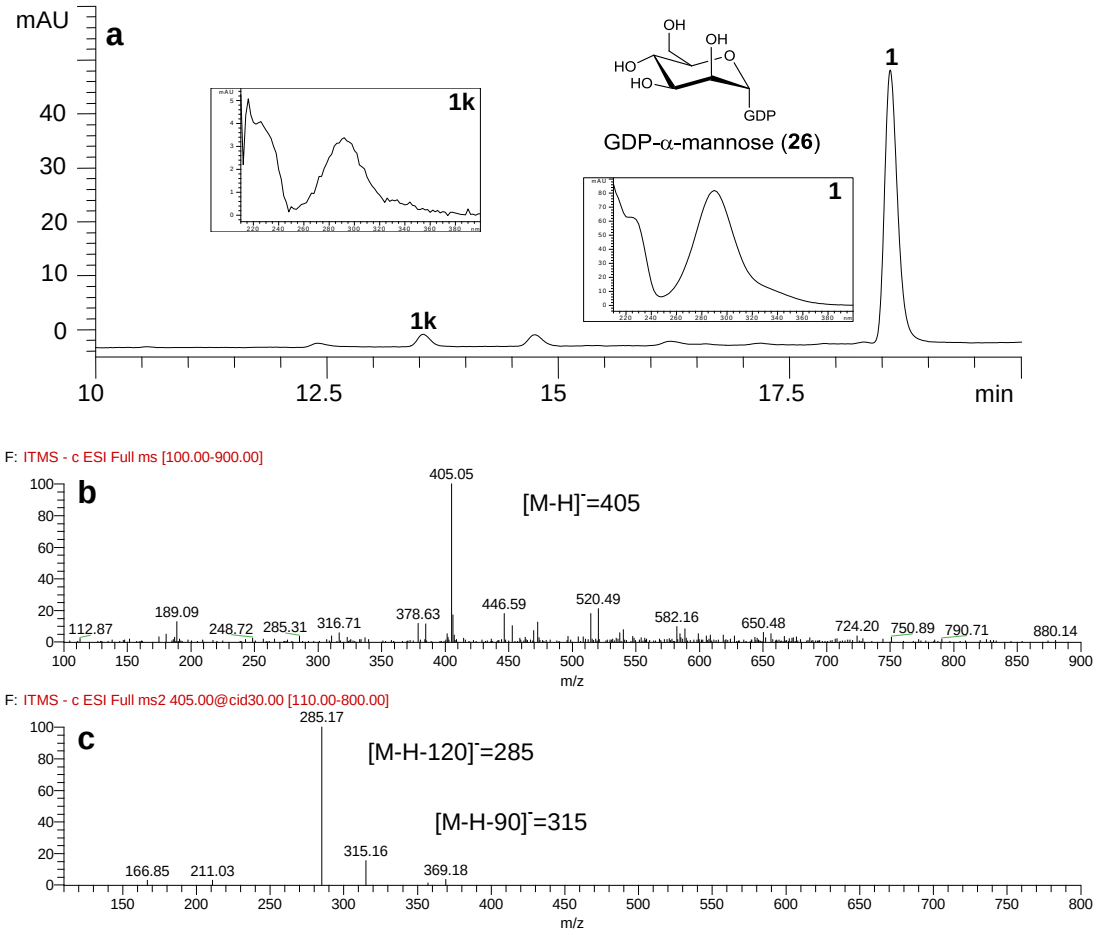

Figure S25. HPLC-DAD/ESI-MS analyses of enzymatic product using **26** as a sugar donor and **1** as an acceptor. (**a**) HPLC chromatogram and UV spectra of enzymatic product **1k**; (**b**) and (**c**) Typical negative ion MS and MS^2 spectra for **1k**.

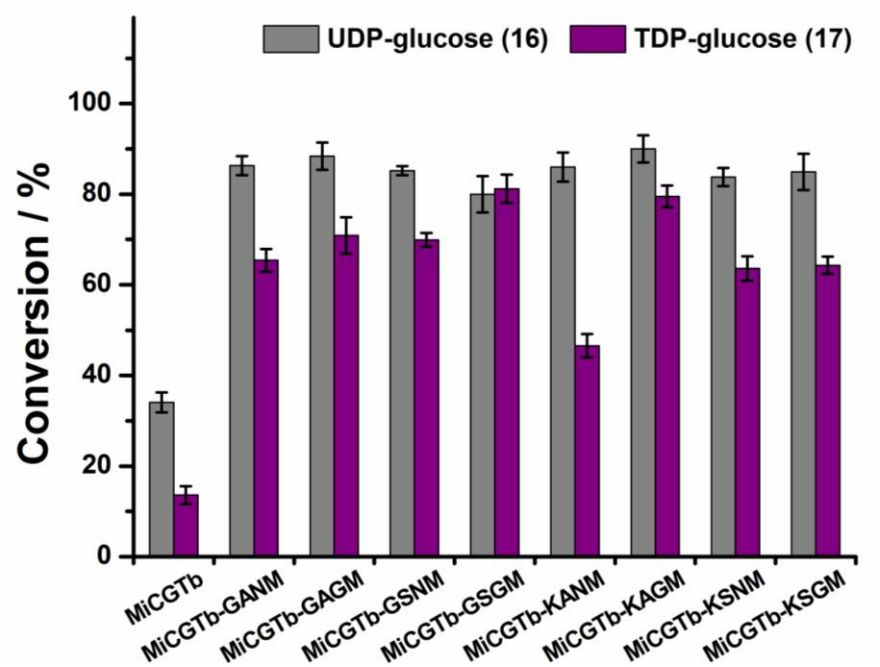

Figure S26. Percent conversion of **1a** by MiCGTb mutants towards glucose and TDP-Glc. The above reactions were conducted using **1** as the sugar acceptor at 30 ℃ and pH 9.0 for 12 h.

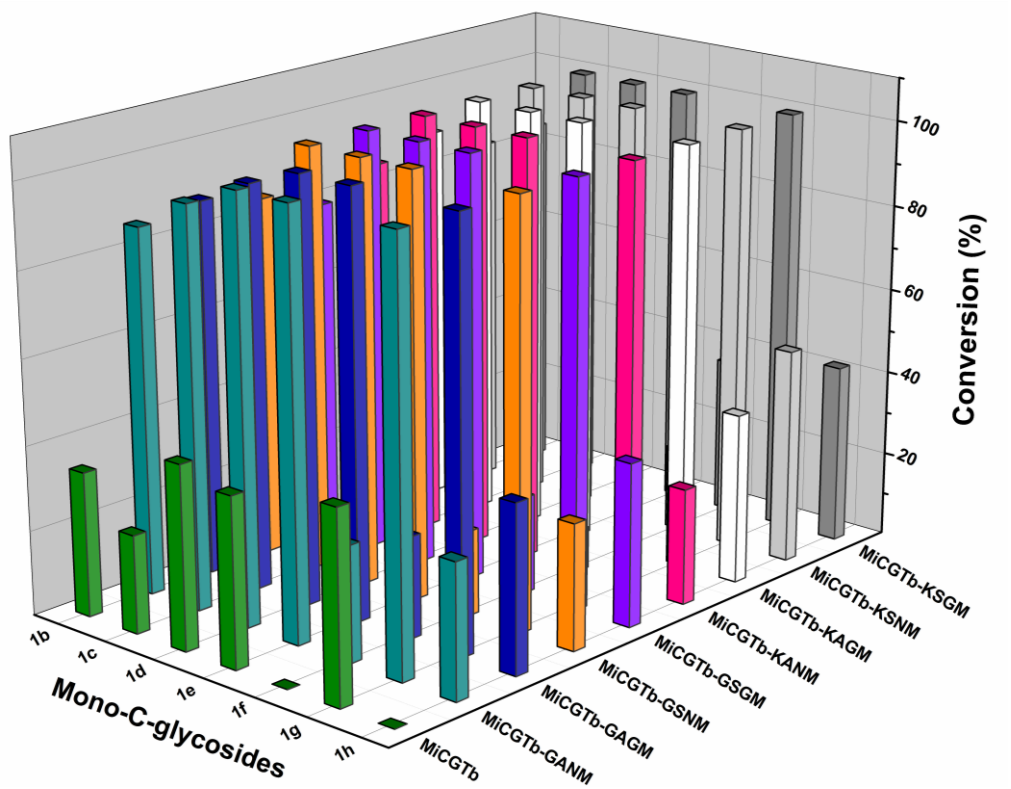

Figure S27. Percent conversion of bis-*C*-glycosides by MiCGTb mutants using mono-*C*-glycosides (**1b**–**1h**) as acceptors and UDP-Glc as a sugar donor. The above reactions were conducted at 30 ℃ and pH 9.0 for 12 h.

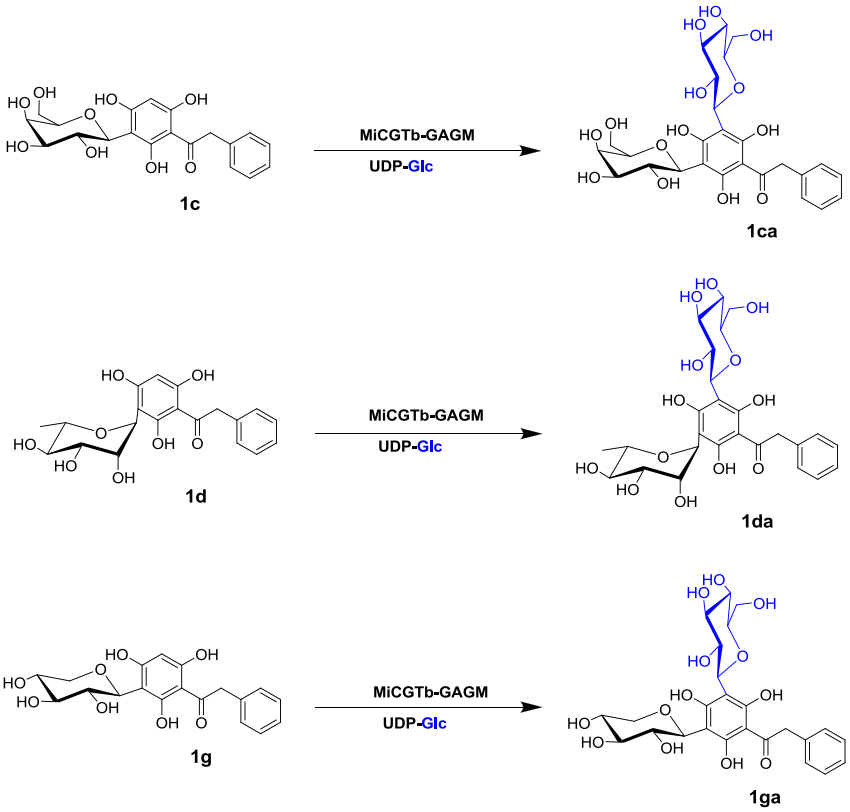

Figure S28. Mono-*C*-glycosides were catalyzed by MiCGTb-GAGM using UDP-Glc as the sugar donor to generate structurally diverse bis-*C*-glycosides with two different sugar moieties. The above reactions were conducted at 30 ℃ and pH 9.0 for 12 h. The bis-*C*-glycosides (**1ca**, **1da** and **1ga**) were prepared and structurally identified by MS, ^{1}H and ^{13}C NMR.

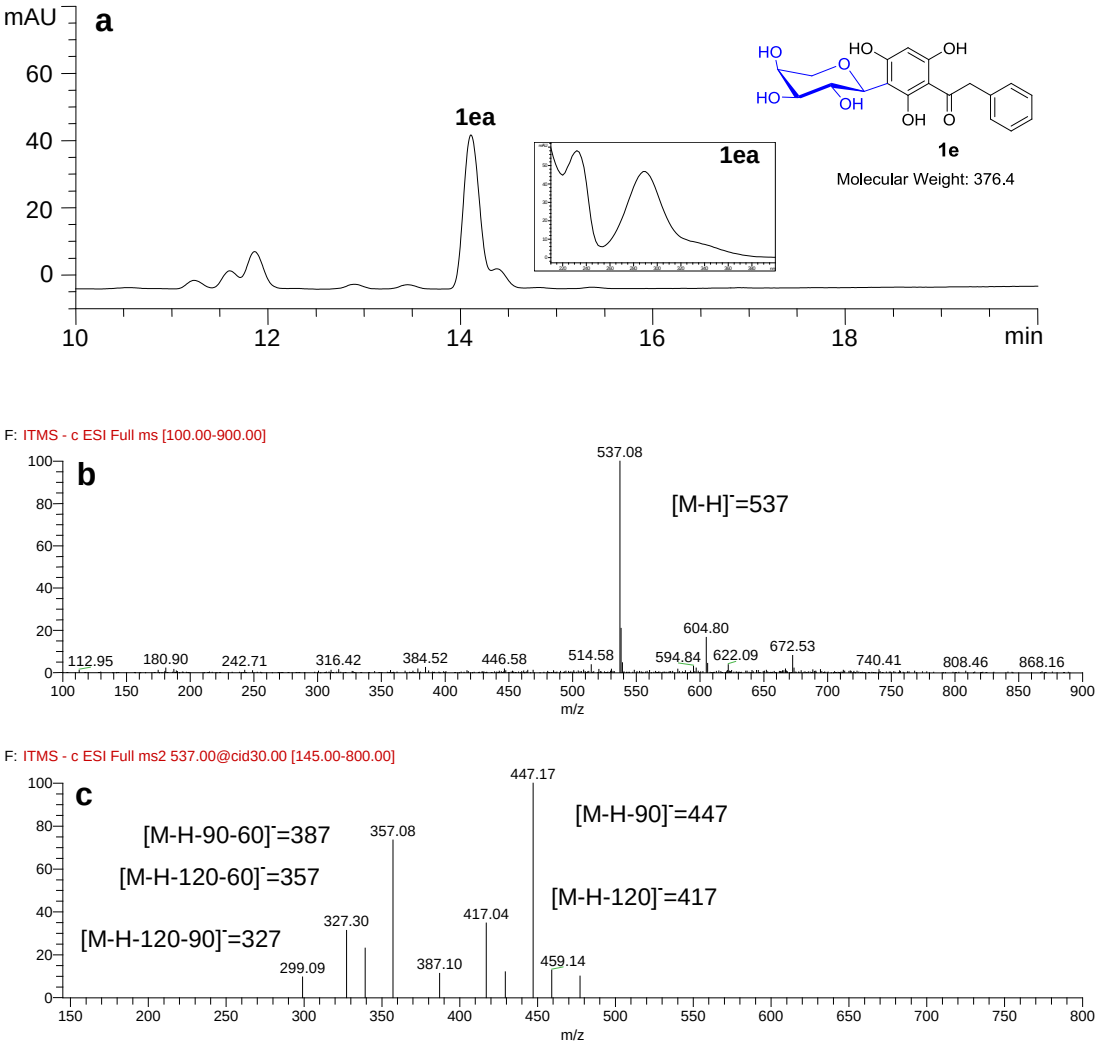

Figure S29. HPLC-DAD/ESI-MS analyses of bis-*C*-glycosylated product using **1e** as an acceptor and UDP-Glc as a sugar donor. (**a**) HPLC chromatogram and UV spectra of enzymatic product **1ea**; (**b**) and (**c**) Typical negative ion MS and MS^2 spectra for **1ea**.

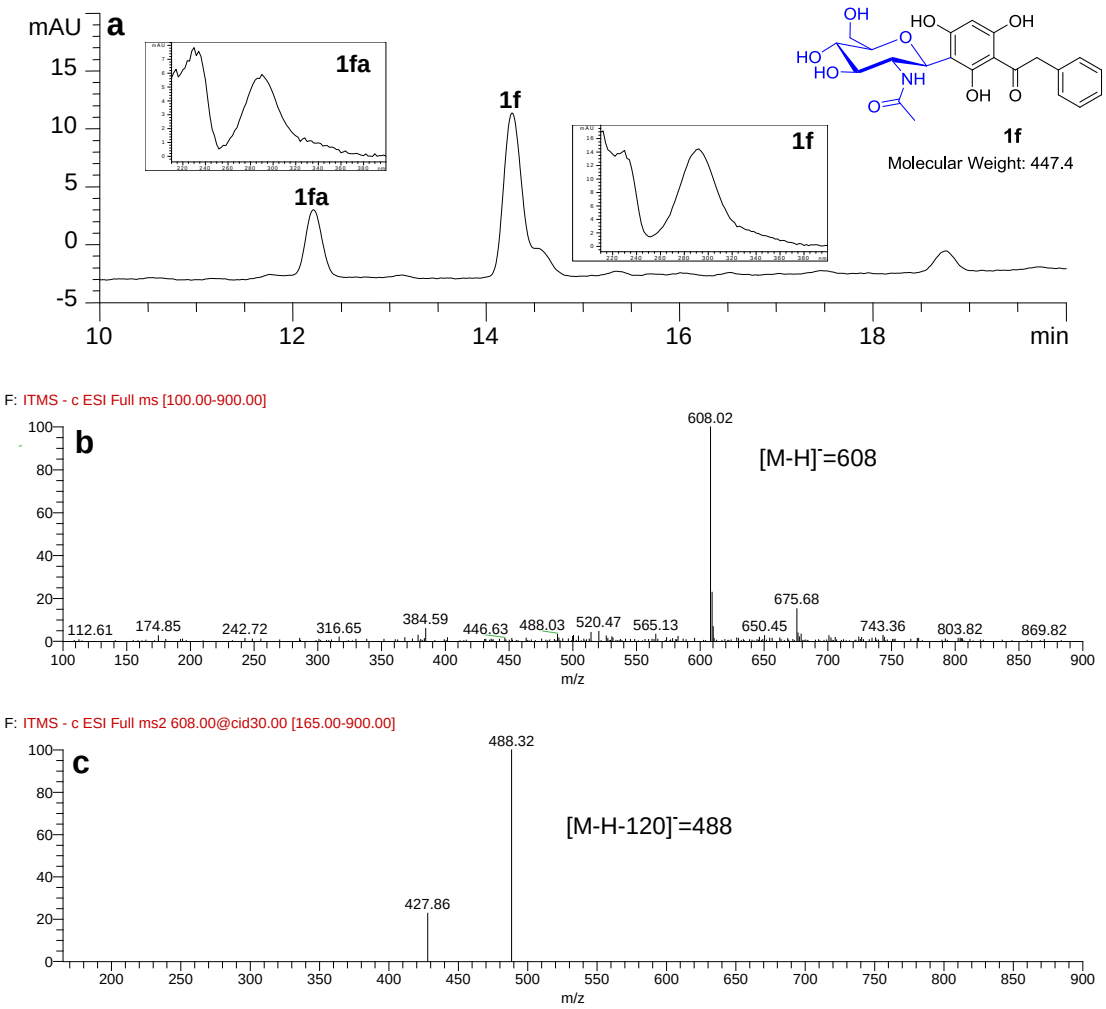

Figure S30. HPLC-DAD/ESI-MS analyses of bis-*C*-glycosylated product using **1f** as an acceptor and UDP-Glc as a sugar donor. (**a**) HPLC chromatogram and UV spectra of **1f** and enzymatic product **1fa**; (**b**) and (**c**) Typical negative ion MS and MS^2 spectra for **1fa**.

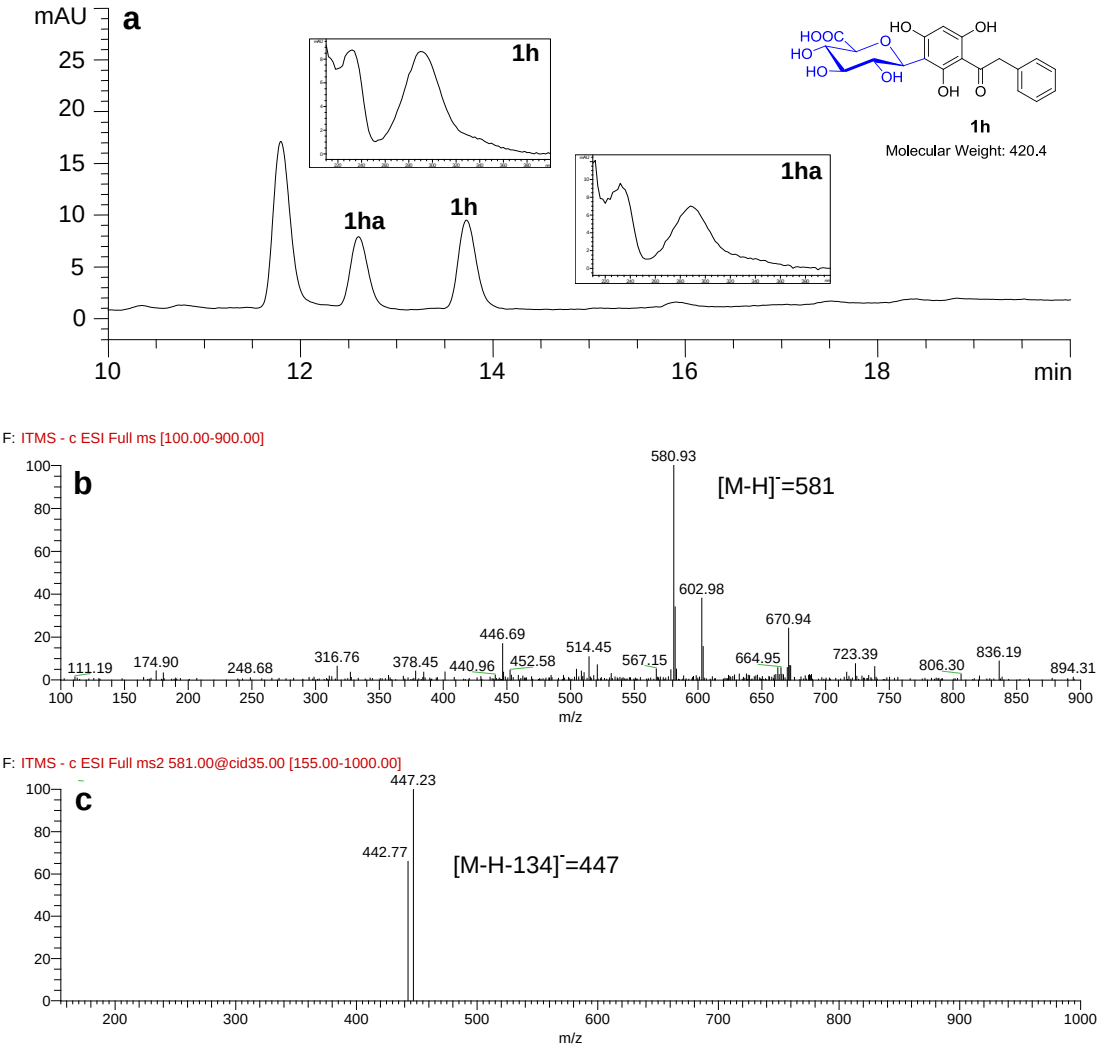

Figure S31. HPLC-DAD/ESI-MS analyses of bis-*C*-glycosylated product using **1h** as an acceptor and UDP-Glc as a sugar donor. (**a**) HPLC chromatogram and UV spectra of enzymatic products **1ha** and **1h**; (**b**) and (**c**) Typical negative ion MS and MS^2 spectra for **1ha**.

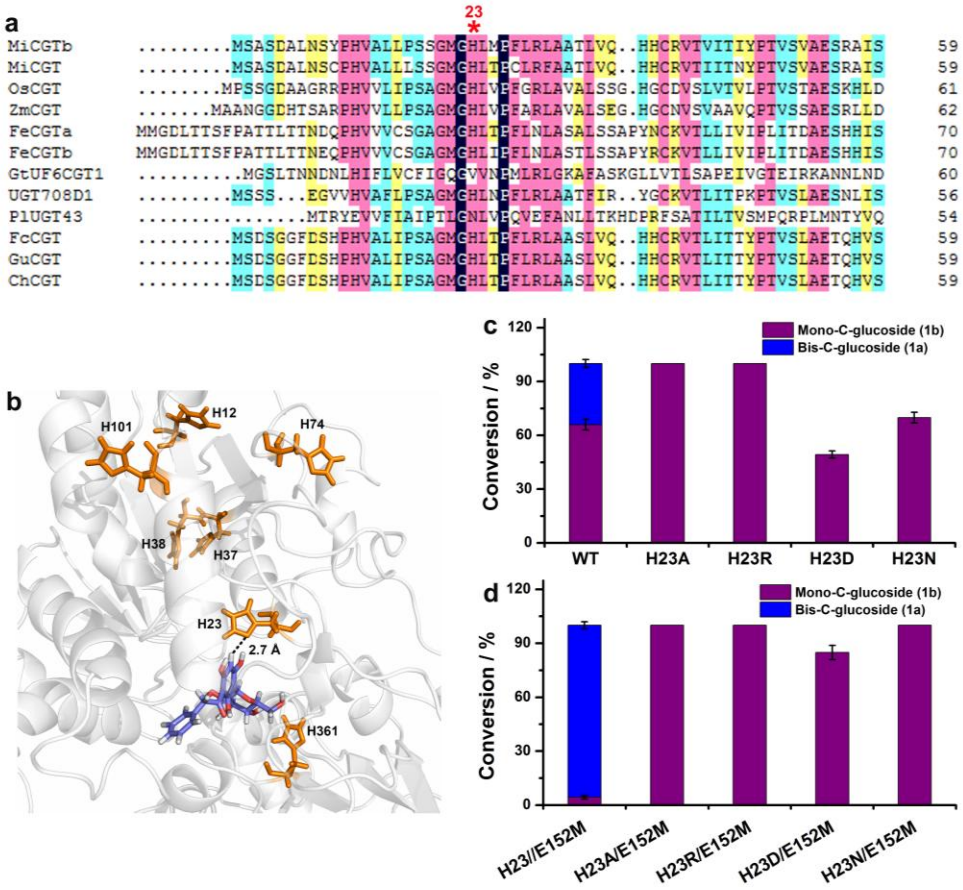

Figure S32. The H23 of MiCGTb and MiCGT as catalytic residue for the bis-*C*-glycosylation. (**a**) Alignment of the N-terminal amino acid sequences of MiCGTb and MiCGT with other plant *C*-glycosyltransferases. MiCGT and MiCGTb used in this study from *Mangifera indica*; OsCGT from *Oryza sativa*;[11] ZmCGT from *Zea mays*;[12] FeCGTa and FeCGTb from *Fagopyrum esculentum*;[13] GtUF6CGT1 from *Gentiana triflora*;[14] UGT708D1 from *Glycine max*;[15] PlUGT43 from *Pueraria lobata*;[16] FcCGT from *Fortunella crassifolia*, CuCGT from *Citrus unshiu* and ChCGT from *Citrus hanaju*.[17] (**b**) Histidine surrounded the homology modeling of MiCGTb bound with **1b**. The crystal structure of UGT71G1 (PDB code 2ACW) was used as a model for homology modeling; (**c**) Conversion of mono- and bis-*C*-glucoside of H23 mutants in MiCGTb. WT: wild type; (**d**) Conversion of mono- and bis-*C*-glucoside of H23 mutants in MiCGT-E152M.

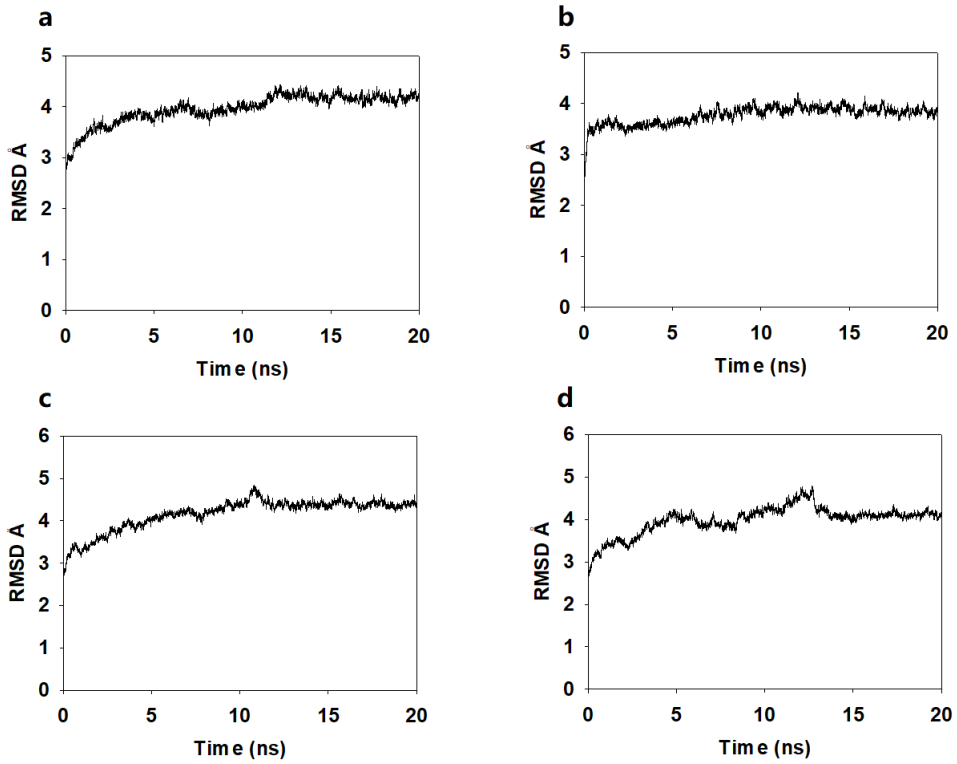

Figure S33. Time dependences of root mean square deviation (RMSD) of backbone Cα atoms from the initial structure of mutants. (**a**) MiCGT–**1b**; (**b**) MiCGT-E152I–**1b**; (**c**) MiCGTb–**1b**; (**d**) MiCGTb-I152E–**1b**. The corresponding values converge around 4.0 Å after 10 ns simulation and show no more significant fluctuation afterwards, revealing that the structure remained stable during the molecular simulations.

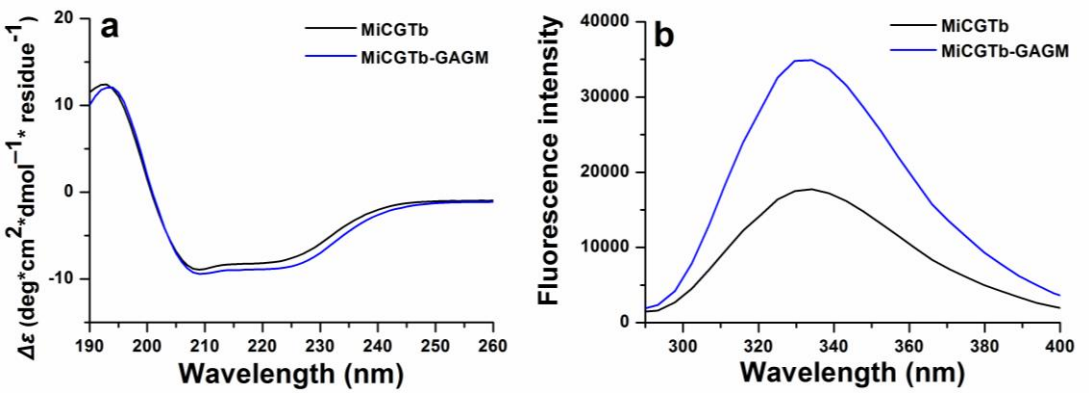

Figure S34. Circular dichroism and fluorescence spectroscopy of MiCGTb and the MiCGTb-GAGM mutant.

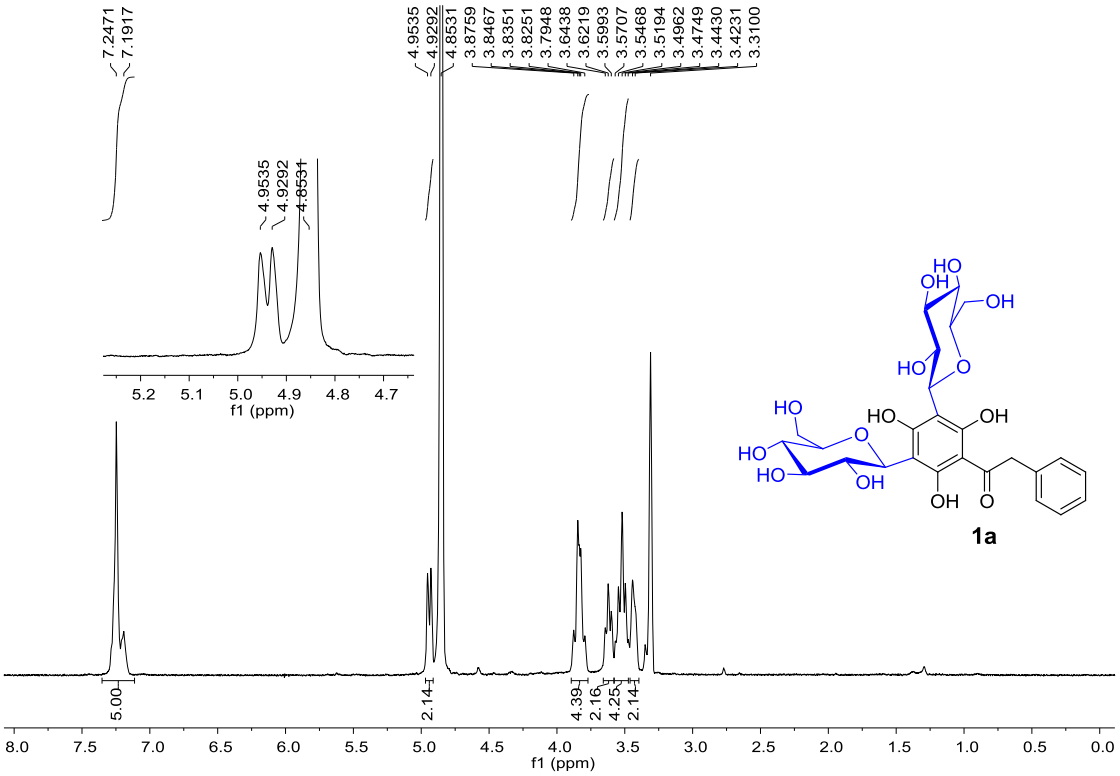

Figure S35. ^{1}H NMR spectrum of **1a** (CD_3OD-d_4, 400 MHz).

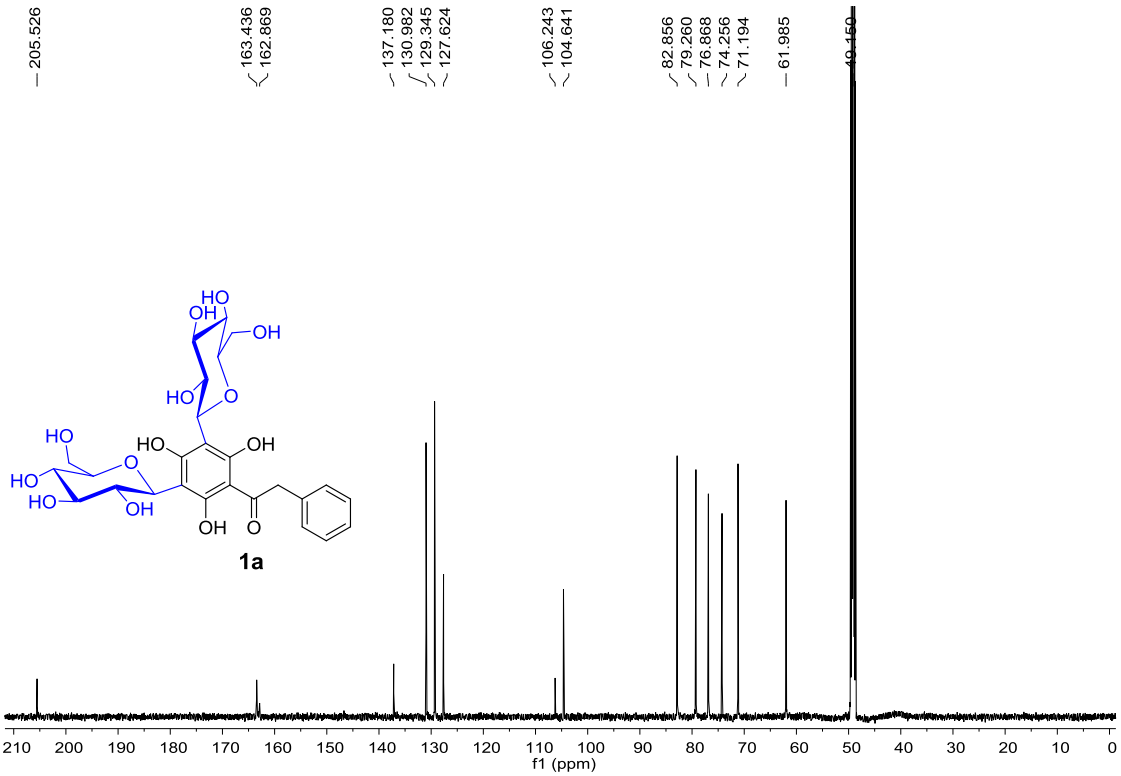

Figure S36. ^{13}C NMR spectrum of **1a** (CD_3OD-d_4, 150 MHz).

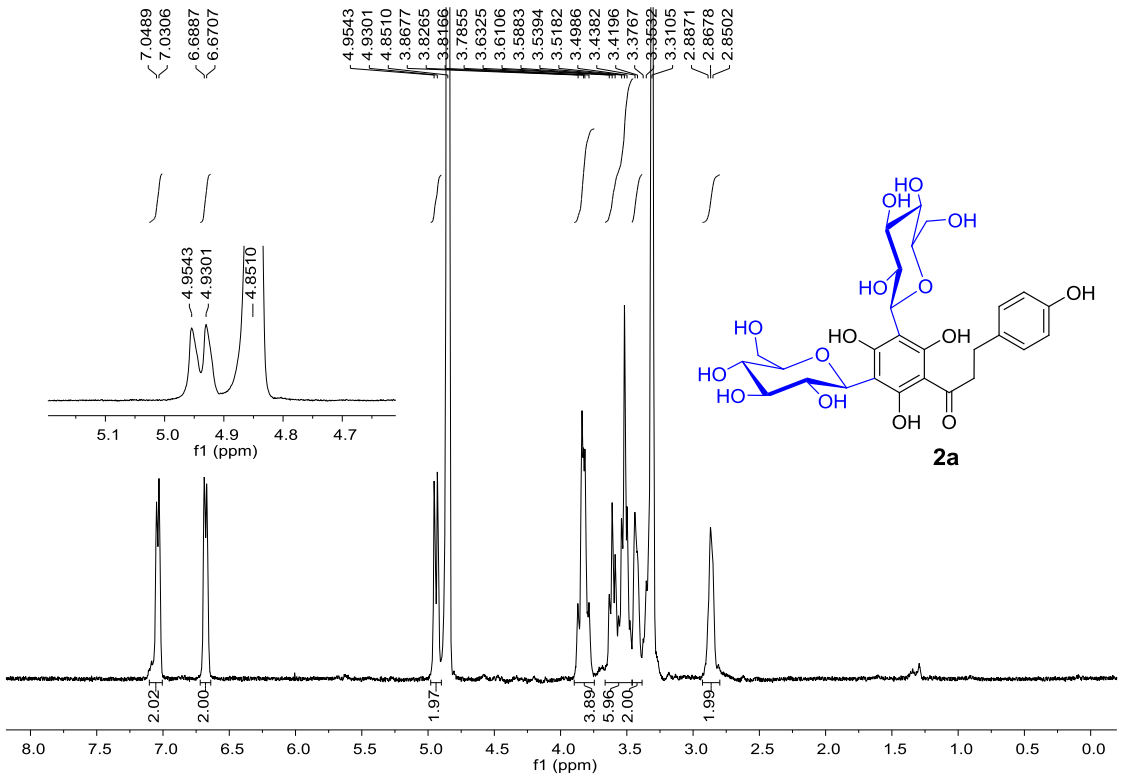

Figure S37. ^{1}H NMR spectrum of **2a** (CD_3OD-d_4, 400 MHz).

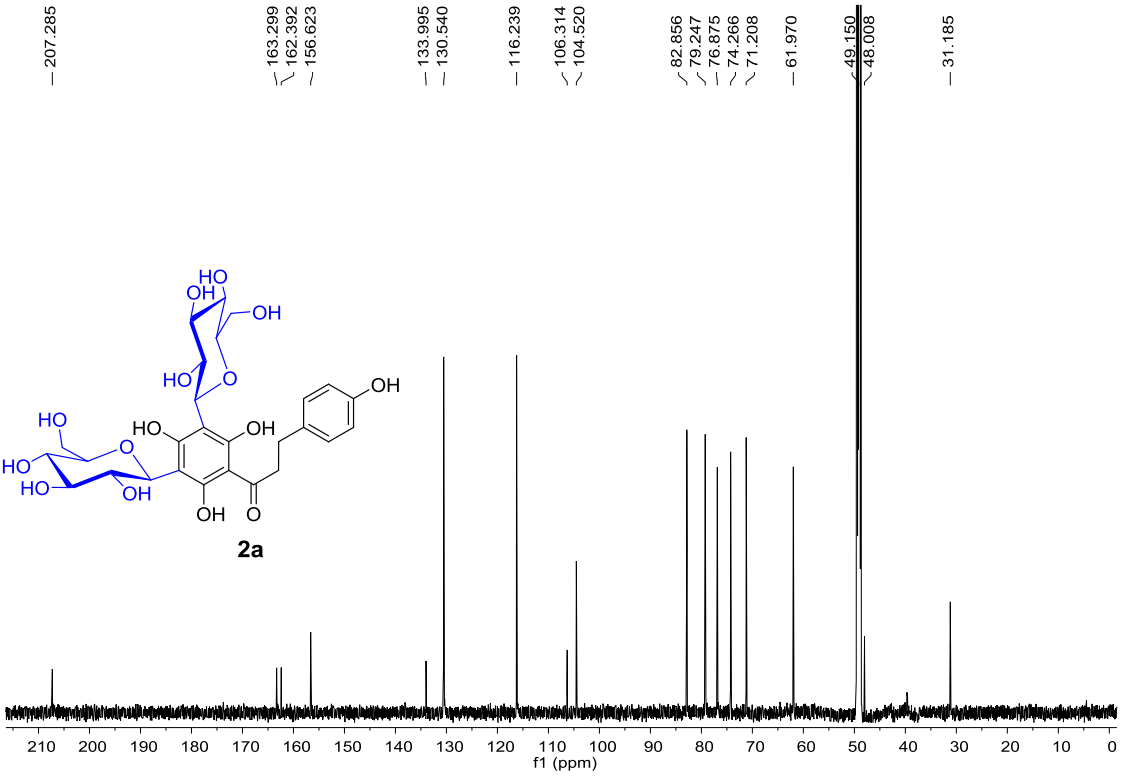

Figure S38. ^{13}C NMR spectrum of **2a** (CD_3OD-d_4, 150 MHz).

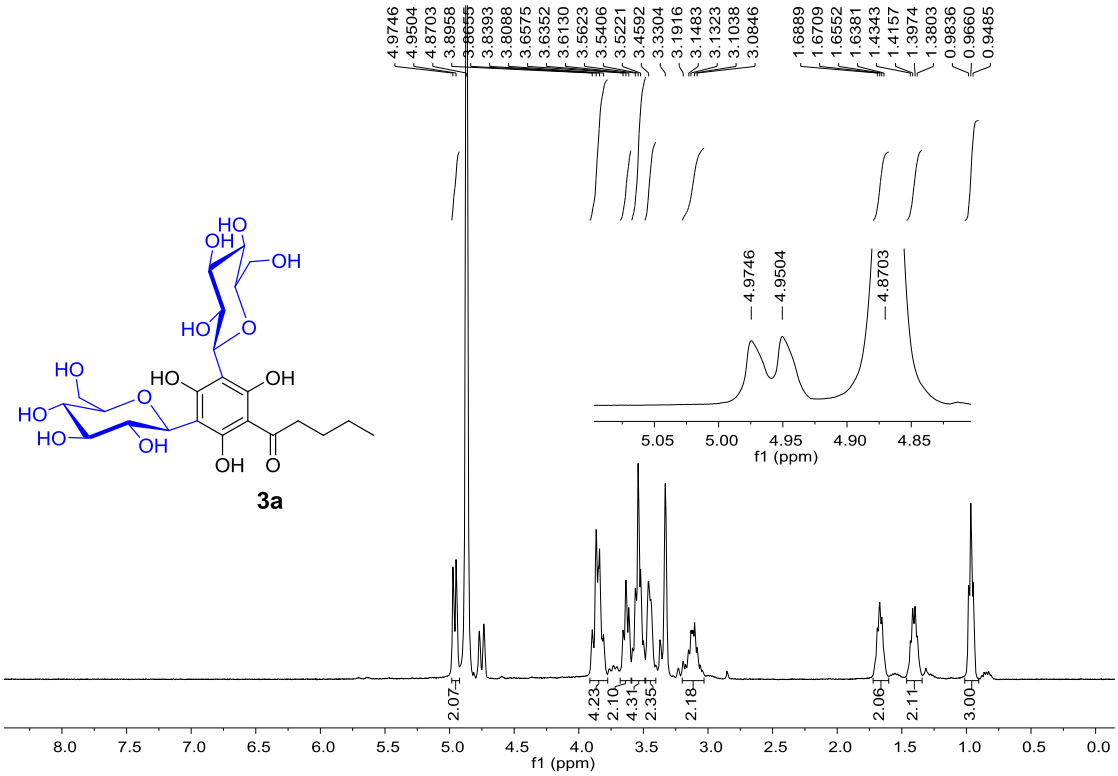

Figure S39. ^{1}H NMR spectrum of **3a** (CD_3OD-d_4, 400 MHz).

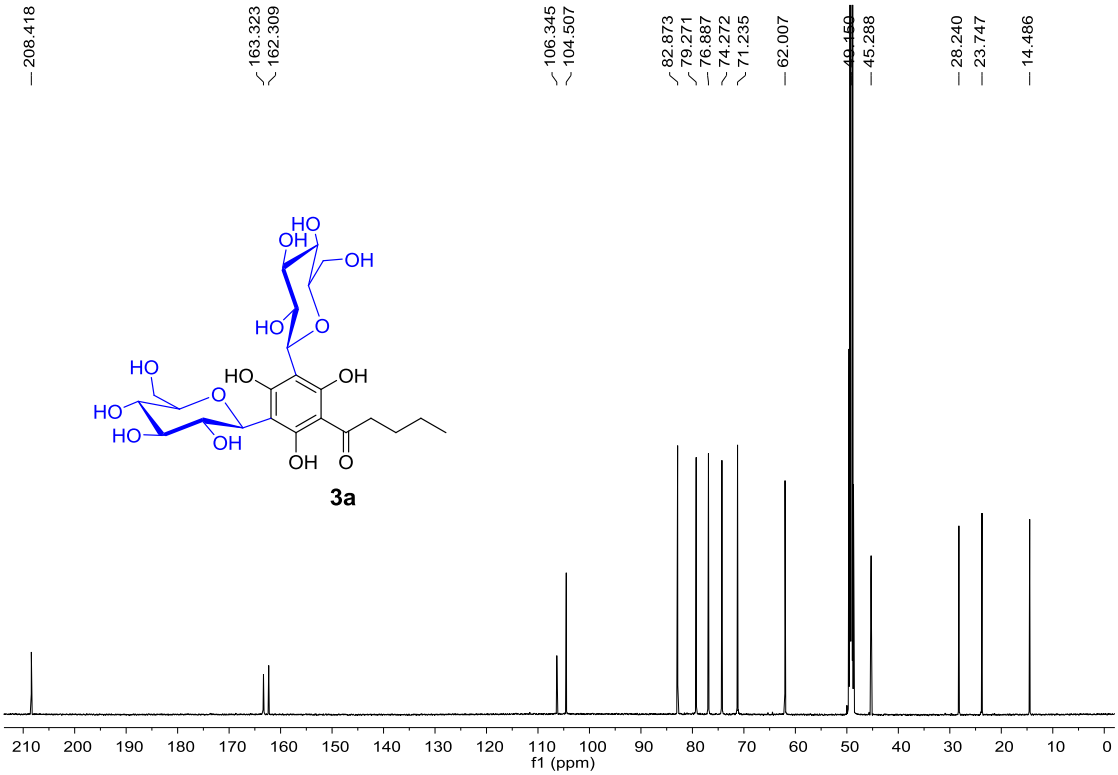

Figure S40. ^{13}C NMR spectrum of **3a** (CD_3OD-d_4, 150 MHz).

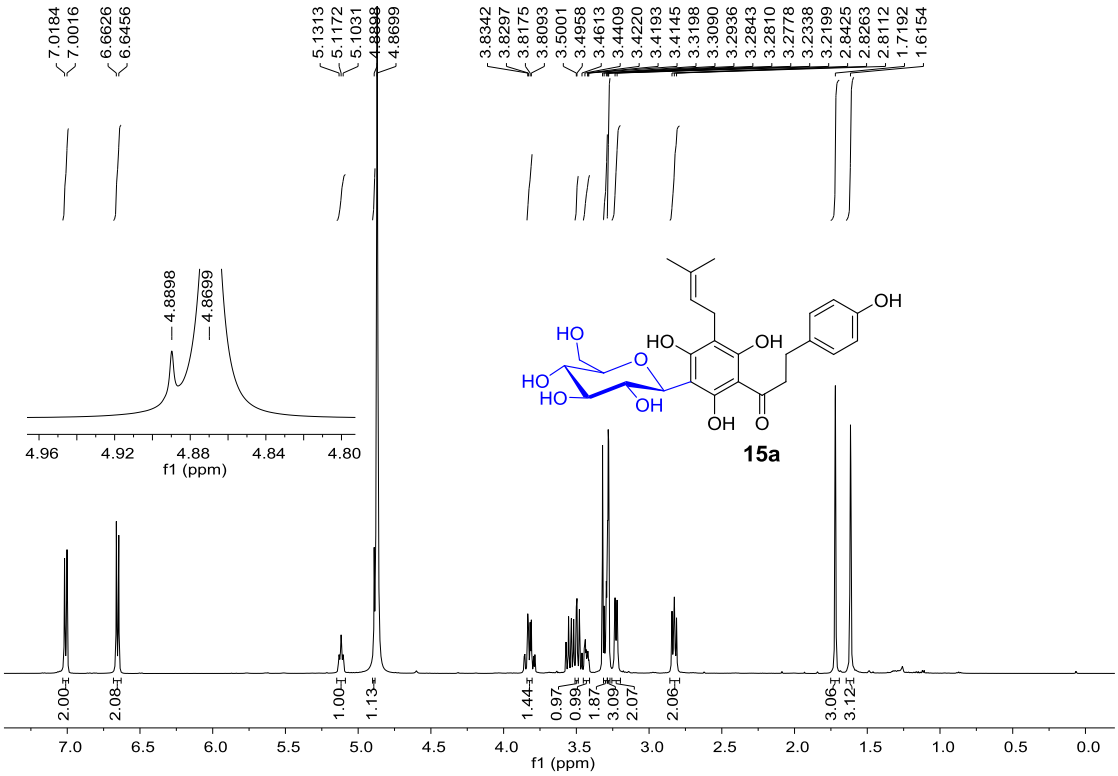

Figure S41. ^{1}H NMR spectrum of **15a** (CD_3OD-d_4, 400 MHz).

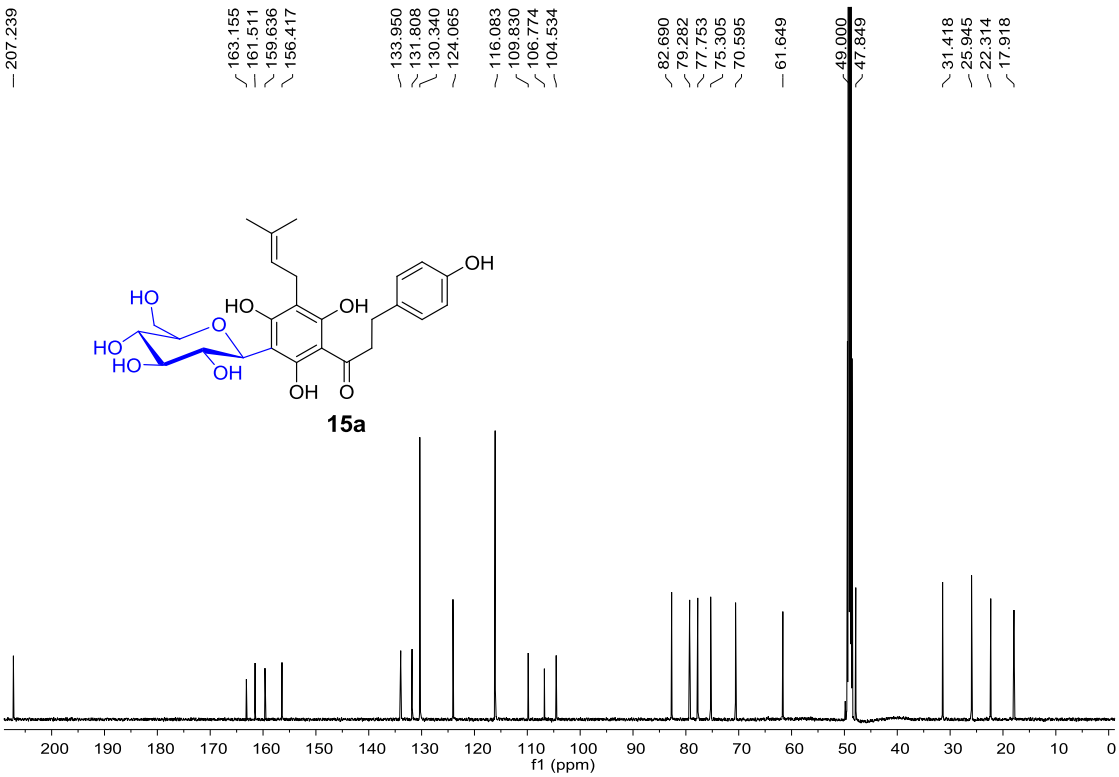

Figure S42. ^{13}C NMR spectrum of **15a** (CD_3OD-d_4, 150 MHz).

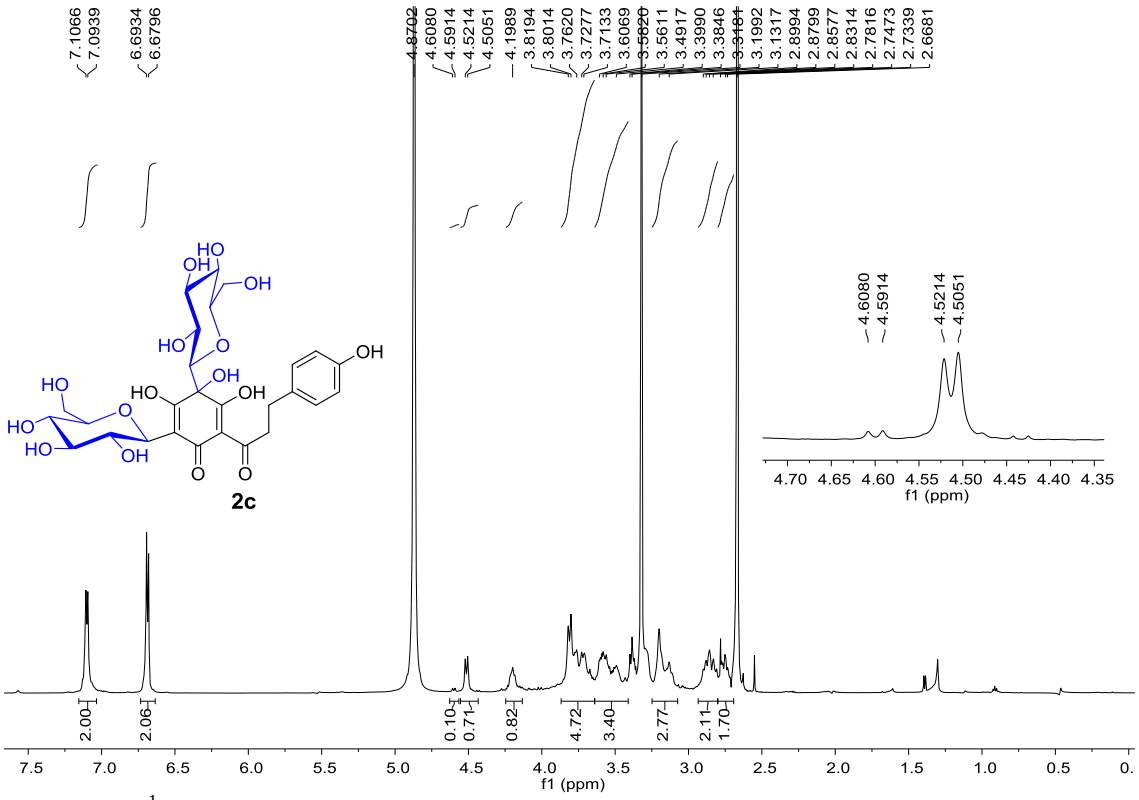

Figure S43. ^{1}H NMR spectrum of **2c** (CD_3OD-d_4, 600 MHz).

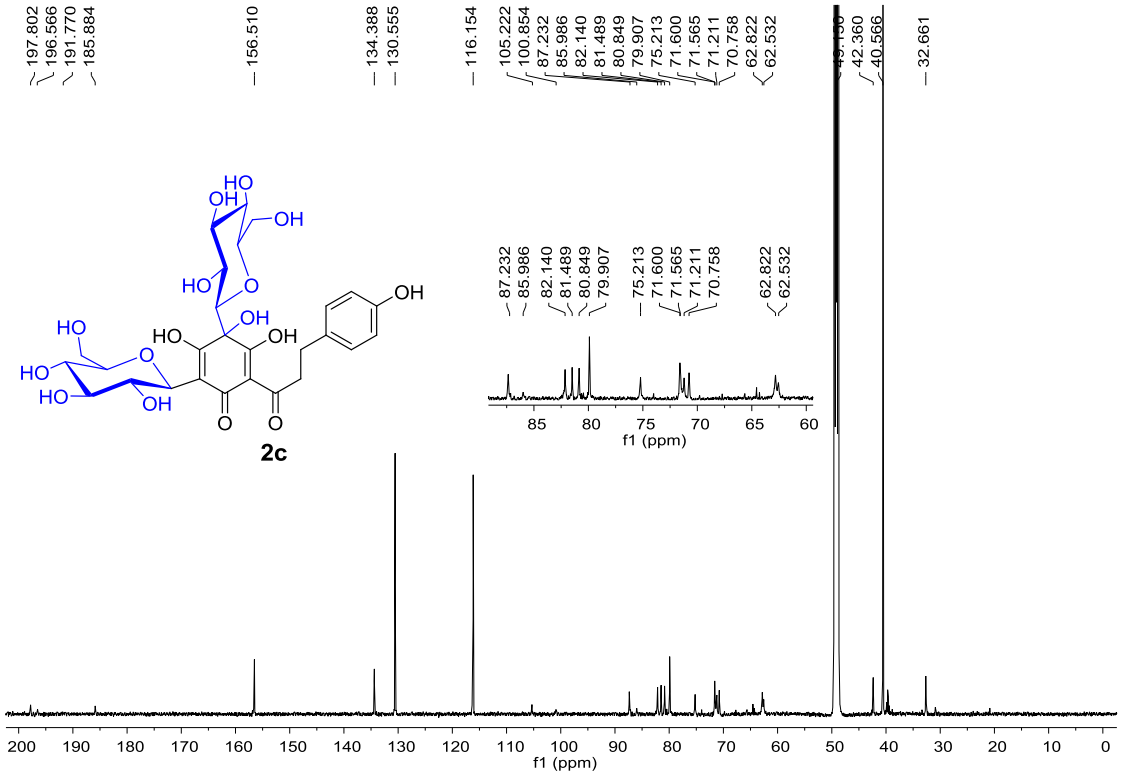

Figure S44. ^{13}C NMR spectrum of **2c** (CD_3OD-d_4, 150 MHz).

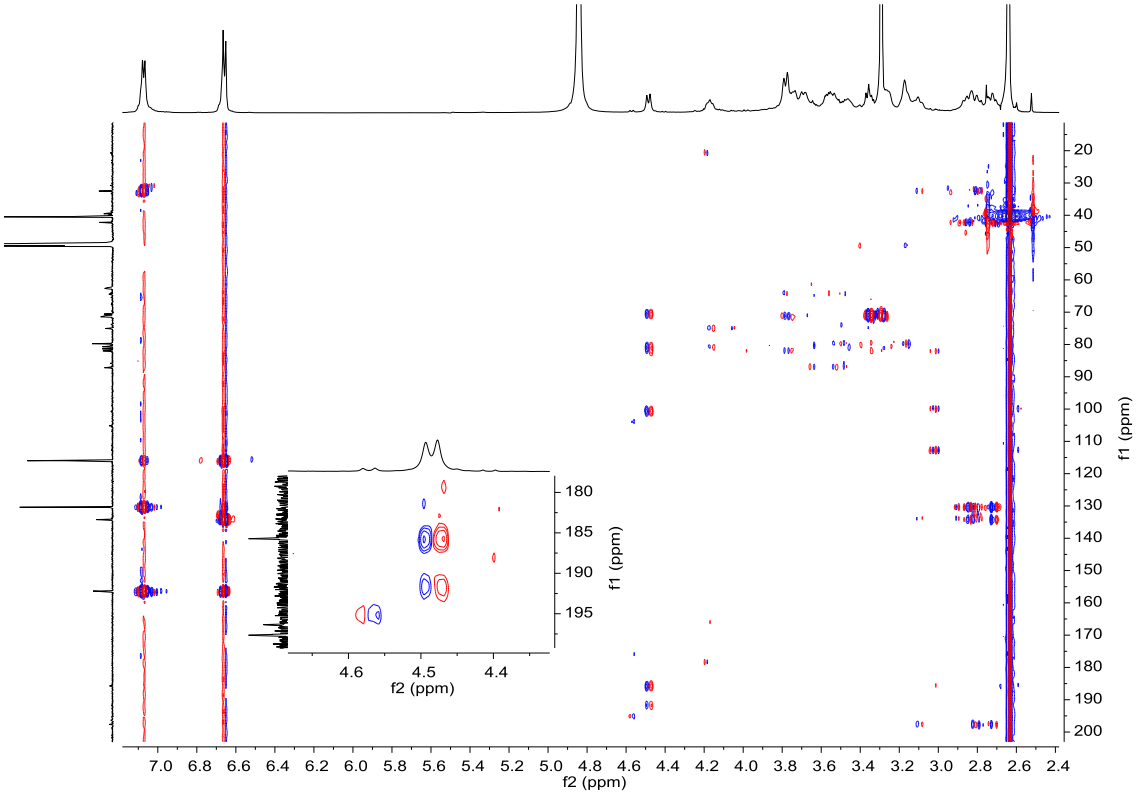

Figure S45. HMBC spectrum of **2c** (CD_3OD-d_4, 600 MHz).

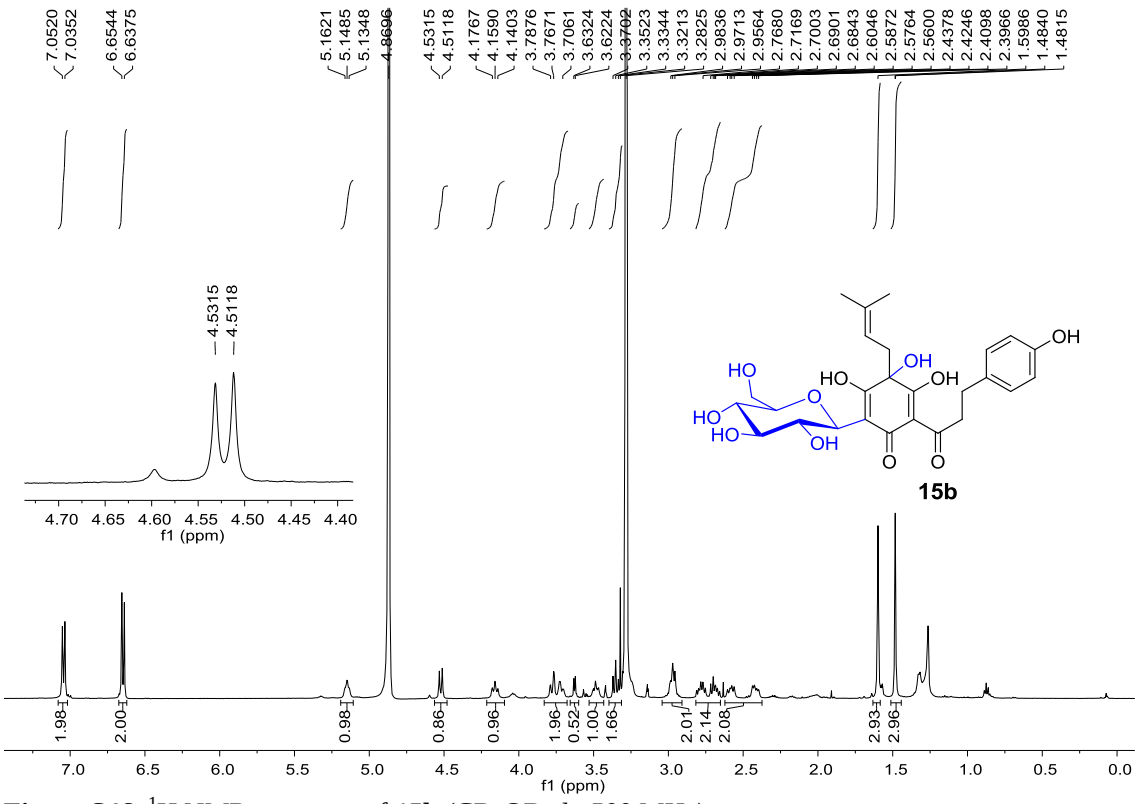

Figure S46. ^{1}H NMR spectrum of **15b** (CD_3OD-d_4, 500 MHz).

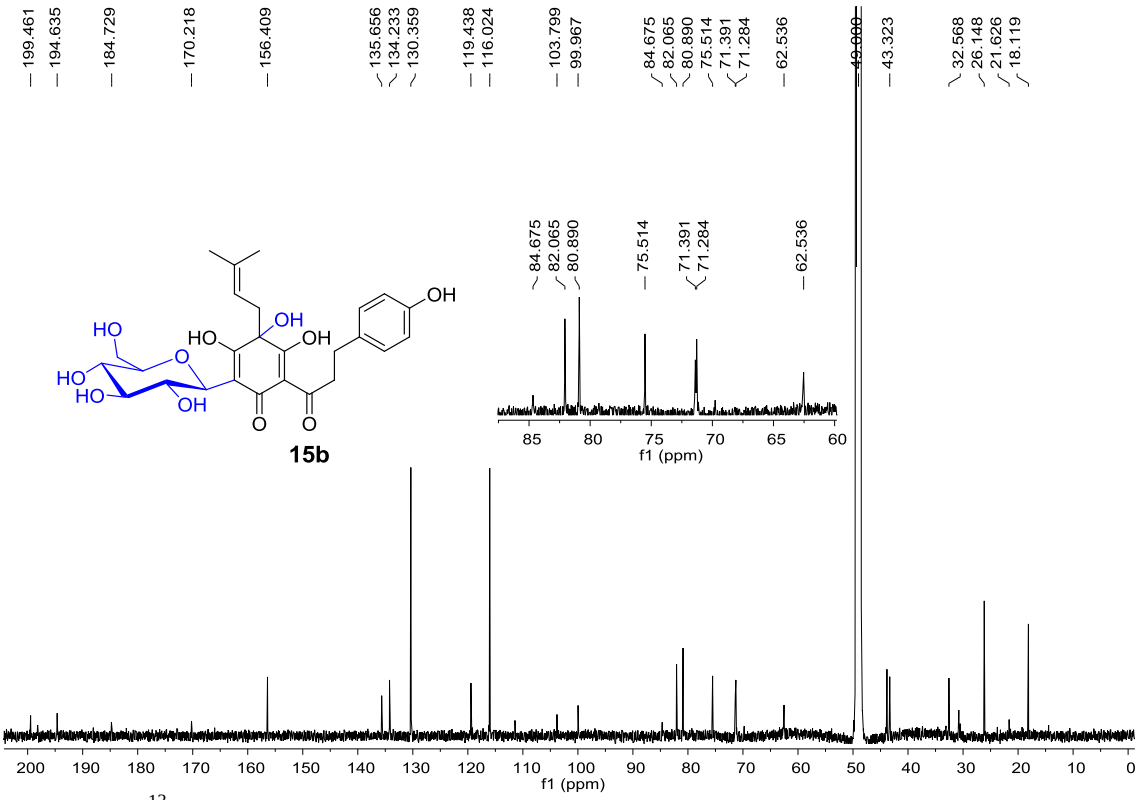

Figure S47. ^{13}C NMR spectrum of **15b** (CD_3OD-d_4, 150 MHz).

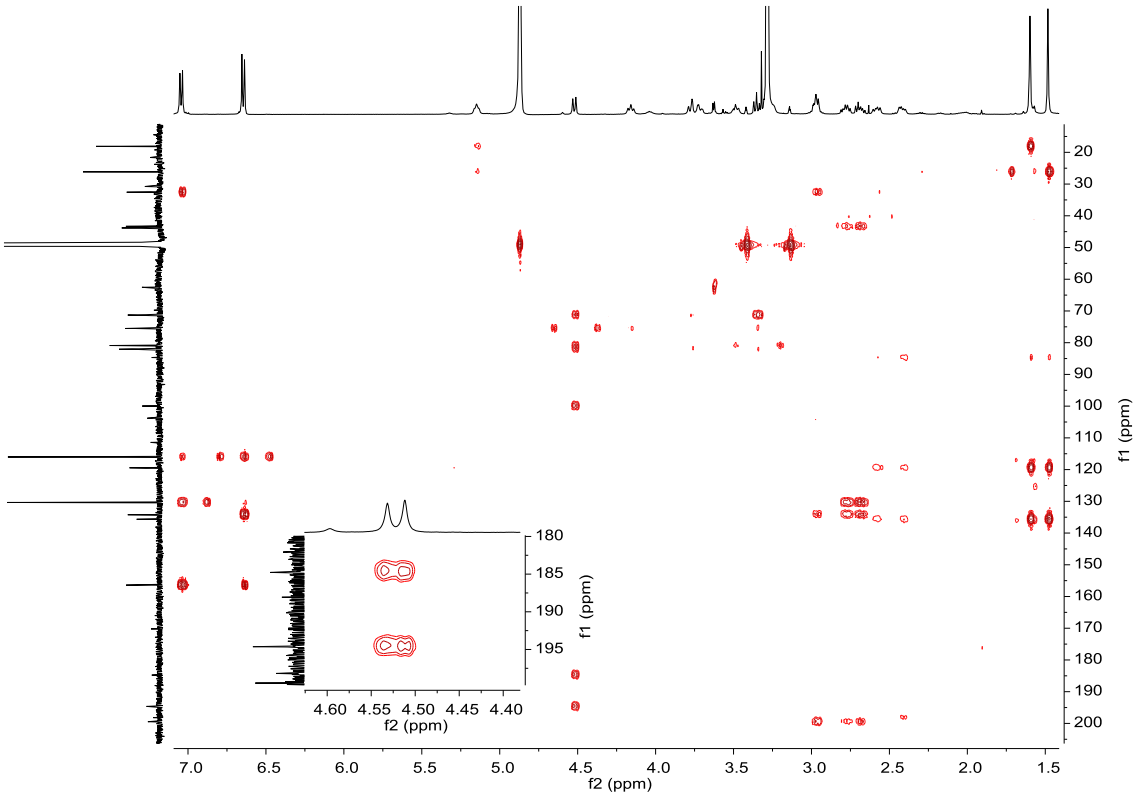

Figure S48. HMBC spectrum of **15b** (CD_3OD-d_4, 500 MHz).

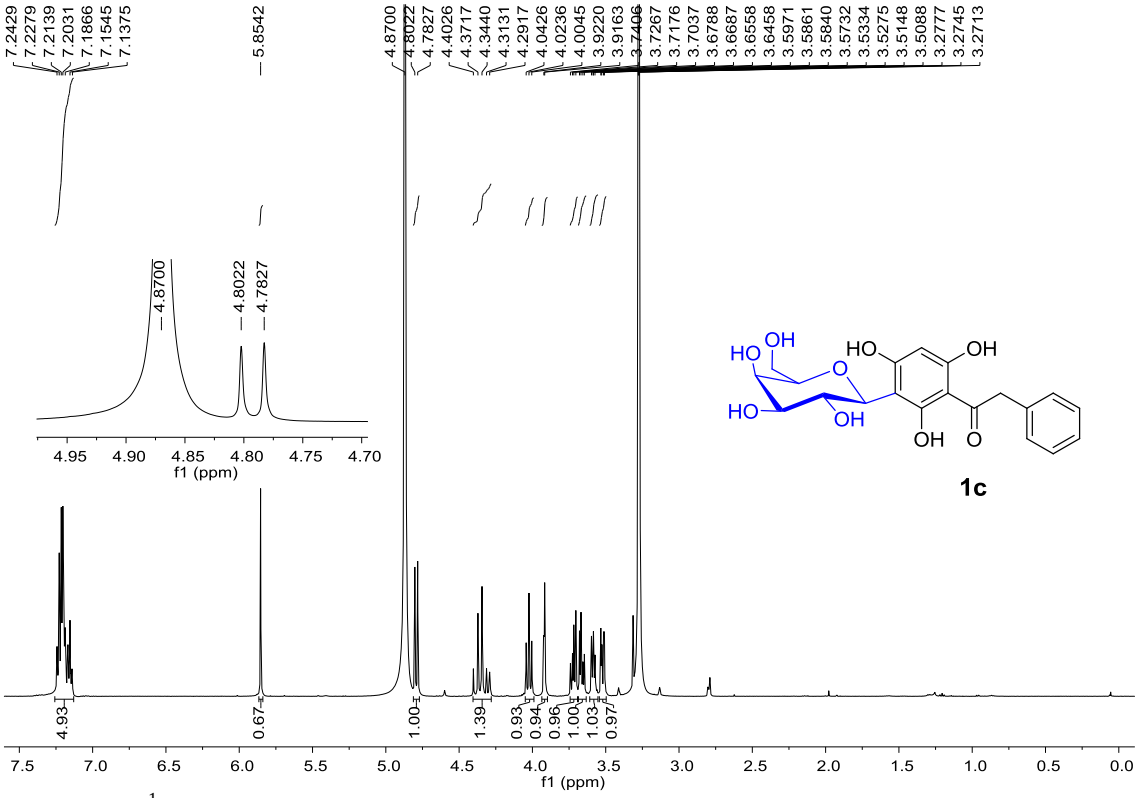

Figure S49. ^{1}H NMR spectrum of **1c** (CD_3OD-d_4, 500 MHz).

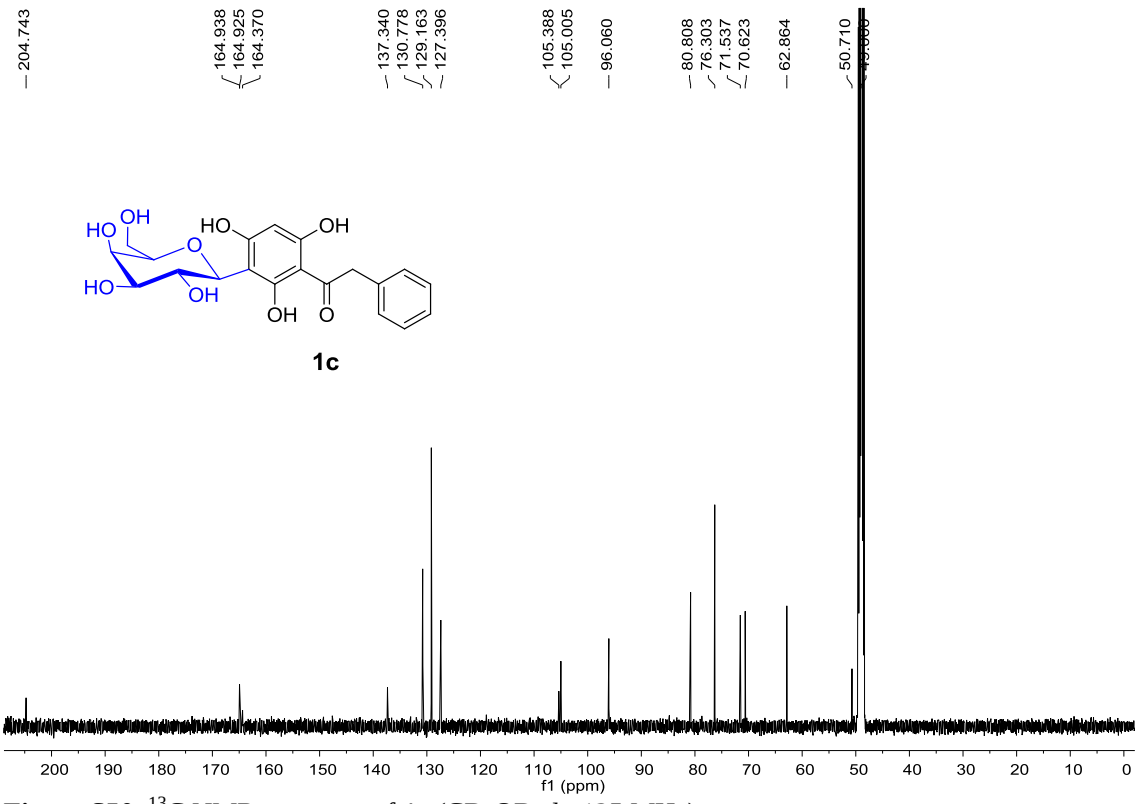

Figure S50. ^{13}C NMR spectrum of **1c** (CD_3OD-d_4, 125 MHz).

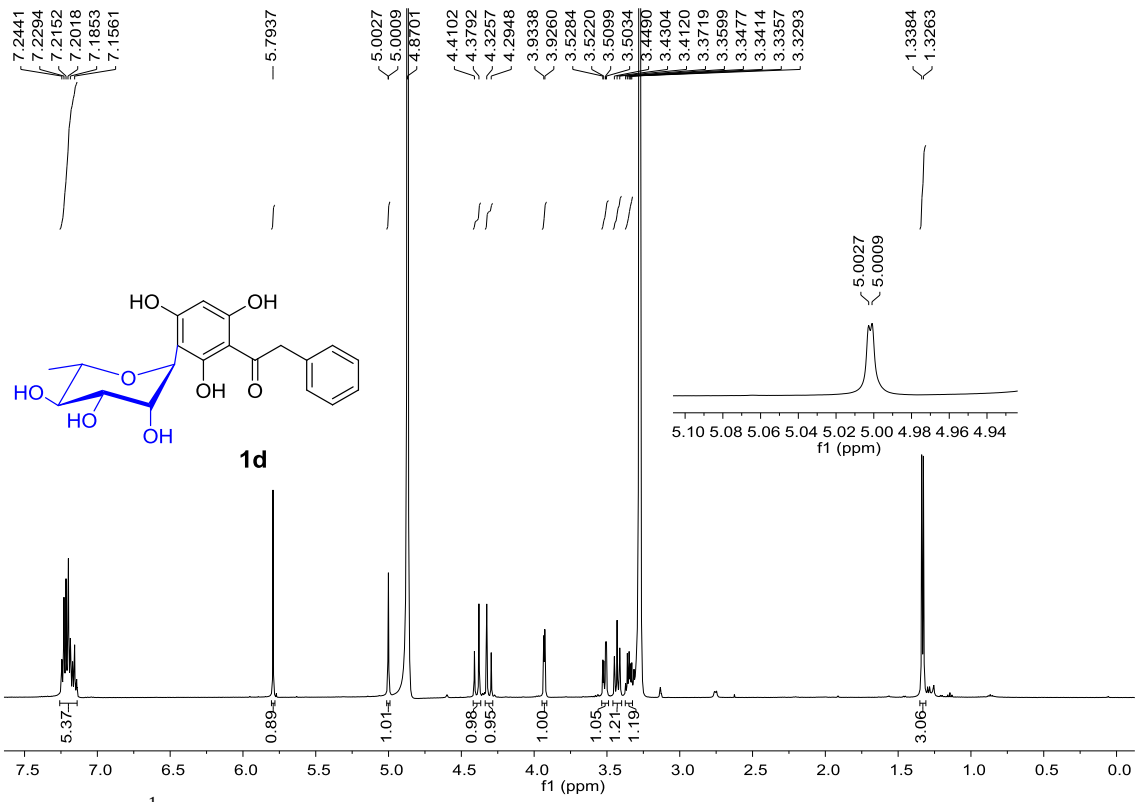

Figure S51. ^{1}H NMR spectrum of **1d** (CD_3OD-d_4, 500 MHz).

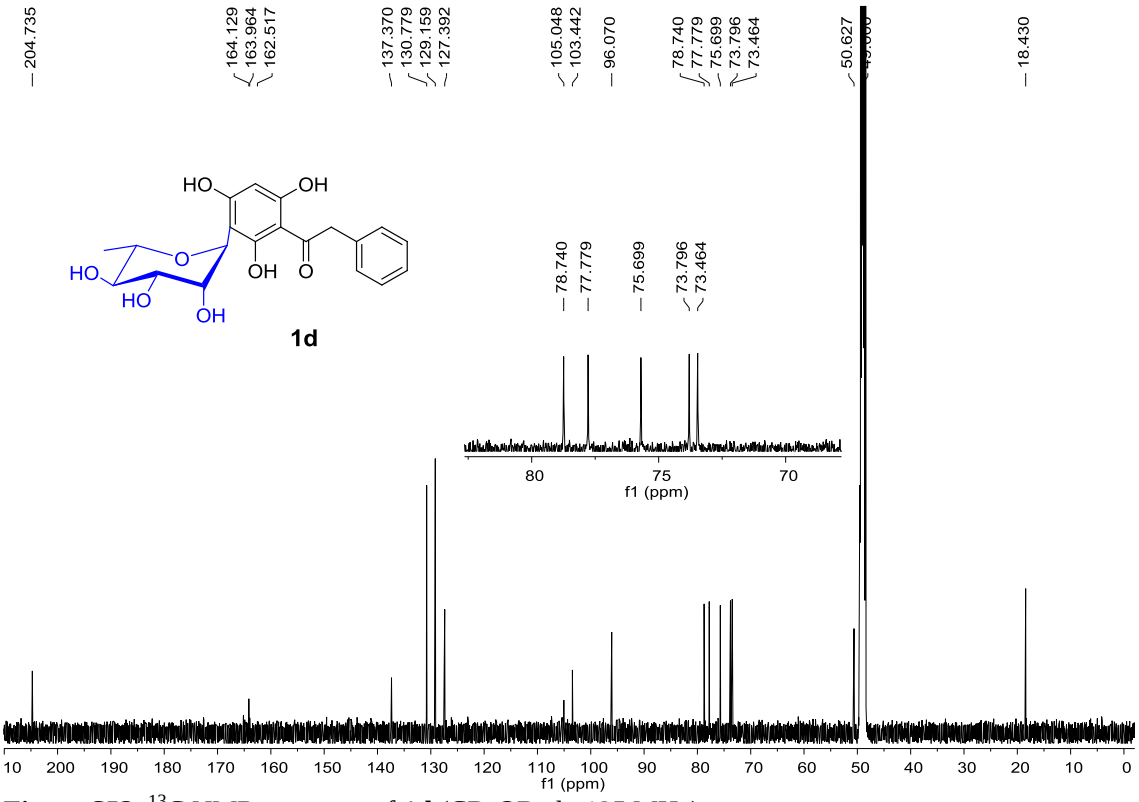

Figure S52. ^{13}C NMR spectrum of **1d** (CD_3OD-d_4, 125 MHz).

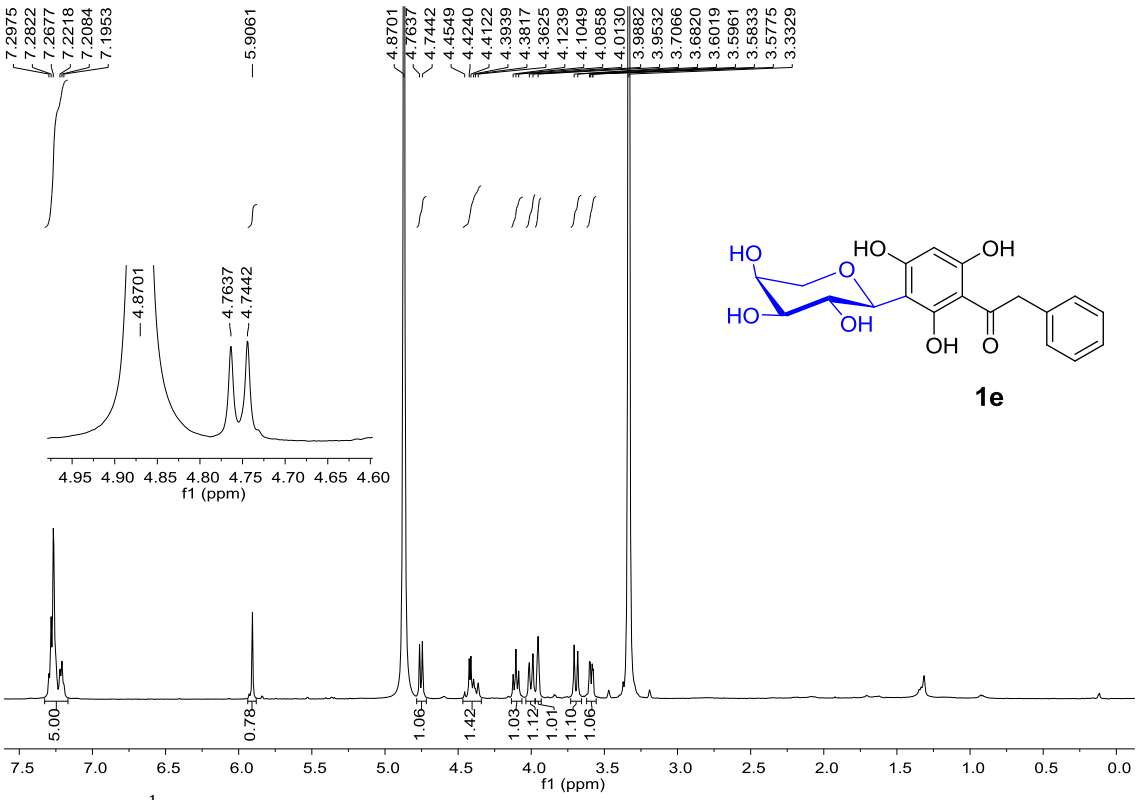

Figure S53. ^{1}H NMR spectrum of **1e** (CD_3OD-d_4, 500 MHz).

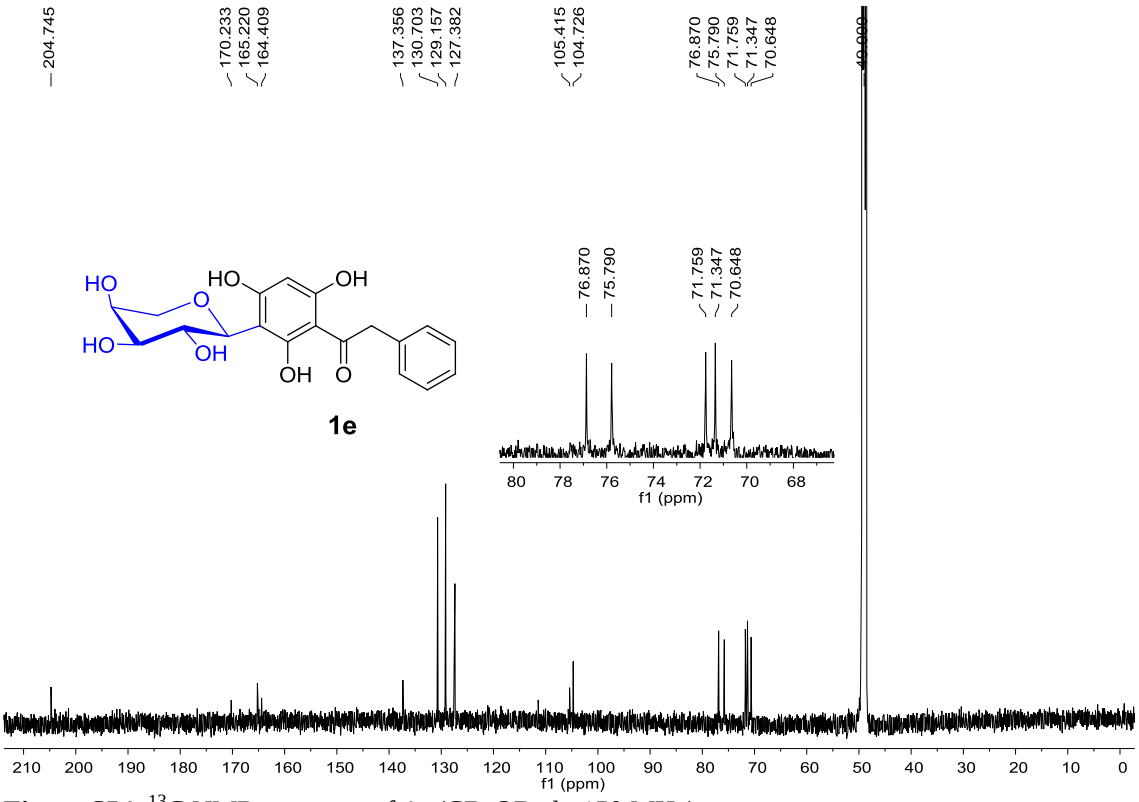

Figure S54. ^{13}C NMR spectrum of **1e** (CD_3OD-d_4, 150 MHz).

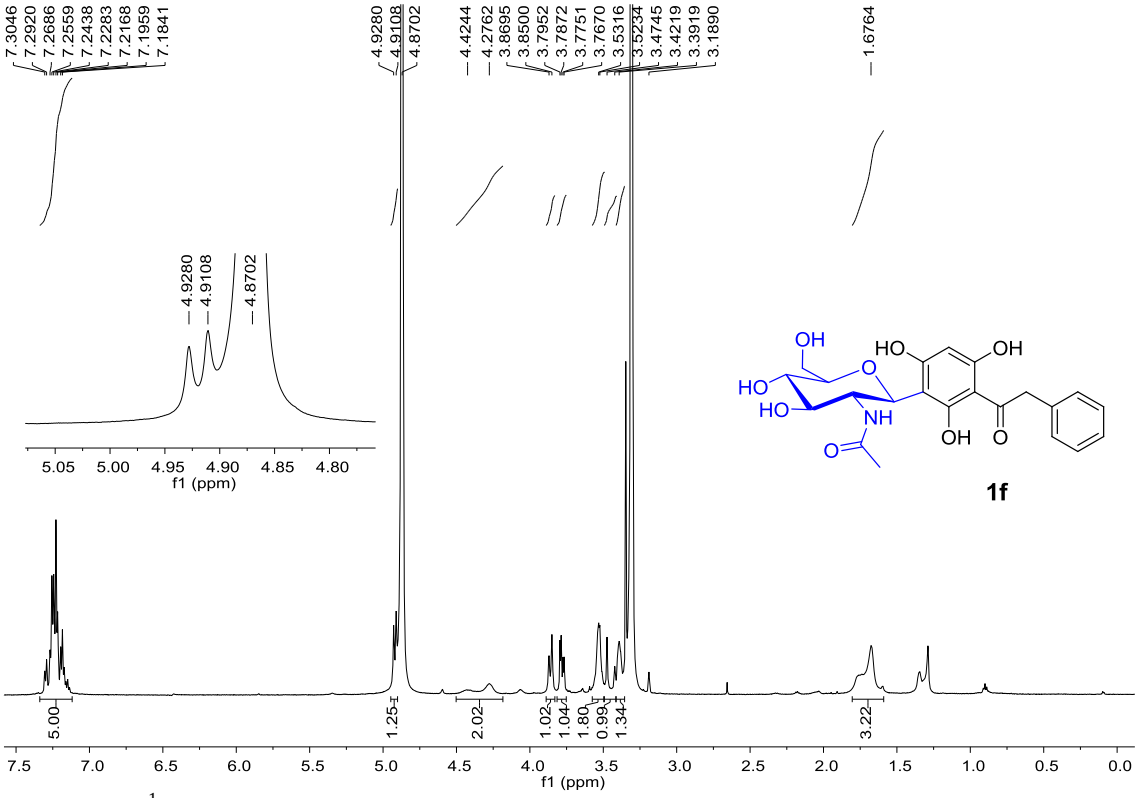

Figure S55. ^{1}H NMR spectrum of **1f** (CD_3OD-d_4, 600 MHz).

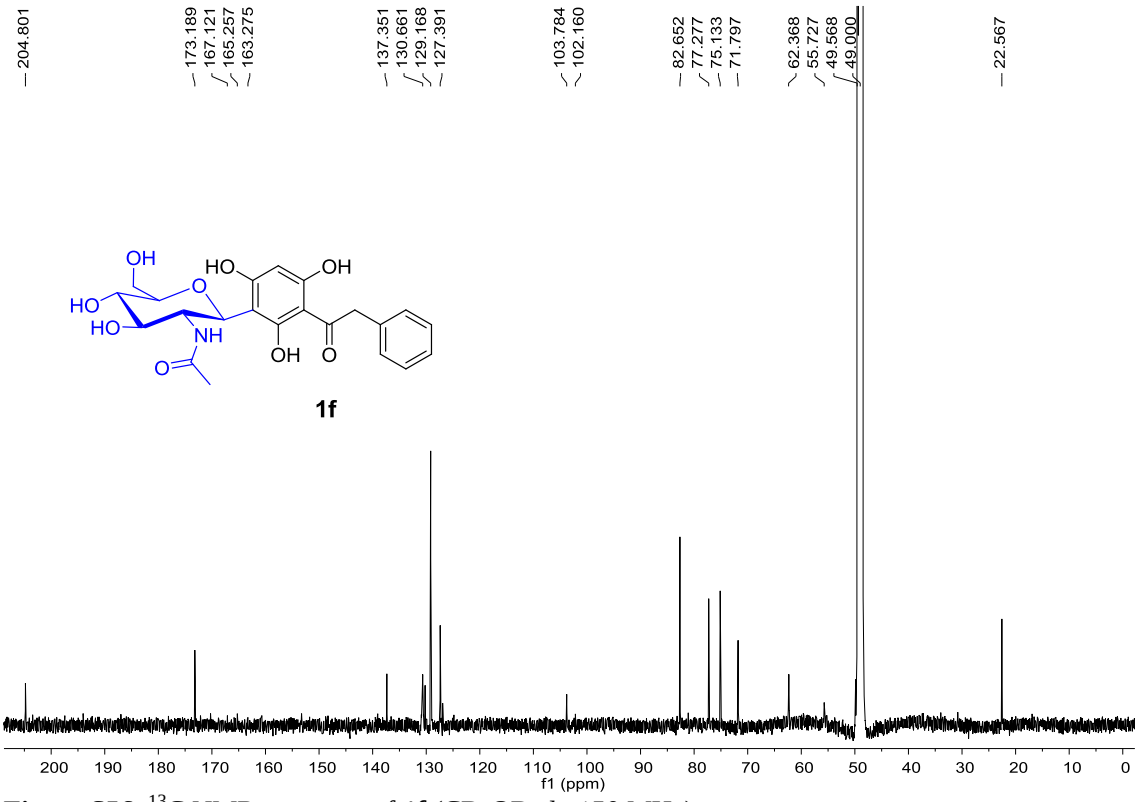

Figure S56. ^{13}C NMR spectrum of **1f** (CD_3OD-d_4, 150 MHz).

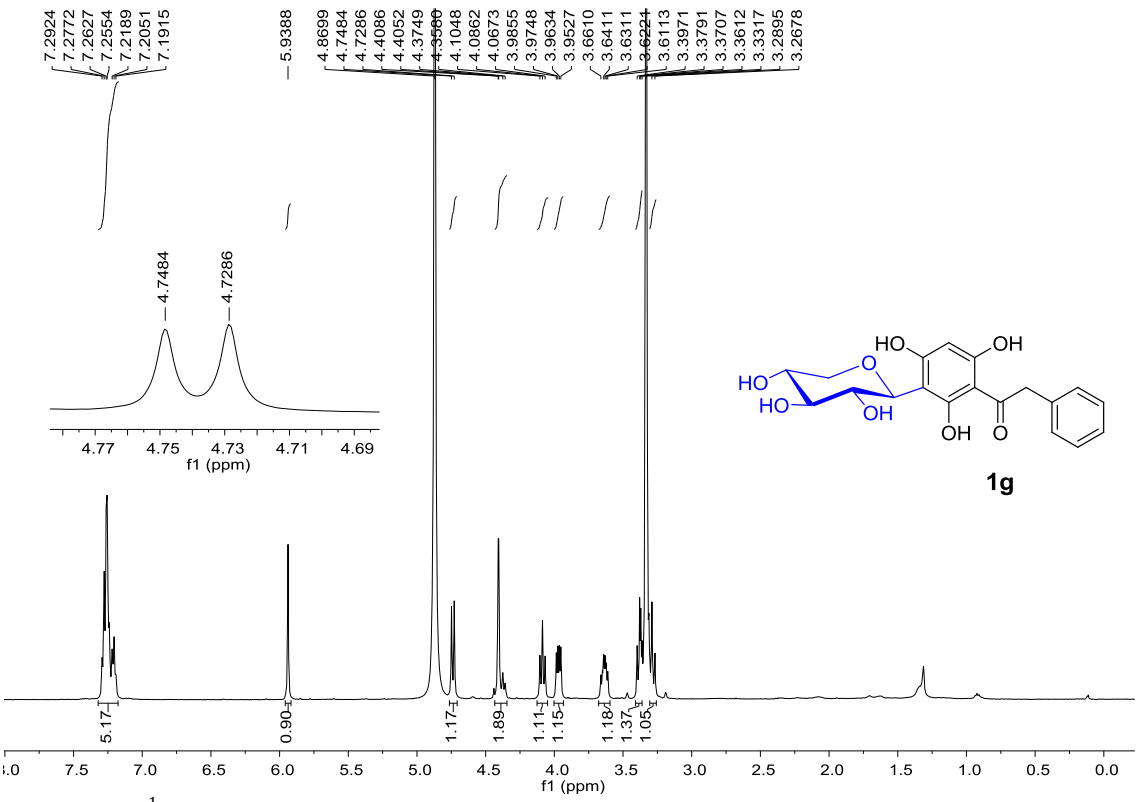

Figure S57. ^{1}H NMR spectrum of **1g** (CD_3OD-d_4, 500 MHz).

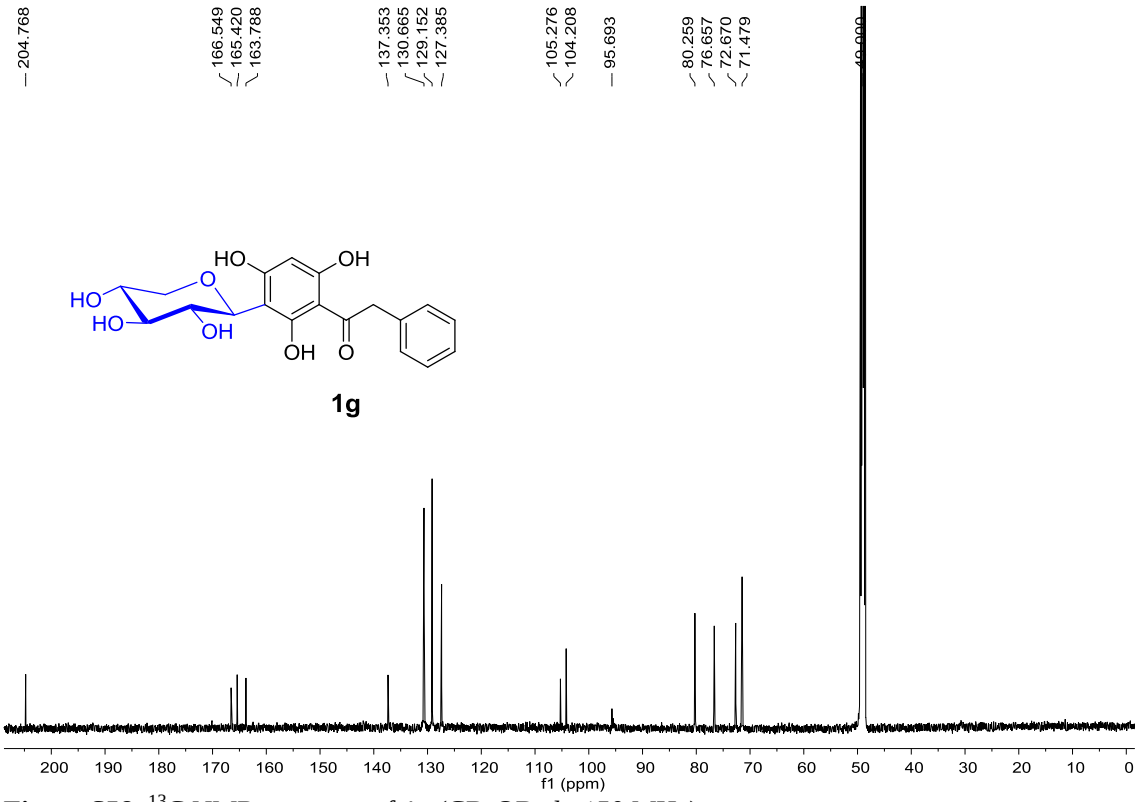

Figure S58. ^{13}C NMR spectrum of **1g** (CD_3OD-d_4, 150 MHz).

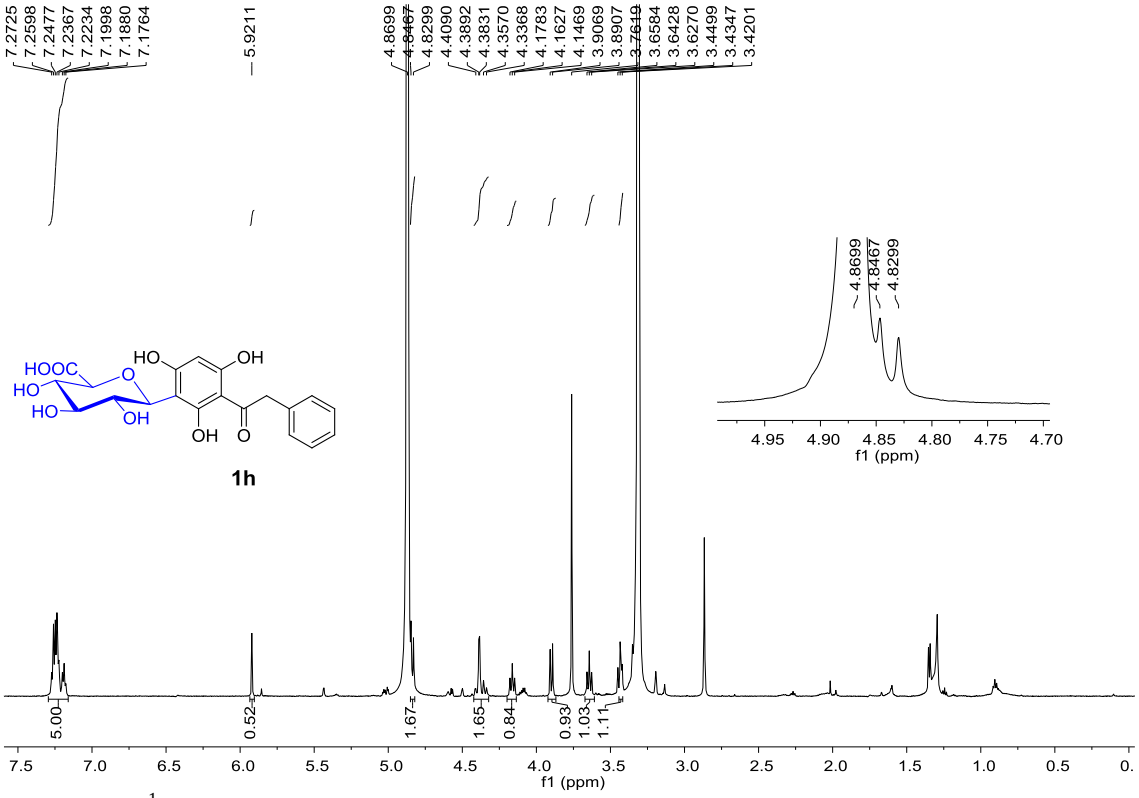

Figure S59. ^{1}H NMR spectrum of **1h** (CD_3OD-d_4, 600 MHz).

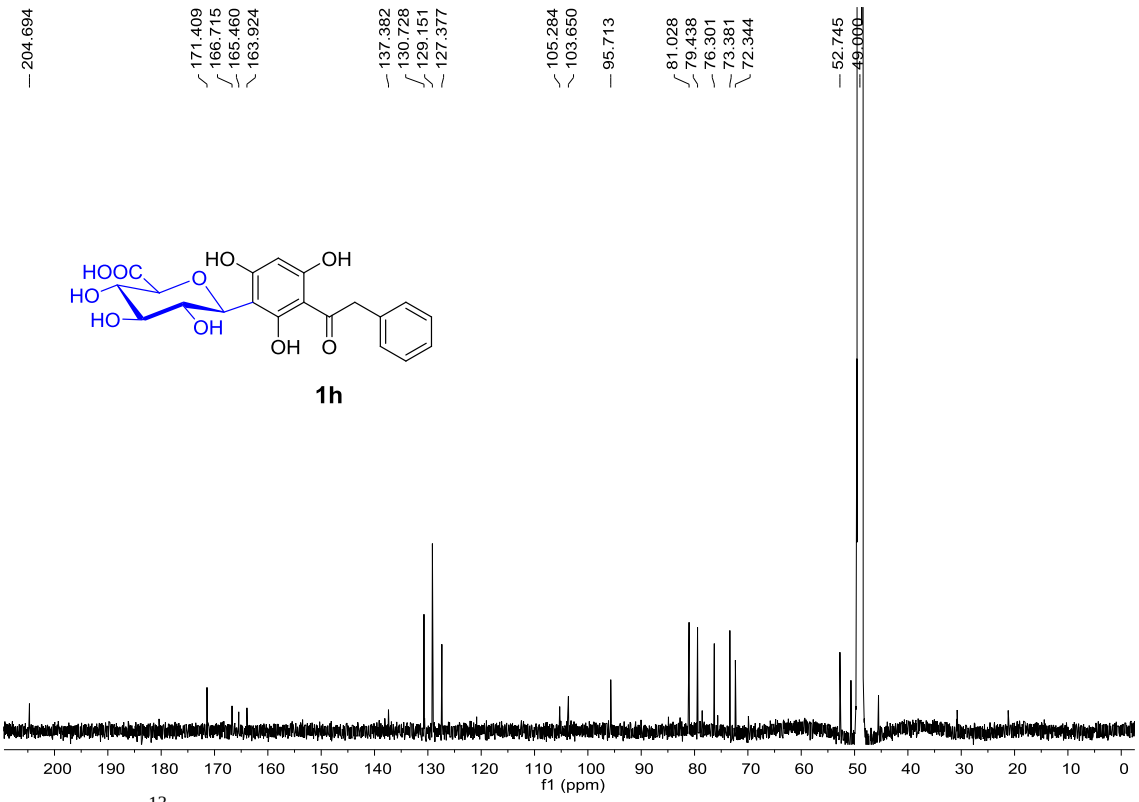

Figure S60. ^{13}C NMR spectrum of **1h** (CD_3OD-d_4, 150 MHz).

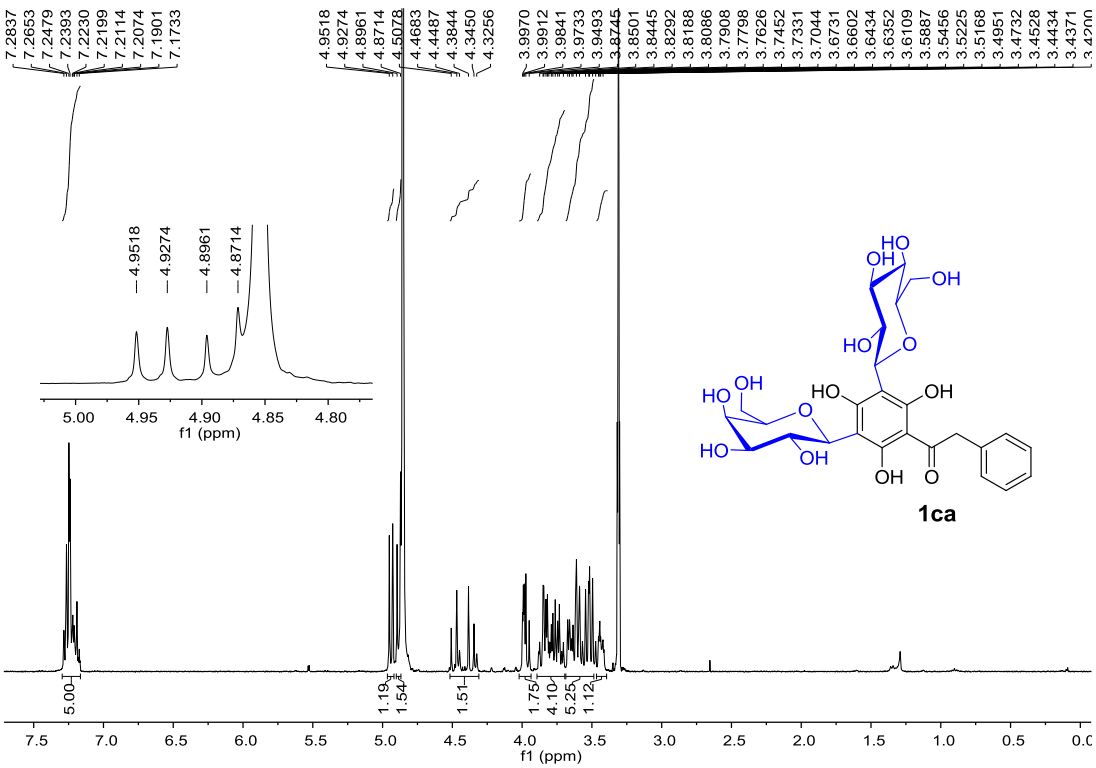

Figure S61. ^{1}H NMR spectrum of **1ca** (CD_3OD-d_4, 400 MHz).

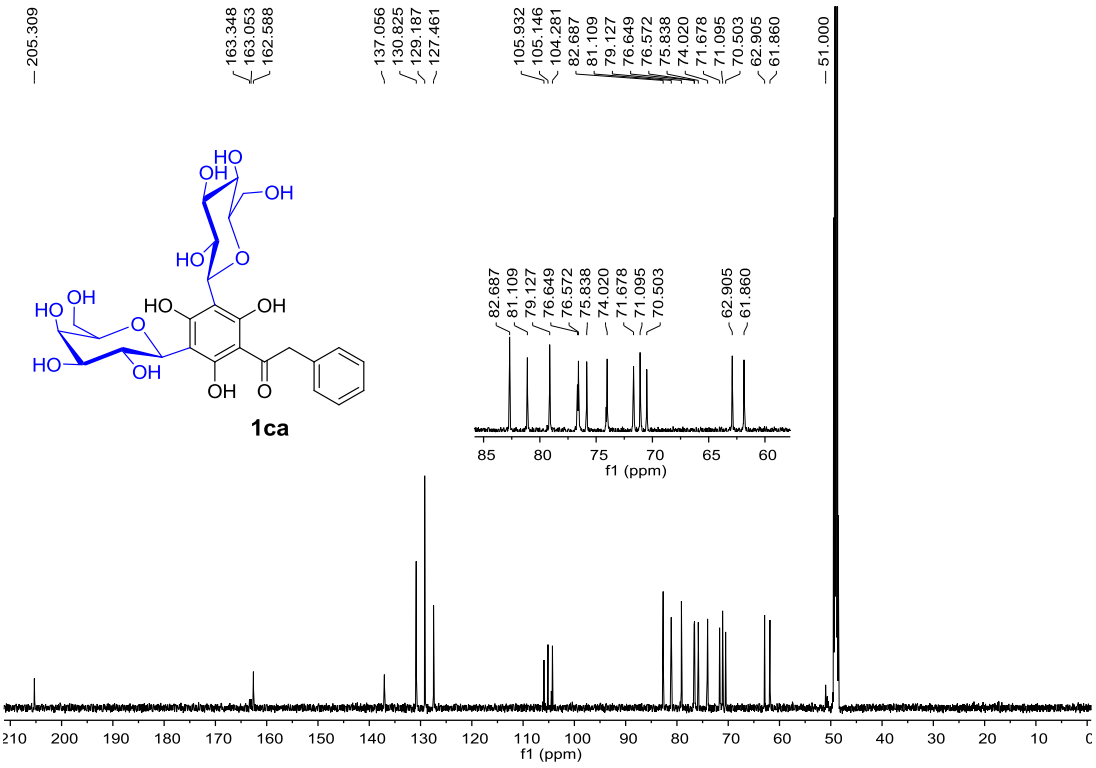

Figure S62. ^{13}C NMR spectrum of **1ca** (CD_3OD-d_4, 150 MHz).

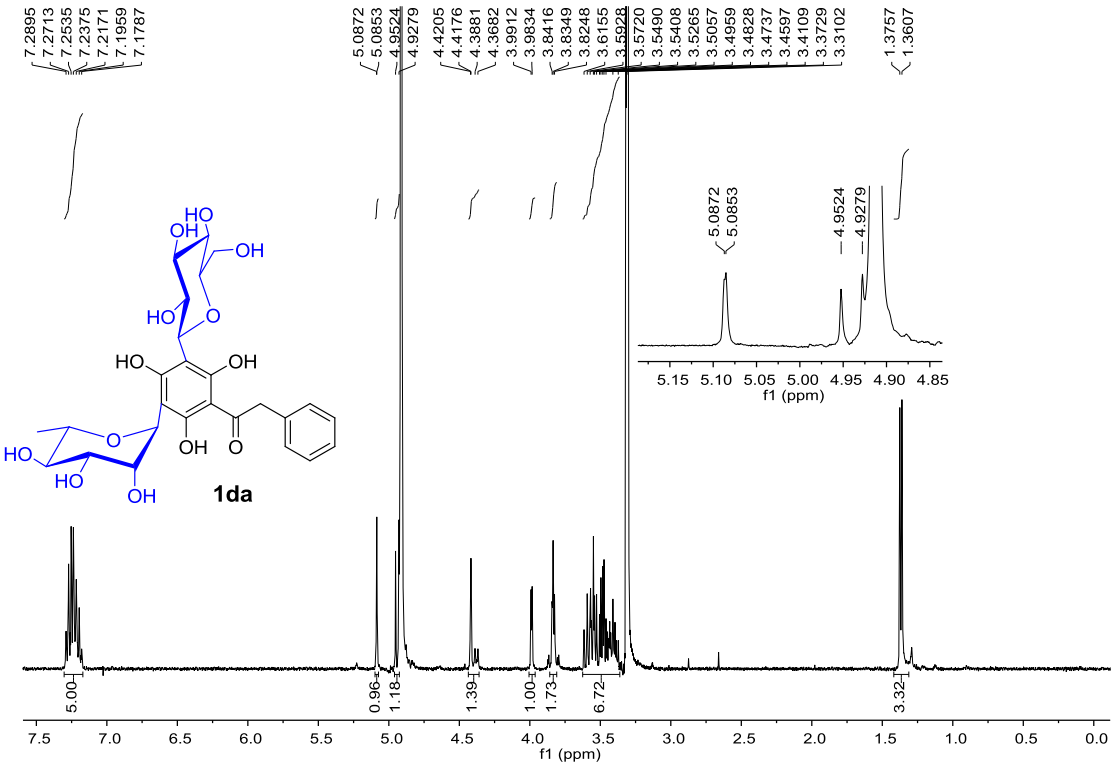

Figure S63. ^{1}H NMR spectrum of **1da** (CD_3OD-d_4, 400 MHz).

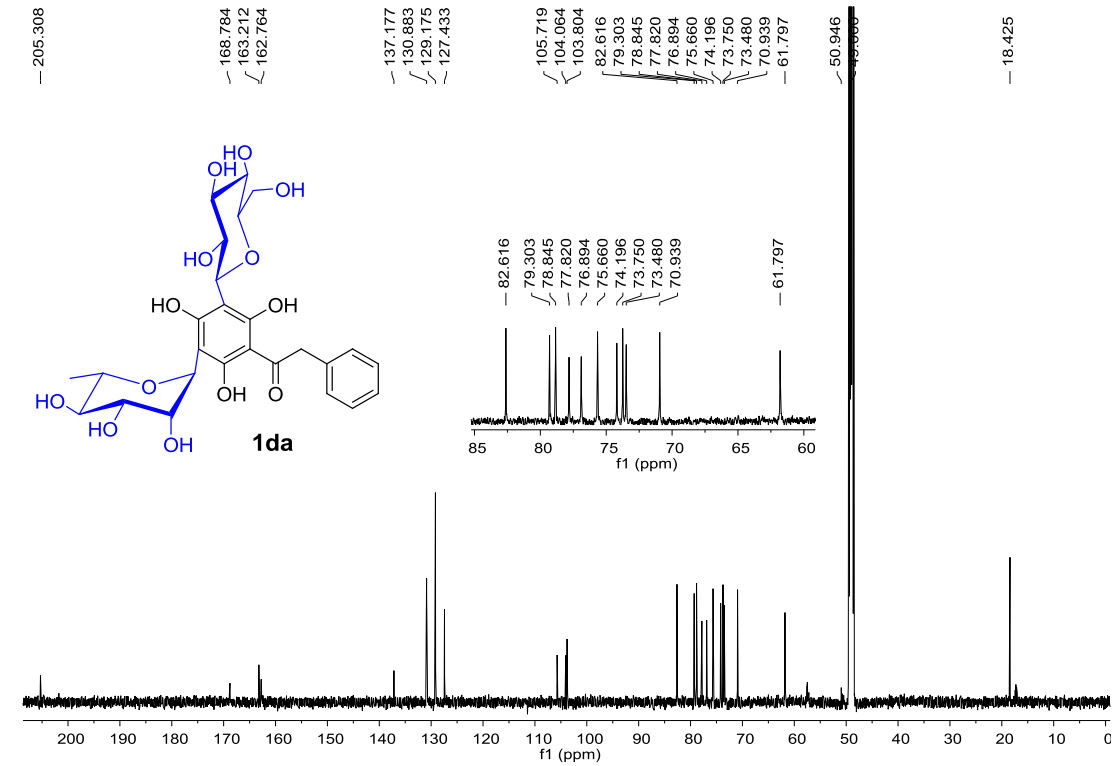

Figure S64. ^{13}C NMR spectrum of **1da** (CD_3OD-d_4, 150 MHz).

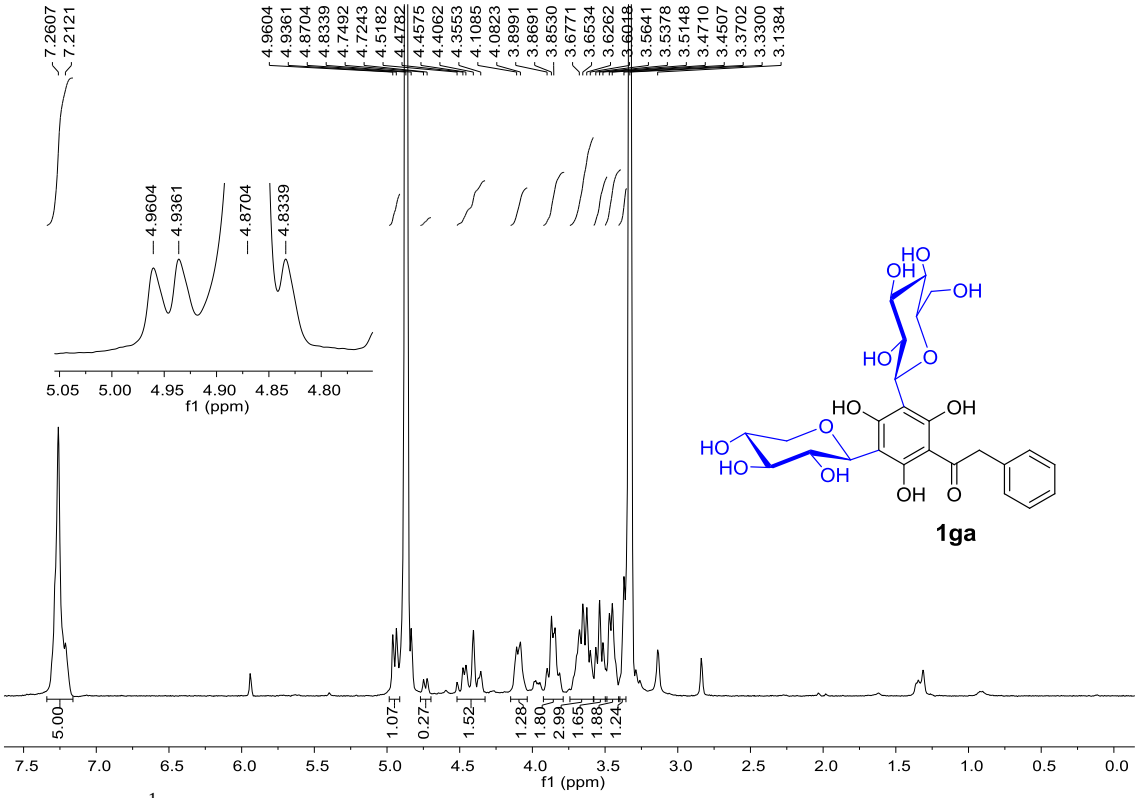

Figure S65. ^{1}H NMR spectrum of **1ga** (CD_3OD-d_4, 400 MHz).

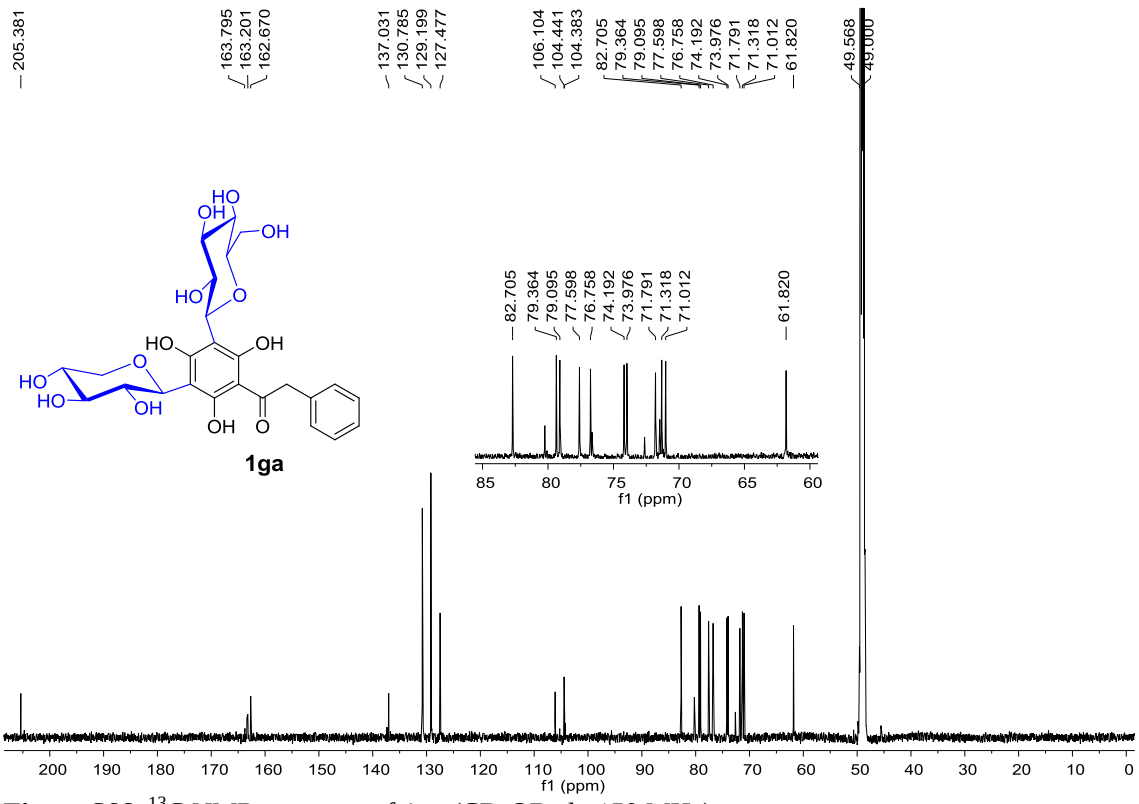

Figure S66. ^{13}C NMR spectrum of **1ga** (CD_3OD-d_4, 150 MHz).

4. References

(1) Sato, S.; Akiya, T.; Nishizawa, H.; Suzuki, T. Total Synthesis of Three Naturally Occurring 6,8-Di-*C*-glycosylflavonoids: Phloretin, Naringenin, and Apigenin Bis-*C*-β-D-glucosides. *Carbohydr. Res.* **2006**, *341*, 964–970.

(2) Santos, R. G.; Xavier, N. M.; Bordado, J. C.; Rauter, A. P. Efficient and First Regio- and Stereoselective Direct *C*-Glycosylation of a Flavanone Catalysed by $Pr(OTf)_3$ Under Conventional Heating or Ultrasound Irradiation. *Eur. J. Org. Chem.* **2013**, *8*, 1441–1447.

(3) Ng, C. H.; Rullah, K.; Aluwi, M. F. F. M.; Abas, F.; Lam, K. W.; Ismail, I. S.; Narayanaswamy, R.; Jamaludin, F.; Shaari, K. Synthesis and Docking Studies of 2,4,6-Trihydroxy-3-geranylacetophenone Analogs as Potential Lipoxygenase Inhibitor. *Molecules* **2014**, *19*, 11645–11659.

(4) Chen, R.; Liu, X.; Zou, J.; Yin, Y.; Ou, B.; Li, J.; Wang, R.; Xie, D.; Zhang, P.; Dai, J. Regio- and Stereospecific Prenylation of Flavonoids by *Sophora flavescens* Prenyltransferase. *Adv. Synth. Catal.* **2013**, *355*, 1817–1828.

(5) Bai, Y.; Lu, P.; Han, C.; Yu, C.; Chen, M.; He, F.; Yi, D.; Wu, L. Hydroxysafflor Yellow A (HSYA) from Flowers of *Carthamus tinctorius* L. and Its Vasodilatation Effects on Pulmonary Artery. *Molecules* **2012**, *17*, 14918–14927.

(6) Rye, C. S.; Withers, S. G. Elucidation of the Mechanism of Polysaccharide Cleavage by Chondroitin AC Lyase from *Flavobacterium heparinum*. *J. Am. Chem. Soc.* **2002**, *124*, 9756–9767.

(7) Oka, T.; Nemoto, T.; Jigami, Y. Functional Analysis of *Arabidopsis thaliana* RHM2/MUM4, a Multidomain Protein Involved in UDP-D-glucose to UDP-L-rhamnose Conversion. *J. Biol. Chem.* **2007**, *282*, 5389–5403.

(8) Xie, C.; Veitch, N. C.; Houghton, P. J.; Simmonds, M. S. J. Flavone *C*-Glycosides from *Viola yedoensis* MAKINO. *Chem. Pharm. Bull.* **2003**, *51*, 1204–1207.

(9) Křenek, K.; Šimon, P.; Weignerová, L.; Fliedrová, B.; Kuzma, M.; Křen, V. Facile Synthesis of Nitrophenyl 2-Acetamido-2-deoxy-α-D-mannopyranosides from ManNAc-oxazoline. *Beilstein J. Org. Chem.* **2012**, *8*, 428–432.

(10) Panigot, M. J.; Humphries, K. A.; Curley Jr., R. W. Preparation of 4-Retinamidophenyl- and 4-Retinamidobenzyl-*C*-glycosyl and *C*-Glucuronosyl Analogues of the Glucuronide of 4-Hydroxyphenyl-Retinamide as Potential Stable Cancer Chemopreventive Agents. *J. Carbohydr. Chem.* **1994**, *13*, 303–321.

(11) Brazier-Hicks, M. K.; Evans, M.; Gershater, M. C.; Puschmann, H.; Steel, P. G.; Edwards, R. The *C*-Glycosylation of Flavonoids in Cereals. *J. Biol. Chem.* **2009**, *284*, 17926–17934.

(12) Falcone Ferreyra, M. L.; Rodriguez, E.; Casas, M. I.; Labadie, G.; Grotewold, E.; Casati, P. Identification of a Bifunctional Maize *C*- and *O*-Glucosyltransferase. *J. Biol. Chem.* **2013**, *288*, 31678–31688.

(13) Nagatomo, Y.; Usui, S.; Ito, T.; Kato, A.; Shimosaka, M.; Taguchi, G. Purification, Molecular Cloning and Functional Characterization of Flavonoid *C*-Glucosyltransferases from *Fagopyrum esculentum* M. (buckwheat) Cotyledon. *Plant J.* **2014**, *80*, 437–448.

(14) Sasaki, N.; Nishizaki, Y.; Yamada, E.; Tatsuzawa, F.; Nakatsuka, T.; Takahashi, H.; Nishihara, M. Identification of the Glucosyltransferase that Mediates Direct Flavone *C*-Glucosylation in *Gentiana triflora*. *FEBS Lett.* **2015**, *589*, 182–187.

(15) Hirade, Y.; Kotoku, N.; Terasaka, K.; Saijo-Hamano, Y.; Fukumoto, A.; Mizukami, H. Identification and Functional Analysis of 2-Hydroxyflavanone *C*-Glucosyltransferase in Soybean (*Glycine max*). *FEBS Lett.* **2015**, *589*, 1778–1786.

(16) Wang, X.; Li, C.; Zhou, C.; Li, J.; Zhang, Y. Molecular Characterization of the *C*-Glucosylation for Puerarin Biosynthesis in *Pueraria lobata*. *Plant J.* **2017**, *90*, 535–546.

(17) Ito, T.; Fujimoto, S.; Suito, F.; Shimosaka, M.; Taguchi, G. *C*-Glycosyltransferases Catalyzing the Formation of Di-*C*-glucosyl Flavonoids in Citrus Plants. *Plant J.* **2017**, *91*, 187–198.